The Pennsylvania State University

The Graduate School

Department of Materials Science and Engineering

POLYOLEFIN INTERPENETRATED NETWORK FOR OIL SPILL RECOVERY: SYNTHESIS, CHARACTERIZATION, AND APPLICATION

A Dissertation in

Materials Science and Engineering

by

Changwoo Nam

Submitted in Partial Fulfillment
of the Requirements
for the Degree of

Doctor of Philosophy

December 2016

The dissertation of Changwoo Nam was reviewed and approved* by the following:

T.C. Mike Chung

Professor of Materials Science and Engineering

Dissertation Advisor

Chair of Committee

Ralph H. Colby

Professor of Materials Science and Engineering

Michael A. Hickner

Associate Professor of Materials Science and Engineering

Fred S. Cannon

Professor of Civil and Environmental Engineering

Suzanne E. Mohney

Professor of Materials Science and Engineering and Electrical Engineering

Chair of Graduate Program

*Signatures are on file in the Graduate School

ABSTRACT

In light of BP (British Petroleum) oil spill in the Gulf of Mexico in 2010, and despite the government's "all hands on deck" approach to combating the oil spill, there was no effective technology for removing, recovering, and cleaning up oil spills or oil slicks from the surface of sea water and shorelines. A new class of polyolefin copolymers with an interpenetrating network (IPN) structure is considered as a practical and comprehensive solution for oil spill recovery and cleanup.

After discussing some background information (Chapter 1) and current sorbent technology (Chapter 2), I will explain my research approach and experimental results, involving various polyolefin absorbent materials for oil and hydrocarbon spill recovery. To understand the structure-property relationship in polyolefin absorption capacity and kinetics, a systematic study (Chapter 3) was first conducted using a series of semi-crystalline ethylene/1-octene copolymers (LLDPE thermoplastics with a broad range of crystallinity) and amorphous cross-linked 1-decene/DVB (x-D/DVB) copolymers (elastomers with a wide variety of crosslinking density). They are swellable but not soluble in any hydrocarbon liquids under ambient temperature conditions. The absorption evaluation involved various hydrocarbon liquids, including solvents (hexane, cyclohexane, and toluene), refined oil products (gasoline, diesel, and petroleum oil) and Alaska North Slope (ANS) crude oil. In general, the absorption capacity is controlled by the network structure. The maximum absorption capacities of semi-crystalline LLDPE and amorphous x-D/DVB elastomer with toluene can reach 35 and 43 times that of the polymer mass, respectively. However, with the complex oils, the absorption profile is determined by a

combination of absorbate composition and absorbent network structure and morphology. Both polymer systems exhibit poor absorption performance with ANS crude oil.

The systematic study provides important information about how the polymer structure and morphology affects the hydrocarbon absorption capacity and kinetics. Thus, a new polyolefin IPN structure was designed and fabricated by the combination of two polyolefin copolymers, including semicrystalline LLDPE thermoplastics and amorphous x-D/DVB elastomers (Chapter 4). The IPN structure allows the formation of porous morphology with relatively high free volume between two intertwined rigid and soft polymer chains, which enhances the diffusion of highly viscous hydrocarbon liquids and the swelling capacity of the polymer matrix. Some resulting polyolefin IPN structures show a very high hydrocarbon absorption capacity (>40 times by weight) and fast kinetics for all examined hydrocarbon absorbates, independent on the type of organic solvents and oils. The selective oil absorption (without water) offers buoyancy, stability, and easy recovery on water surfaces. In addition, the recovered oil swollen gel, containing >97% oil and <3% polyolefin (which is completely thermally degradable to small hydrocarbon molecules), is suitable for the regular oil-refining process (an economical, no waste, and no pollutant approach).

Once the desirable polyolefin IPN structure was validated in the laboratory, a scale-up study was performed with the target of developing a commercial process that can be used for the large-scale production (Chapter 5). More than 20 pounds polyolefin IPN material have been delivered to DOI BSEE for an operational test at the Ohmsett (NJ, USA) facility. They had successfully examined the recovery of ANS crude oil spilled in seawater (salinity 29-33 ppt) under outdoor cool weather environment with similar 40 times ANS oil

absorption capacity and fast kinetics. In addition, the tests were focused on the recovery of resulting absorbed oil adduct (gels) on the water surface by skimmers and the pumping ability of the fully swollen gel by common crude oil delivery methods.

In economic considerations, polyolefins are the least expensive polymeric materials, with a large production capability in the United States and around the world. With a conservative estimate, the production cost of new polyolefin INP material may be below $2 per pound in the large-scale industrial production. One pound of this polymer with 40 times absorption capacity can recover more than 5 gallons of the spilled oil (that would become pollutant/waste) to be used as regular crude oil that is worth more than $8 (based on $60/barrel). Most importantly, it can mitigate the huge environmental impacts caused by oil spills.

Overall, this new polyolefin IPN absorbent material exhibits a combination of benefits in oil recovery and cleanup, including

(i) High oil absorption capability (over 30 g/g)

(ii) Fast kinetics (30 times within 2 hr)

(iii) No water absorption

(iv) Easy recovery from water surface and transporting to storage tank

(v) The recovered oil-swelled i-Petrogel as regular crude oil for refinery

(vi) No waste in natural resources and no air/water pollutions

(vii) Cost effective and economic feasible.

TABLE OF CONTENTS

LIST OF FIGURES

LIST OF TABLES

ACKNOWLEDGEMENTS

“Your word is a lamp for my feet, a light on my path.”

- Psalm 119:105-

I would, first and foremost, like to offer this endeavor to our GOD almighty for the wisdom he bestowed upon me, good health, and funding in order to finish this research.

This dissertation becomes reality with the kind support of many people. I would like to express my sincere thanks to all of them.

I would like to express my gratitude towards my family for the encouragement which helped me in completion of this dissertation. My beloved and supportive mother (Bongsun), father (Jongchul), and brother (Jinwoo).

I would like to express my appreciation to Dr. Chung, my principle advisor, for all the support and guidance he provided during my study. I have learned so much from him starting from research techniques, how to think as a scientist. Without his help, I would not have grown as a scientist and as an individual as I have over the past years.

I would like to express my thanks to my committee members Dr. Ralph Colby, Dr. Michael Hickner and Dr. Fred Cannon, for the insightful feedback during scientific discussions about my research and accommodating the scheduling of my comprehensive examination and oral thesis defense.

My thanks and appreciations also go my colleagues (Dr Chung’s group members, Dr. Hickner’s group members, MatSE Korean students, and Korean Church Members) who have willingly helped me out with their abilities.

Chapter 1

Introduction

1.1 Motivation

Massive oil spillage is always considered as a challenging task around the world. This spillage is mostly caused by cracking of storage tanks and pipes and tanker ship accidents. The number of oil spill accidents on offshore oil rigs is increasing while tanker ship accidents tend to decrease every year. Although less than 8% of petroleum out of total oil production in North American Ocean is produced by offshore oil rigs, concerns over oil spillage prevail due to the cost associated with these incidents (Figure 1.1). Therefore, further research is necessary to develop advanced technology for removing crude oil spillage from the water surface.

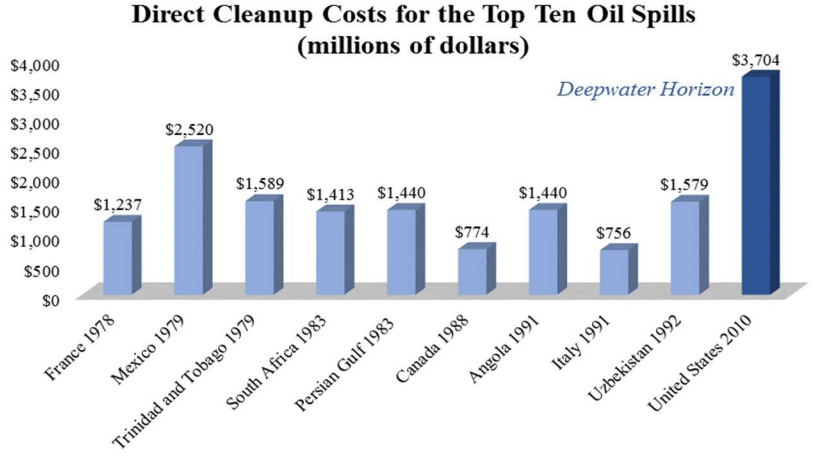

Figure 1-1. Direct cleanup cost for the top ten oil spills, 1970 to 2010. (Anne Casselman, Popular Mechanics, 2015)

Unlike other refined fuels or light oils, removing crude oil on the water surface is cost-inefficient and time-consuming due to its weathering and high viscosity. Unfortunately, crude oil spillage on the ocean and shorelines also causes a long-term impact on the marine environment.[1] In the event of an oil spillage in a remote ocean, a fast response is required. However, the "weathering" process (i.e. spreading, emulsification, and evaporation) of spilled oil makes it harder to get rid of spilled oil from the water surface when it exposed to the open environment (Figure 1.2). The crude oil coats the rock surfaces, animal skins, shorelines, and it can block the sunlight and reduce air circulation in the ocean.[2] If the crude oil stays on the water surface for few days, the oil will become completely emulsified in water, which makes it even harder to minimize the long-term environmental impact.[3]

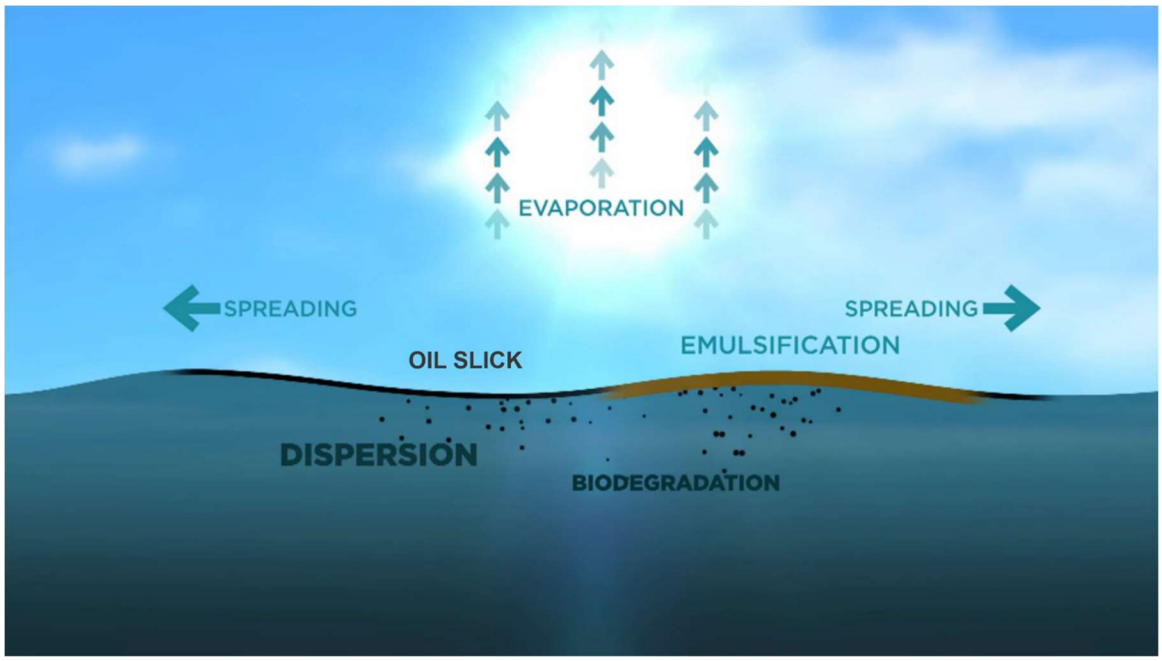

Figure 1-2. Schematic illustration of an oil weathering process. (ITOPF image)

1.2 Current Technologies in Oil Spill Response

Several standard methods are commonly applied to combat an oil spill on the open sea, including booms, oil skimmers, dispersant, in situ burns and sorbents (Figure 1.3).[4–6] Booms create a boundary around contained oil and prevent the spreading of oil, helping to pick up oil by a skimmer. However, heavy wind or unsteady ocean currents prevent booms from reaching their full potential as an initial response to trap oil from the water surface. The in situ burn of oil, is limited to conditions such as fresh oil under good weather condition. Additionally, burning can create micro dust and release toxic gas into the air which can affect the ecosystem. Bioremediation agents or chemical oil dispersant can be applied on a large oil spilled area to break down oil into a smaller size of dispersed oil droplets.[7] However, there are concerns that environmental tradeoff such as tar balls and difficult to pick up the oil by the skimmer.

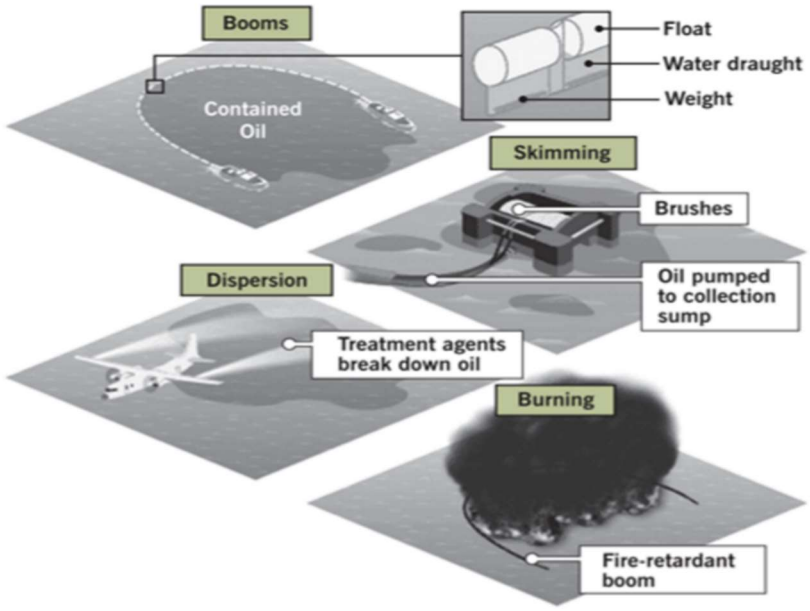

Figure 1-3. Current techniques in oil spill response.[8]

These traditional remediation methods have been used for years to treat oil spillage, but they are cost-inefficient both in terms of labor and equipment. The United States Coast Guard reported that only 10 percent of the 2010 BP oil spill in the Gulf of Mexico was removed by skimmer. 42 million gallons of dispersants were used in the Gulf, and the negative impact on the ecosystem is obvious, but it was the fastest way to remove massive amounts of oil from the water surface. With current methods, most of the spilled oils are wasted, becoming pollutants in air and waters. Recovering even small fractions of oil generates a large quantity waste. About 40,000 tons of solid waste and more than 7.7 million gallons of oily liquid waste have been collected in the BP oil spill. They are treated as an industrial waste, so they are only allowed to be buried at specially-designated dumps.[9] Herein, we refer to this as secondary pollution.

Sorbents are the most often used the method to cleanup small scale oil spillage and prevent oil spreading.[10–14] For example, polypropylene sorbent pad (PP pad) has been used for shoreline oil spill area. However, the PP pad is not useful for large oil spills. It is only effective for light oils due to it's low swelling capacity. Also, after oil is absorbed, the PP pad cannot be recycled and must be disposed of in a landfill. Although many sorbent technologies have been studied for recovering the crude oil spillage, they also show limits, such as cost-inefficiency, low absorbing capacity, and low recyclability.[15] To improve these inefficiencies; the research has to be continued to find new material, structure, and functionality of sorbents. The suitable sorbent should recover the spilled crude oil with fast kinetics, high capacity, cost-effective, and without secondary pollution.

1.3 Crude Oils

Crude oil consists of different size hydrocarbons and various organic compounds (tars, wax-like hydrocarbons) and can be converted into petroleum-based fuels (diesel, gasoline, other fuel oils, and gas). Crude oil varies greatly in properties (density, viscosity, and solubility) depending on the geographical location of oil fields (Table 2.1). Crude oil arrives in the United States from many different areas like Texas, Alaska, western Canada or the Middle East and South America by marine tankers.

In this research, we mainly focused on Alaska Northslope (ANS) crude oil which consists of aliphatic hydrocarbons (65-75%) and aromatic hydrocarbons (15-20%), with the molecular size from C_5 to C_{20} and some non-volatile waxes, asphalts, resins, and a few inorganic impurities (Figure 1.4). ANS crude oil tends to mix quickly with water and from 15-20 % of the composition evaporates in the first day of a spill. Furthermore, ANS crude oil forms a stable oil/water mixture up to 60-80% water content, and it changes the physical properties of the oil. The oil/water mixture is densified and the oil changes color from dark brown to light brown during emulsifying. The continued exposure of weathered oil to wave action continues to stretch and tear patches of the mousse into smaller bits, resulting in small patches, and tiny tar balls.

Based on a US National Oceanic and Atmospheric Administration (NOAA) study on the 1989 *Exxon Valdez* oil spill in, Alaska, the weathering of ANS spill oil starts as soon as it is exposed to the open environment (wave, the wind, temperature, sunlight, microbes).[16] The more exposed to the elements oil is, the more rapidly it weathers and more difficult it

becomes to be recovered. Thus, it is essential to develop an oil spill recovery strategy that also offers a fast response to prevent weathering of spilled crude oil.

Table 1-1. Various oil-spill sorbent materials.

Name	δ $(cal/cm^3)^{1/2}$
water	23.5
dimethylformamide	12.1
Benzene	9.15
THF	9.3
polystyrene	9.1
toluene	8.9
n-heptane	7.4
crude oil	7.0-10.0[17]

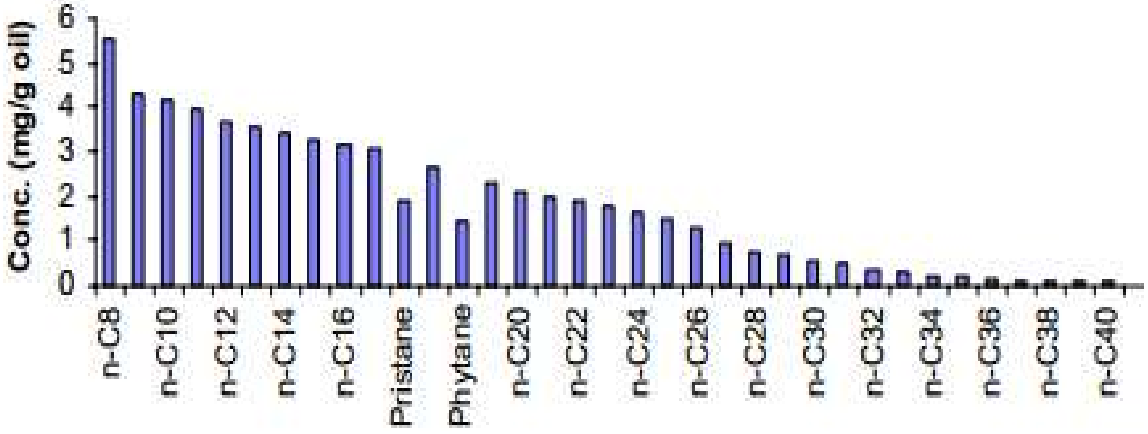

Figure 1-4. The oil composition of ANS crude oil.

1.4 Hydrogels and Petrogels

Hydrogels are hydrophilic polymers that feature three-dimensional (3-D) networks in aqueous solution when they swelled; They are widely used in many commercial applications, including personal hygiene, biomedical, and agrochemical products due to their high affinity for water.[18–21] Most of the hydrogels are formed based on acrylate, methacrylate and cellulose polymers with hydrophilic (polar and ionic) moieties in the side chains.[22–24] Interestingly, some superabsorbent hydrogels (SAPs) can absorb water up to a thousand times their own dry weight.[25] The swelling (absorption) capacity of hydrogel depends on the number of ionic groups in hydrogels. The counterions must remain in the gel for charge neutrality and make a huge osmotic pressure that swells the hydrogel.

Also, the swelling ratio depends on the crosslinking density. However, it is challenging to prepare a completely connected 3-D network with a very low crosslinking density which tends to be soft and floppy in some low Tg rubbery materials. These properties do not allow the preparation of a product with high surface area to enhance absorption kinetics. Theoretically, absorbents with high swelling capacity like hydrogel can be developed after designing oil absorbent with low crosslinking density and high oil affinity. Petrogels are the opposite of Hydrogels. They are hydrophobic hydrocarbon networks and are swollen by hydrocarbon (oil) molecules with high oil absorption capacity (oil-SAP). Our group has designed and investigated a series of the polyolefin based on oil-SAP copolymer networks (Petrogels) that are composed of aliphatic and aromatic side chains that have similar solubility parameters with the hydrocarbon (oil) solutes. These oil-SAP materials are amorphous with lightly crosslinked structure, which showed rapid oil swelling kinetics

with up to 45 times absorption capacity with a crude containing 70% volatile light oils and 30% nonvolatile heavy oils. According to the experimental results, polyolefin based oil-SAP copolymer network has not only high oil absorption capacity but also is applicable to a broad range of organic solvents and refined oil products. However, they are not effective for the complex crude oils with a broad range of chemical compositions and high viscosity, for which they show slow kinetics and low absorption capacity.

1.5 Adsorption and Absorption Mechanisms

A sorbent is a material that recovers liquids through either absorption, or adsorption, or both mechanisms (Figure 1.5). Adsorption occurs only on the surfaces of the substrate with the diffusion of the adsorbate into the interstices by the capillary effect.[27] The adsorption capacity is linearly proportional to the specific surface area of the sorbent.[28] Many adsorbents with high surface areas are used for various sorption (storage) applications, especially for gas molecules.[28–32] However, the weak liquid-substrate interaction at the surfaces usually causes an easy bleeding of the liquid under a slight external force.[33]

Absorption occurs when the absorbate penetrates into the absorbent matrix and expands its volume (swelling).[34–36] When a gas or liquid is absorbed inside the substrate, absorption cannot be reversed by single force which is suitable for long-term liquid or gas storage applications. As expected, the degree of swelling in the matrix determines the absorption capacity (1000X for superabsorbent hydrogels).[37–39] However, except for some superabsorbent hydrogels, volume expansion speed is relatively slow to reach the saturation level in most cases.[40–44] The saturation level is affected by the combination of crosslinking density and the polymer-solvent interaction, as explained by Flory-Rehner.[45–49]

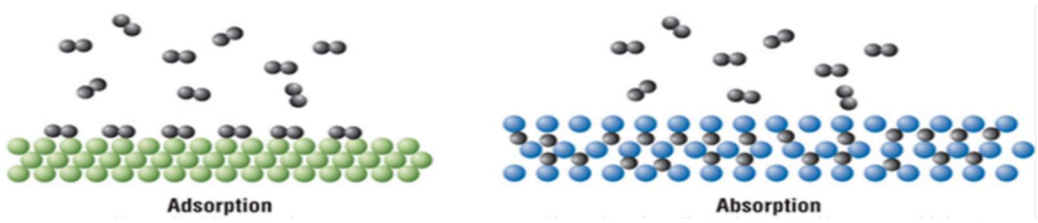

Figure 1-5. Schematic illustration of adsorption (left) and absorption (right) mechanism.

1.6 Synopsis of Research

As will be discussed in Chapter 2, all currently reported hydrocarbon (oil) sorbent materials show a significant shortfall in their performance for oil spill recovery and cleanup. Some of them capture more water than hydrocarbons. A new oil-SAP material is clearly needed, which would exhibit a combination of high sorption capacity and kinetics, oil selectivity (no water), and be cost-effective. Polyolefin represents an important family of hydrophobic/oleophilic polymers; with a broad range of commercial applications due to the combination of tough thermoplastic properties, excellent stability, and low cost. They are downstream petroleum products with naturally good affinity for hydrocarbons, including solvents, refined oil products, and crude oil itself. However, due to chemistry difficulties, there are only a few polyolefin compositions available. In the past three decades, our group has developed several chemical routes, with the combination of single-site metallocene catalysts and selective comonomers and chain transfer agents, to prepare many new polyolefin compositions and structures, including functional and crosslinked polyoelfins. Some of the polyolefin copolymers were also applied to hydrocarbon absorbents (Petrogels) with good absorption capacity for solvents and light oil products. They showed several advantages over the commercial sorbents. However, the low crude oil absorption capacity and slow kinetics were also evident and had hindered the implementation of these materials in crude oil spill cleanup applications. There were some attempts to increase the surface area of the absorbent to facilitate the crude oil diffusion into the polyolefin network. However, the experiment was not successful due to the

instability of the porous morphology in a soft hydrocarbon network with low crosslinking density.[50,51]

In this thesis, I will discuss how we overcame the problems (bleeding, low capacity, poor oil/water selectivity and low recycability) by developing a new polyolefin-based interpenetrating polymer network (IPN) that is composed of a semi-crystalline LLDPE thermoplastic and an amoprhous crosslinked 1-decene/divinylbenzene (x-D/DVB) elastomer, called i-Petrogel. IPN refers to two polymer networks in which different morphology coexist, and having a network that is homogeneous. The combination of rigid and soft polyolefin chains with the IPN structure allows the formation of porous morphology and eases crude oil penetration into the polymer matrix, which increases the crude oil absorption capacity and kinetics. This new i-Petrogel material can effectively transform a marine oil spill into a floating solid (oil swelled gel), ready for collection (recovery by skimmer and transported by pumping). The recovered material is suitable for refining as a regular crude oil (no disposal issues and no waste in natural resources). Specifically, Chapter 3 will summarize a systematic study on individual semi-crystalline polyolefin thermoplastics and amorphous cross-linked polyolefin elastomers to understand their structure-property relationships with various hydrocarbon liquids, including solvents (hexane, cyclohexane, and toluene), refined oil products (gasoline, diesel, and petroleum oil) and Alaska North Slope (ANS) crude oil. Chapter 4 will explain the experimental results and the molecular design that lead to the discovery of i-Petrogel with the most suitable composition. Once the i-Petrogel absorbent was validated on the laboratory scale, a scale-up study was performed with the target of developing a commercial process that can be used in large-scale production. Chapter 5 explains the experimental details to scale

up i-Petrogel material with consistently high quality. This chapter will also include the operational testing results conducted by Department of the Interior (DOI), Bureau of Safety and Environmental Enforcement (BSEE) at the Ohmsett (government-owned) facility. The last Chapter will provide some comments and suggestions for future research.

Chapter 2

Current Oil Sorbent Materials

2.1 Introduction

As previously discussed, crude oil spill in the sea is of continuing concern due to the long-term impacts to the marine environment.[52–55] The currently-used remediation methods (booms and skimmers, dispersants, and *in situ* burning) to combat the oil spill are not effective. Especially, dispersants create tar balls into ocean which are more harmful to food chain than crude oil itself. These concerns have prompted the desire to investigate some more efficient remediation technologies that can directly remove oil from water.[63–69] Currently, sorbents are mostly used to recover (also prevent) oil spillage on the shoreline areas or the small oil spills in different manufacturing and service facilities.[63] Due to economic and environmental reasons, many research activities are focused on natural sorption materials, such as various porous inorganic materials and biodegradable organic products. However, most of them are hydrophilic in nature and only show limited oil sorption capacity and also absorb water, thus making the recovered solids unsuitable for calcinations; most of them end up in the landfills, causing secondary pollution.

Polymers are the primary materials used to make commercial sorbents.[72–74] It is relatively easy to produce the porous structure with high surface area that is necessary to enhance the oil adsorption kinetics and capacity.[67] A broad range of modified and synthetic polymers have also been investigated involving both sorption mechanisms, including adsorption (surface sorption) mechanism and absorption (matrix sorption/swelling)

mechanism. The most attractive property of polymeric sorbents is their diversity in forming various structures and surfaces. It has been shown that by adjusting these parameters (details discussed in the following sections), can enhance oil sorption performance. Furthermore, the synthetic polymers represent the reliable, scalable, and low to moderate cost resources, which is an important consideration for dealing with the massive scale of oil spill cleanup application.[68]

Figure 2-1. Commercial sorbents including polypropylene pads, paper waste booms.

Fiber-based polypropylene (PP) pads (made from meltblown PP fibers) are one of the most used polymeric sorbents (Figure 2.1), which are based on the adsorption mechanism. The PP pad selectively adsorbs oil (no water) in their interstices via capillary action. However, for large-scale crude oil spilled on the distant ocean, the PP pad shows some shortfalls. It only exhibits a relatively low crude oil adsorption capacity (<10g/g) and is expensive for large-scale application. In addition, due to the weak oil-substrate interaction (adsorption mechanism), the fiber-based absorbers exhibit many disadvantages, including failure to maintain oil of low viscosity and easy re-bleeding of adsorbed oil under a slight external force. Once the PP pad adsorbs oil it causes another environmental concern due to the fact oil can not squeeze out or separate from the pad hence it must be disposed of in a landfill.[69]

Polymer absorbent provides enough swelling space to overcome the adsorption drawback with high sorption capacity and the retention of absorbed liquid. To prevent the dissolution of the polymer in oil or hydrocarbon solvents, it is necessary to form a crosslinked network structure. Some reports are disclosing the usage of hydrophobic alkyl acrylate oil absorbents, such as cross-linked styrene/acrylate, 1-octene/acrylate, and octadecene/maleic anhydride copolymers.[41,70,71] However, these resins contain some hydrophilic polar groups and require an additional procedure for cross-linking reaction after copolymerization. Also, this method has the drawback of a long absorbing time, especially for aliphatic hydrocarbon components. Some synthesized rubbers, such as polybutadiene, butyl rubber, SBR, and EPDM, were modified (grafting and cross-linking) to achieve the network structure for oil absorption.[38,72,73] However, the solution cross-linking is hardly controlled due to the combination of broad molecular weight distribution and composition distribution in the polymer and some side reactions; they usually require extensive solvent extraction to remove the soluble fraction. The resulting sol-free materials possess various degrees of cross-linking density, reducing the overall oil swelling capability. Some methods, (i.e. milling, electrospinning, and foaming of the oil absorbents) to increase specific surface area,[74–76] have also been applied to improve oil absorption kinetics.

Recently, several papers[74,75] applied the high surface area materials, including nanowire membranes, nanocellulose aerogels, and carbon nanotube aerogels, to increase oil adsorption capacity. However, the treatment of the recovered solid absorbents is always a major concern, including waste disposal, recyclability, biodegradability, and cost. Overall, it is still a major scientific challenge to develop a suitable oil-superabsorbent polymeric (oil-SAP) material that can offer a comprehensive solution for combating future oil spills.

This chapter reviews the major advances in designing sorbent materials with both adsorption and absorption mechanisms. The discussion focuses on the research approaches that can improve oil recovery performance. After a brief review of the general adsorption behaviors of natural sorbent materials, I will concentrate on the synthetic polymer adsorbents that are usually in the form of foams and fibers. They exhibit high specific surface area and fast liquid (adsorbate) diffusion kinetics. Some experimental results explain the effect of a porous morphology on the oil/water selectivity and overall oil adsorption capacity and kinetics. In the next section, I will discuss surface modification and wettability of adsorbents to improve their hydrophobicity and oleophilicity for enhancing oil/water adsorption selectivity and overall capacity. Lastly, the discussion will move to the hydrocarbon polymers with absorption mechanism, especially polyolefins that are downstream petroleum products with good affinity for oil (hydrocarbon) molecules. In this absorption mechanism, the oil/water selectivity is usually excellent. However, the oil absorption performance is controlled by a combination of polymer swelling ability and the diffusion rate of specific oil molecules.

2.2 Natural Sorbents

Natural sorbents can be categorized into two major classes: inorganic mineral products and organic vegetable products. Mineral products, including perlite, vermiculites, and sorbent clay, do not show adequate buoyancy retention and exhibit low oil sorption capacity. Except for low cost, they are not considered as candidates for remediating large scale oil spills. On the other hand, some organic vegetable products, such as cotton fibers, flax, and kapok, are widely used for shoreline oil spill remediation due to the sorbents being non-toxic and can be easily handled by people.[79–83] However, most of these natural sorbents have low oil/water selectivity.[83] Thus, overall oil adsorption capacity is relatively lower than oleophilic polymeric sorbents and these create a problem for disposing of the recovered oil sorbent wastes.

Previous studies have demonstrated that oil/water selectivity of the natural sorbent can be enhanced by surface modification.[85] Wang et al., demonstrated a kapok fiber with further enhanced hydrophobicity and oleophilicity by incorporating silica nanoparticles with many long alkyl chains on the surface of kapok fiber, which involves the application of the hydrolyzed dodecyltrimethoxysilane (DTMS) (Figure 2.2a). Removal of the plant wax of the kapok fiber is the key step to incorporate the nanoparticles that reveals the hydrophobic effect on the surface of kapok fiber. In addition, the treated surface becomes rough and improves the surface area of the kapok fiber (Figure 2.2b). Consequently, the treated surface has low surface energy which increases its oil affinity (Figure 2.2c). The sorption capacity of treated kapok fiber is about 46.9 g/g for diesel and 58.8 g/g for soybean oil. These results suggest that the treatment of natural sorbents with silica nanoparticles are

an effective way to improve the oil/water selectivity and oil absorption capacity. However, this study did not discuss the sorption performance of crude oil and the issues associated with the adsorption mechanism and natural products discussed in the previous section. Natural sorbents are not suitable for large oil spillage such as the BP oil spill because natural absorbents are not readilty availble in large quantities (needs more than 44 million kilograms base on 10 times oil adsorption capacity to remove 110 million gallons on spilled oil).

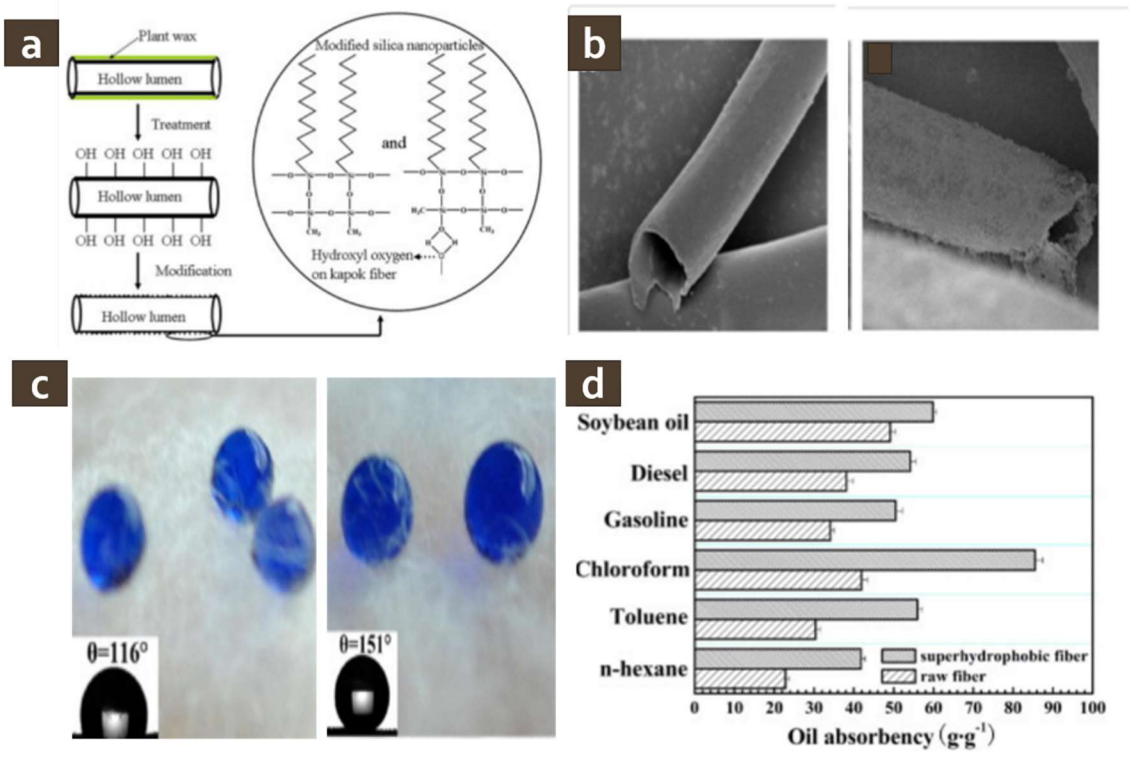

Figure 2-2. (a) Schematic image of surface treatment of kapok fiber. (b) SEM image of raw (left) and coated (right) kapok fiber. (c) Image of a water droplet on the surface treated kapok fiber surface. (d) Oil sorption capacities of raw and treated kapok fiber with various oils.[86]

2.3 Polymeric Adsorbents with Porous Morphology

Polymeric adsorbents with a porous morphology have been intensely studied over the last decades for oil cleanup due to their high specific surface areas, fast kinetics, and moderate prices.[85,86] Polymer foam adsorbents provide some advantages; easily scalable fabrication, light weight, fast kinetics, and simple operation procedure comparing to many other oil cleanup methods.[88–90] In early 1971, Pier et al. [92] performed oil sorption tests with twenty different types of sorbent materials, including cellulose fiber, polystyrene (PS), polypropylene (PP), and polyurethane (PU) foams. When using PU foam for Bunker C oil (high viscosity fuel oil) sorption, the result showed highest oil sorption capacity (79 g/g). However, the results also revealed that the water sorption capacity (80.0 g/g) was also high, which reduces the oil sorption capacity of PU foam in removing the spilled oil on the water surface (poor oil/water selectivity).

Recently, Peng et al.,[93] fabricated a hydrophobic PU sponge that was modified by hydrolysis and polymerization of trimethylchlorosilane (TMCS)/tetracthoxysilane (TEOS) to improve hydrophobicity (Figure 2.3a). It was demonstrated that the as-prepared polyurethane sponge shows random roughness and spherical particles on the surface (Figure 2.3b,c). This spherical particle increased the surface roughness and anchored the hydrophobic group (-CH_3) onto the porous structure of the PU sponge which is essential for the selectivity of the water and oil. In addition, this hydrophobic PU foam can be reused for many cycles (Figure 2.2d) However; the PU sponge still had some interspaces after the oil adsorption; hence water diffused into the remaining space (Figure 2.3e). This result indicates that the water diffusion cannot be fully prevented by controlling the surface of

the skeleton of the porous structure. Thus, porous types of adsorbent is not the best option to enhance high oil/water selectivity and overall adsorption capacity.

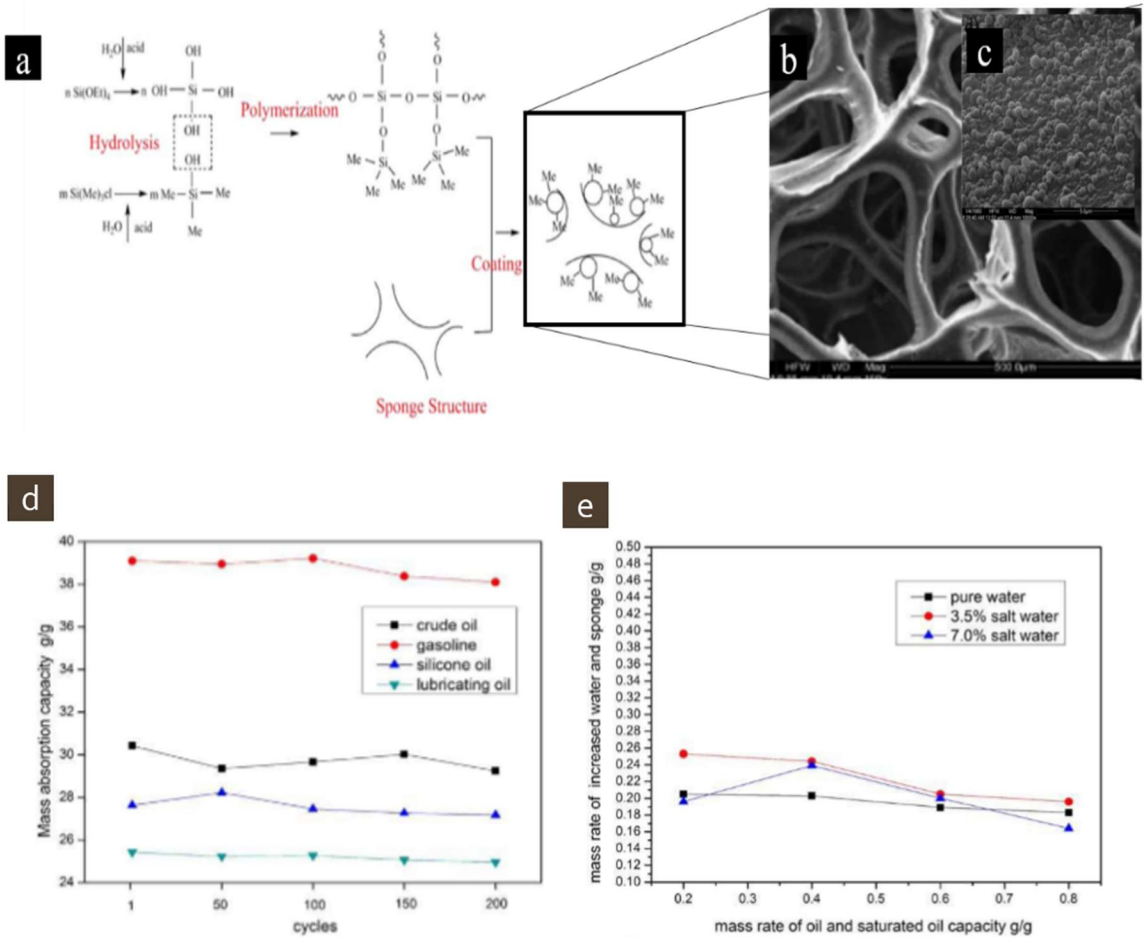

Figure 2-3. (a) Polymerization process of TEOS modified PU sponge with a hydrolysis process. SEM images of modified PU sponge at (b) 500µm and (c) 5 µm. (d) Oil adsorption capacity of coated PU sponge with four different types of oil (e) Water adsorption capacity of PU sponge under different water types.[93]

Designing a pore structure of porous adsorbents is important for oil cleanup performance.[94,95] Interestingly, Zhao et al.,[96] directly fabricated poly(dimethylsiloxane (PDMS) sponges with porous morphology and hydrophobic surfaces by a simple fabrication method using NaCl microparticles as the pore templates during the thermal curing of silicone elastomer (Sylgard® 184A) with the thermal curing agent (Sylgard® 184B) (Figure 2.4a). The silicone elastomer and curing agent were diluted with a different amount of dimethicone (silicone oil), then mixed with NaCl particles. Dimethicone was used to dilute the silicone elastomer and the curing agent, which tune the density of the silicone elastomer sponge. The dimethicone and NaCl micro particles was washing out with ethanol and warm (40 °C) water, a relatively uniform porous morphology is formed in the silicone elastomer network. This porous network morphology can be controlled by the NaCl particles (65-297 μm) and the silicone oil quantity , which then influences the oil absorption capacity and mechanical properties. The oil absorption capacity decreases evidently with decreasing the size of NaCl micro particle. The oil sorption capacity of the sponge reached a maximum when the size of the particle was 150-297 μm. The oil adsorbency of the sponge was higher than 17g/g for dichloromethane when at the composition between of silicone elastomer / silicone oil was 3:7. However, over 80 % of silicone oil content shows only 5g/g for dichloromethane. As-prepared sample shows high oil/water selectivity (Figure 2.4b). However, the oil sorption capacity of the sponge is dependent on the oil types. A representative sample adsorbs only 5g/g for diesel comparing to the adsorption capacity for chloroform (21 g/g) (Figure 2.4c).

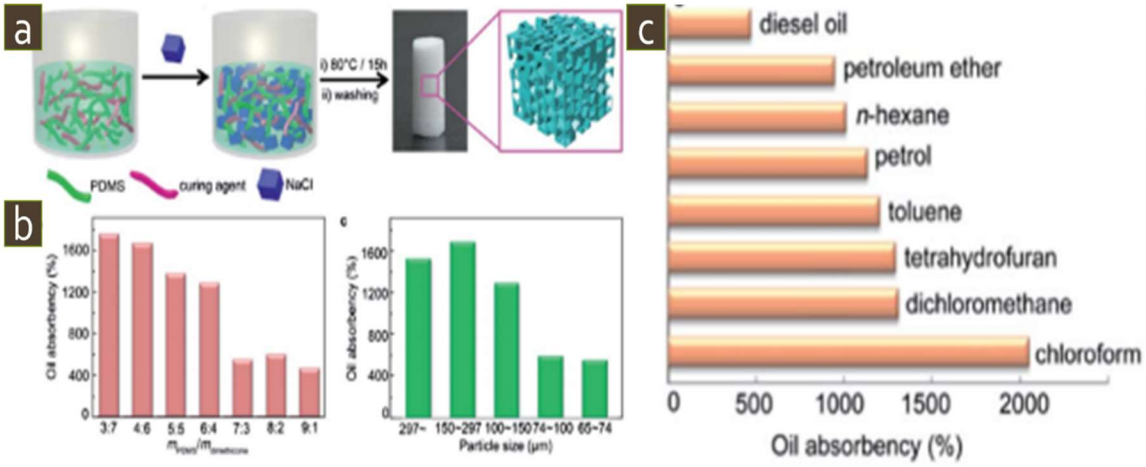

Figure 2-4. (a) Schematic image of preparing porous PDMS sorbent with NaCl microparticles and photo image of PDMS sorbent. (b) Oil absorbency of PDMS sponge with different composition and NaCl particle size. (c) Swelling capacity for various solvents with a representative PDMS sorbent.

Overall, various porous polymer sorbents have been successfully fabricated and investigated for removing oils. Most of them are based on the adsorption mechanism with oil molecules adsorbed on the surfaces of pores, and some water molecules can also be captured inside the void space. The similar situation also happens in the fiber form with both oil and water presented in the intersticial areas. In general, the porous structure that improves permeability for high viscous oil also leads to a decrease in oil/water selectivity.[97,98] This delicate tradeoff between permeability and selectivity makes it challenging to develop an effective adsorbent material.[99] Also, the oil removal efficiency is strongly dependent on the viscosity of the oil. In many cases, high viscosity oil can clog the pores located near the surfaces and stop (at least significantly slow down) the entire liquid diffusion process. The resulting oil/water/polymer mixed adducts are diffuicult to be recycled and reused. It remains a scientific challenge to take advantages of the porous structure in polymer sorbents for oil spill recovery in water. The ideal polymer material should exhibit a combination of high specific surface area, high oil/water selectivity, high oil sorption capacity and kinetics for a broad range of oil species (including crude oil), excellent recyclability, and be cost effective.[100–103]

2.4 Surface Modification and Wettability

As discussed, some natural sorbents with high porosity and surface area are effective in collecting oil. Despite their many advantages including abundance, biodegradability, and low cost, it is not efficient for removal of large volumes of spilled oil in water due to poor oil/water selectivity. Also, after the oil/water mixture adsorbed, it also creates a significant amount of oily solid wastes. Thus, some significant effort has been devoted to improving the oil/water selectivity by controlling the surface wettability. This approach can be applied to a broad range of existing natural materials and polymeric adsorbents (foams and fibers).

Surface modification or wettability is a key property of materials that plays important roles in many commercial products. Several chemical routes have been employed to modify various adsorbent surfaces to enhance their hydrophobic properties to improve oil/water selectivity. Both roughness and surface hydrophobicity affect oil (hydrocarbon) wettability. One common approach involves grafting or deposition of fluorine, silicone or hydrocarbon chain containing polymers onto the original adsorbent surfaces (Figure 2.5).[104,105] Both covalent bonding and hydrogen bonding to attach the desired polymer on the adsorbent surface can improve the hydrophobicity of sorbent and the oil/water selectivity.

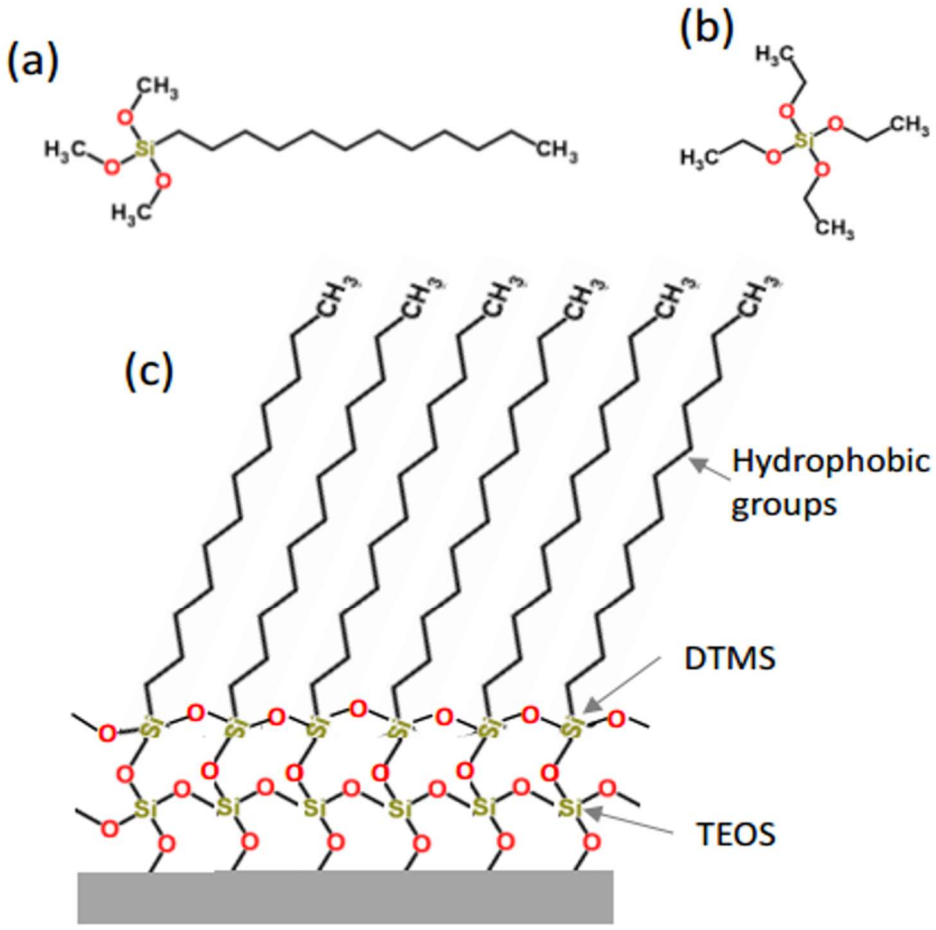

Figure 2-5. (a) Chemical structure of dodecyl(trimethoxy)silane (DTMS), (b) Triethoxysilane, and (c) Sol-gel films formed on the surface of sorbent.

Zhu et al.[106] reported a simple way to prepared hydrophobic and oleophilic polyurethane sponge through solution-immersion processes (Figure 2.6b). Oils are simply removed from the water and collected by the mechanical squeezing process (Figure 2.6a). The original sponge was modified with nanoparticles of copper-$C_{11}H_{23}COOAg$. The morphology of the pristine PU sponge has a smooth surface while as-prepared PU sponge has roughness due to coating different size nanoparticles (from 100 to 200 nm). The hydrophobicity of coated PU sponge can be affected by the presence of $C_{11}H_{23}COOAg$ and it was confirmed by high water contact angle (170°) of as-prepared PU sponge. These features can be applied to enhance high oil/water selectivity. As expected, as-prepared PU sponge showed no water adsorption and this kind of PU sponge might be a good adsorbent for oil/water separation. However, the oil absorption capacity for lubricating oil is only up to 18 times their own weight, which is relatively lower than another natural adsorbent (cotton fibers, about 30.3g/g).[107]

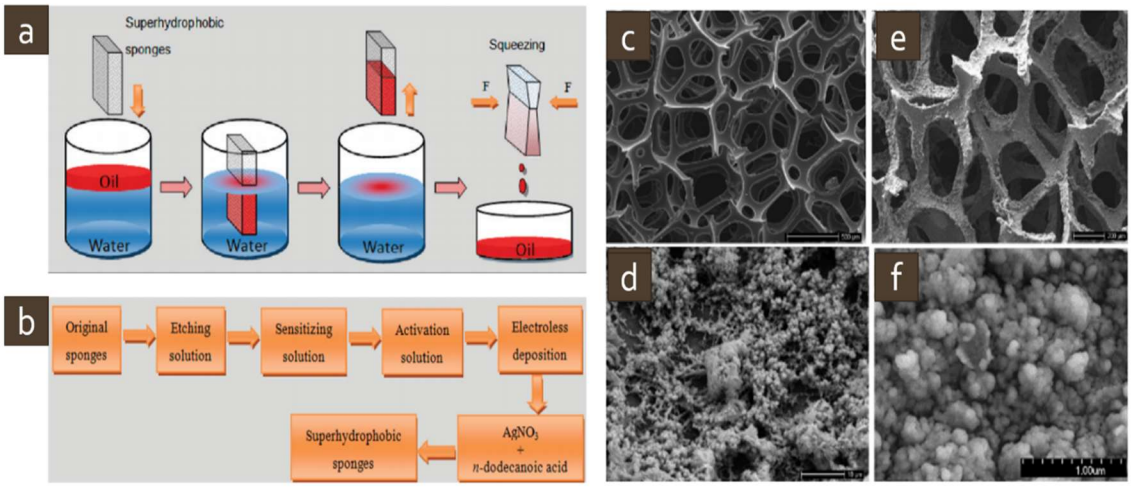

Figure 2-6. (a) Schematic image of oil removal by a hydrophobic PU sponge. (c) Preparation procedure of hydrophobic PU sponge (c) SEM images of original PU sponge (d) and high-magnification SEM images (x2,000) (e) SEM images of coated PU sponge and (f) high-magnification SEM images (x 40,000)

Li et al.[108] studied a graphene coated PU sponge to enhance high oil/water selectivity. The original PU sponge (Figure 2.7b, yellow color) was coated with ɣ-methacryloxypropyl trimethoxy silane (KH-570, Figure 2.7a) and modified graphene (GN) (Figure 2.7b, black color). The methoxy group of KH-570 help to combine with the carboxylic and hydroxyl groups of graphene oxide. The SEM image of the surface of KH-GN PU proves the existence of the coating on the skeleton of the sponge, and also shows the pores (200-400 μm) (Figure 2.7c). The as-prepared KH-GN PU sponge shows high hydrophobicity (contact angle=161°) comparing to the contact angle of original PU sponge (96.9°). Interestingly, the adsorption capacity of the PU sponge also increased with contact angle. The KH-GN PU foam shows 34 g/g for soybean oil while the original PU shows only 10 g/g. Hence, after the modification of the PU sponge with GN, the sponge became more oleophilic. Interestingly, the reusability of the as-prepared PU sponge for diesel was not decreased. This result indicated the good adhesion between the PU skeleton and the KH-GN sheet maintains high oil adsorption performance (Figure 2.7d). However, the desorption test showed some oils remain in the sponge, and it had little effect on the total adsorption capacity. Overall, this research showed how the surface hydrophobicity is important to enhance oil absorption capacity. However, the process of graphene coating process is complex, and the results contain no data on the sorption of heavy crude oils.

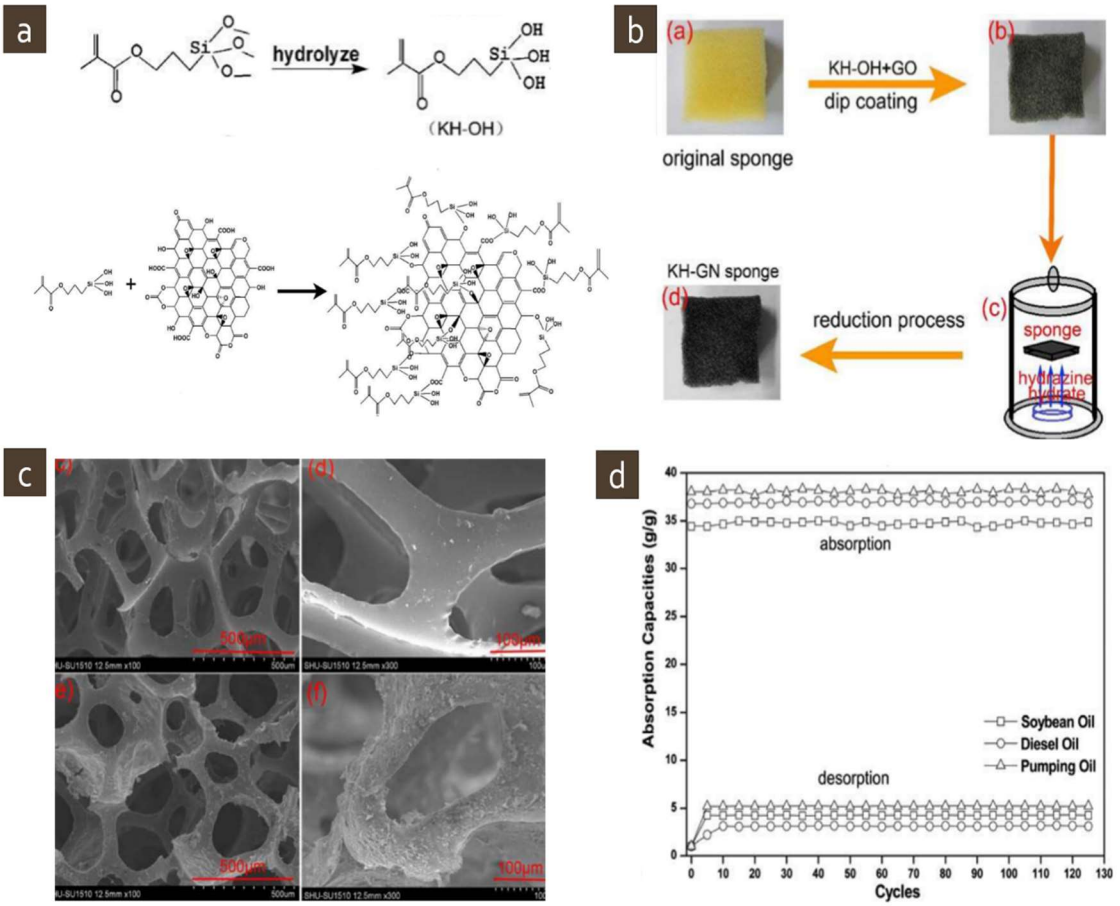

Figure 2-7. (a) The chemical structure of KH-570 (left) and after hydrolyzed (right) (b) Photo and schematic illustrations of the KH-GN sponge. (c) FE-SEM image of (top) original PU sponge and of (bottom) KH-GN PU sponge. (d) adsorption and desorption capacities of the KH-GN PU sponge with different types of oils.

Several other surface modification methods have also been applied to various adsorbents, most of them are hydrophilic in nature, to increase their surface hydrophobicity and enhance their oil/water selectivity. Despite the advantages of already-available porous substrates and relatively simple coating processes, this surface modification method still faces several inherent limitations in the adsorbents, including the limitation to light hydrocarbon molecules, some trapped water molecules in the void space, and the environmental concern in the final disposal of solid wastes. The performance of adsorbents strongly depends on the oil properties, such as viscosity and the composition of oil molecules. In the presence of highly viscous or/and weathered crude oil, it is difficult to prevent clogging the pores in adsorbents. Overall, it is still challenging to develop the adsorbent for large-scale crude oil spill recovery.

2.5 Hydrocarbon Polymer Absorbents

It is logical to use pure hydrocarbon polymers for oil (hydrocarbons) sorption applications. In addition to the hydrophobic surface, with similar solubility parameter, the oil can diffuse into the hydrophobic polymer matrix with absorption mechanism and expansion of the polymer volume. As expected, the combination can potentially provide excellent oil/water selectivity and high oil absorption capacity. However, it is also relatively slow kinetics to reach the saturation level in most cases. In other words, the oil absorption performance (capacity and kinetics) of the hydrocarbon polymers are very dependent on the polymer structure, including crystallinity, branch length, polymer molecular weight and molecular weight distribution, and crosslinking density.[109–112] The semi-crystalline polymer is usually not the favorable choice for absorbent material due to its low swelling. On the other hand, when an amorphous hydrocarbon polymer is exposed to a good solvent with a low interaction parameter (<0.5), oil molecules will diffuse into the polymer matrix, which results in the polymer matrix swelling and volume expansion.[113] To prevent the polymer dissolution in the hydrocarbon solution, the polymer chains have to be cross-linked to form a network structure. The absorption capacity is proportional to the swelling ability of the absorbent polymer, which is controlled by a combination of the cross-linking density and the absorbate–substrate χ-interaction parameter, as explained by Flory.[45] The potential advantages of oil/water selectivity and oil absorption capacity motivate the research interest to investigate several hydrocarbon polymers for removing oil from water.[129,130]

Lin et al. fabricated nanoporous structures in the electrospun polystyrene (PS) fibers using the polymers with different molecular weights, various solvents, and solution concentrations.[117] Polystyrene is a widely used material in food packaging and aqueous solution storage due to its high hydrophobic property, which indicates an excellent oil/water selectivity. The electrospinning process is particularly suitable for the production of fibers with high surface areas and controled fiber morphologies. The as-prepared PS fibers exhibit a wrinkled surface using high molecular weight polymer (350,000 g/mol), while the lower molecular weight PS (200,000 g/mol) results in rough surfaces (Figure 2.8a). Interestingly, the surface morphology and specific surface area (SSA) were dramatically changed by THF: DMF mixing ratio. At the 20:80 THF: DMF mix ratio, the specific surface area of the PS fibers shows the highest SSA (37.72 m^2/g) while THF shows only 0.4 m^2/g. This result indicates that SSA can be tuned by changing the solvent compositions. Importantly, the PS fiber exhibits a rapid oil swelling kinetics with the markedly enhanced oil absorption capacities (84 g/g for motor oil within 2hr) (Figure 2.8c). The performance is significantly dependent on the surface area. However, this research contains no information of the polymer dissolution in the oil or any attempt to control the crosslinking density, which is essential for the absorption mechanism.

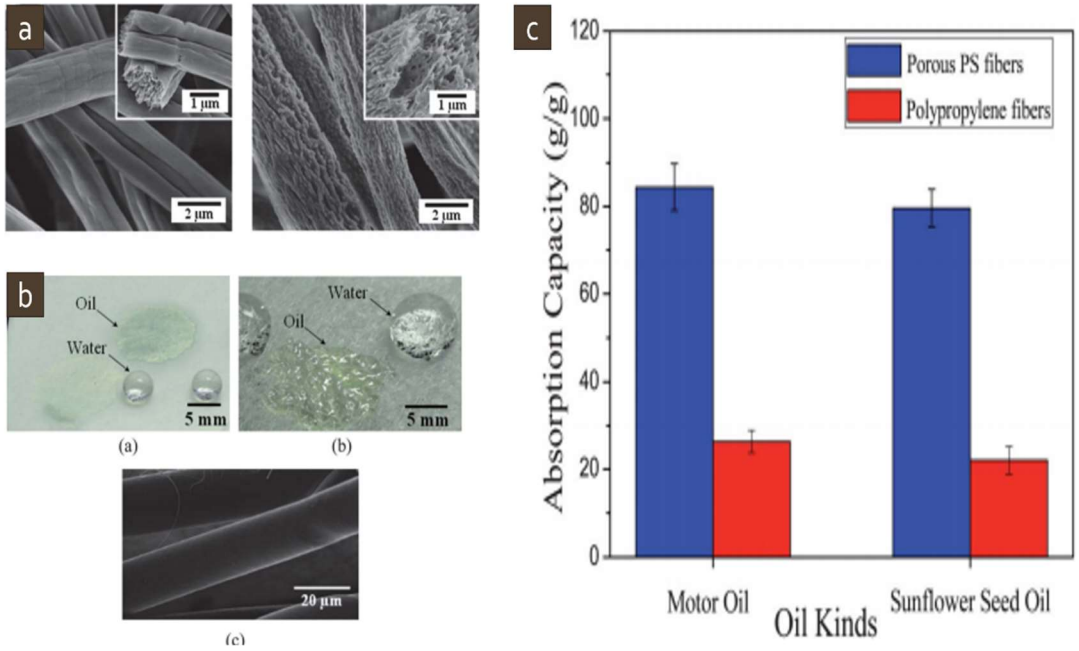

Figure 2-8. (a) FE-SEM image of high molecular weight of (350,000g/mol) PS(left) and low molecular weight (200,000g/mol) of PS fiber. (b) Photo image of water and oil droplet on the as-prepared PS fiber mat (left top) and commercial PP non-woven fabric (right top). SEM image of PP fibers (bottom) (c) Oil absorption capacity of the PS fiber and commercial PP nonwoven fibers for motor and sunflower seed oil.

.

Polyolefin is the most important family of commercial polymers, commonly used in consumer goods and industrial products because of the combination of chemical and physical properties, recyclability, and affordability. They are the petroleum downstream products with the best match in solubility parameters with the crude oils. Wu et al. investigated a complex polyolefin network by copolymerization of 4-tert-butylstyrene (t-BS) and divinylbenzene (DVB) monomers in the presence of ethylene-propylene-diene (EPDM), and studying the effect of the crosslinking density to the swelling behavior and mechanical properties.[118] EPDM is an amorphous low Tg (soft) elastomer, while the t-BS/DVB copolymer is an amorphous high Tg (brittle) plastic. Both EPDM and t-BS/DVB copolymer are crosslinkable by themselves under free radical condition. In addition, some grafting reaction between two polymer chains is also expected to form a very complex network structure. Both polymer chains are hydrophobic and oleophilic with good oil/water selectivity. However, the oil absorption capacity is very dependent on the network composition and crosslinking density (Figure 2.9a). The absorption (swelling) capacity reaches to a maximum of 34g/g with chloroform in the network containing 60 wt% of EPDM and 3 wt% of DVB crosslinker units. Furthermore, the results showed that increases of DVB crosslinker units reduce the oil absorption capacity (Figure 2.9b) because high content of DVB shortens the chain length between crosslinks, which reduces the oil swelling capability. The stress-strain relationship for the crosslinked polymer shows that the t-BS content largely affects the mechanical properties (Figure 2.9c). Unfortunately, this paper only reported the absorption capacity for organic solvents and low molecular weight fuel oil.

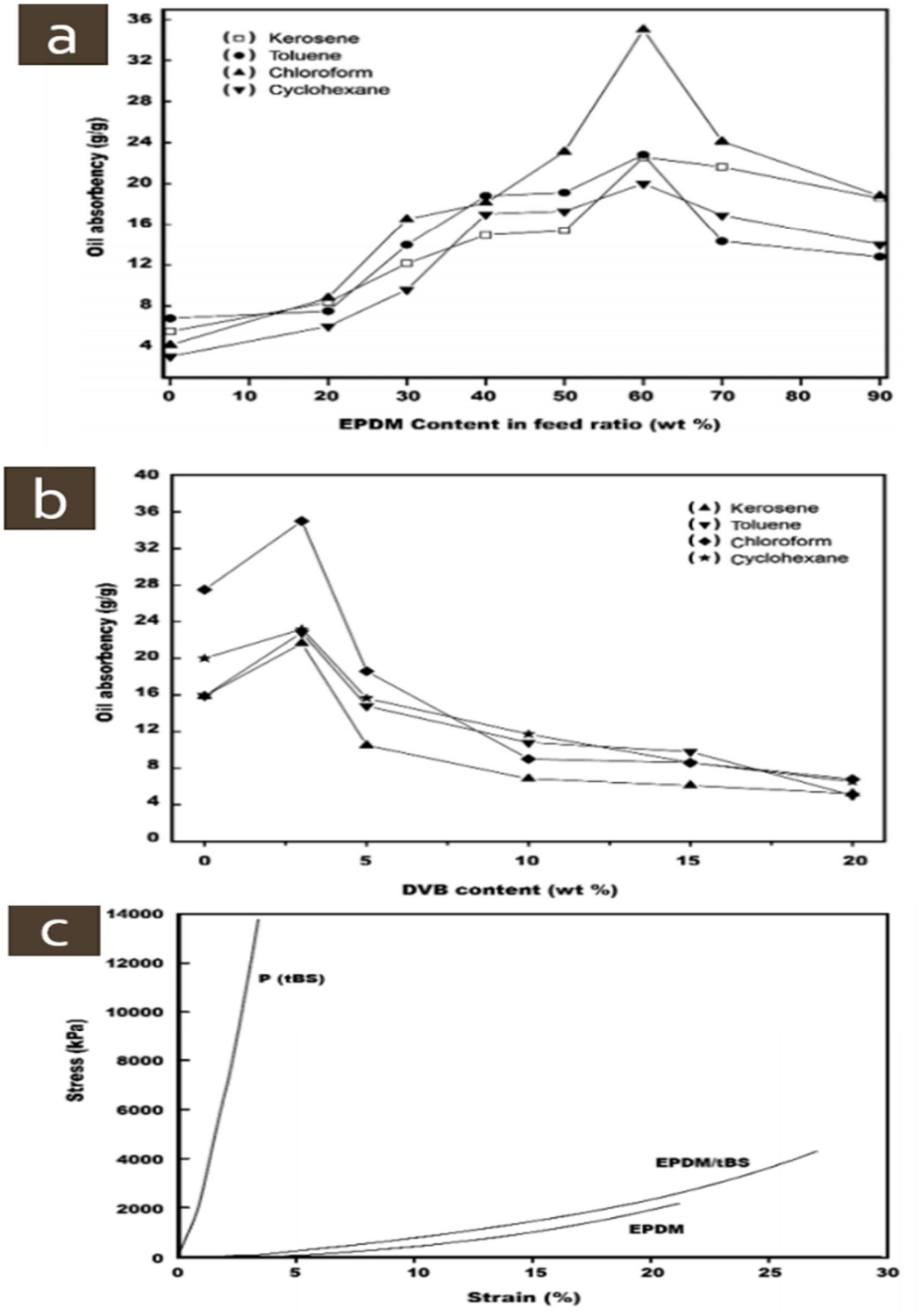

Figure 2-9. Oil absorption capacity of the network structures having (a) various EPDM contents and (b) different DVB concentration with four different solvents. (c) strain-stress curves of poly(t-BS), EPDM, and EPDM/poly(t-BS).

Dr. Chung's group, previously developed a lightly crosslinked 1-octene/styrene/DVB (x-OS-DVB) terpolymer network that can remove light oil in water, as shown in Figure 2.10.[51] The aliphatic and aromatic units located along the polymer chains provide the flexibility to match the solubility parameters of various types of hydrocarbon molecules in oil. This amorphous and low Tg (soft) polyolefin network contains the only hydrocarbon in the whole structure, which means the absorbent with high oil/water selectivity is suitable for oil swelling in the polymer matrix. A typical x-OS-DVB sample can effectively absorb light oil from the water surface with a large expansion of its volume (>40 times). Subsequently, the resulting oil-swelled gel floating on the water surface is ready for collection. In addition, the recovered gel can be treated as crude oil, suitable for regular refining processes. The mixtures contain no water and have nearly the same composition as the original crude oil. During refining, the 2–3% of *x*–OS–DVB polymer was thermally decomposed back to $<C_{20}$ hydrocarbons (typically existing in crude oil) without residue.

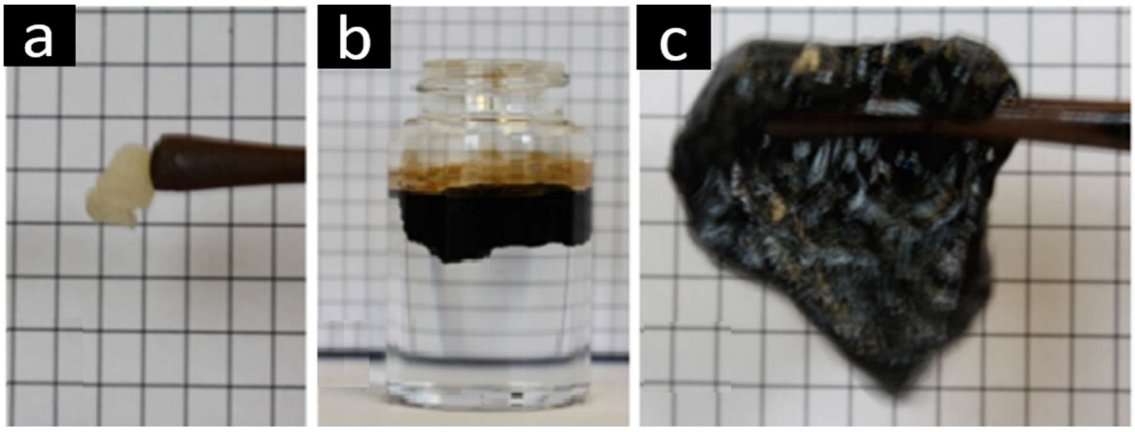

Figure 2-10. Image of oil absorption of (a) 1-octene/styrene/DVB terpolymer. (b)Absorption of toluene (70%)/crude oil (30%) mixture. (c) after swelling 1-octene/styrene/DVB terpolymer with toluene/crude oil mixture.

This x-OS-DVB polyolefin network, with a combination of oleophilic and hydrophobic properties, and amorphous morphology, offers the desirable matrix for hydrocarbon absorption and swelling. The oil uptake is inversely proportional to the cross-linking density. Oil uptake with up to 45 times that of the polymer weight has been observed in a lightly cross-linked *x*–OS–DVB terpolymer. Overall, this new technology exhibits a combination of benefits in oil recovery and cleanup, including (i) high oil absorption capability, (ii) fast kinetics, (iii) easy recovery from the water surface, (iv) no water absorption, (v) no waste in natural resources, and (vi) being cost-effective and economically feasible. However, one major drawback in this x-OS-DVB absorbent is slow absorption kinetics for high molecular weight hydrocarbons with high viscosity and the complex crude oils that contain a whole spectrum of hydrocarbons up to $>C_{30}$. In fact, the absorption of heavy crude oil only occurs at near the surface (only 20 %) of the x-OS-DVB absorbent matrix, and the center portion of the absorbent remained white (without oil absorption), with low overall absorption capacity. Accordingly, there is a continuing need for new absorbent materials that can quickly collect and retain high hydrocarbons, crude oils, and other contaminants. In my research, I intend to develop new polyolefin structure for crude oil cleanup with high absorption capacity and fast kinetics. Furthermore, I introduced interpenetrated polymer network on the absorption to understand structure-property relationship between morphology and oil absorbency.

2.6 Conclusion

The current oil cleanup methods (i.e. booms, oil skimmers, dispersant, and in situ burns) for removing the oil spills are not effective, and most of the spilled oils are wasted, becoming pollutants in our air and waters. The small fractions that are recovered, in fact, generate a large quantity of solid and liquid wastes themselves, from tons of soiled boom and other oily waste. In general, sorbents are most often used in cleaning up oil spillage and prevent oil spreading (Table 2.1). Natural sorbents are hydrophilic in nature and lack of buoyancy, they exhibit low oil sorption capacity. Several surface modification methods have been demonstrated to improve the buoyancy and oil/water selectivity with limited success. Despite the advantages of low cost and biodegradability, natural sorbents are not suitable for large-scale oil spill recovery application. Many research activities have been focused on the polymeric sorbents that are relatively easy to produce in large quantities with tunable material properties. The polymer with the combination of hydrophobicity, porous structure, and high surface area, is desirable for achieving high oil sorption kinetics and capacity.[67] In addition, the ideal sorbent material shall be easily recovered, exhibits good recyclability, and be cost effective.

Table 2-1. Various oil-spill sorbent materials.

Materials	Crude oil (g/g)	10% Crude oil in toluene (g/g)	Toluene (g/g)	Type	Ref.
Recycled tyre rubber	5.49	-	-	Swelling	[76]
cinnamoyloxyethylmethacrylate and isooctyl acrylate copolymers	-	9.29	13.9	Swelling	[68]
polyisobutylene and octadecyl acrylate copolymers	-	32	45.9	Swelling	[69]
Recylced tyre rubber and 4-tert-butylstyrene (tBS)	-	24		Swelling	[77]
crosslinking of butyl rubber (PIB)	-	18.2	20.6	Swelling	[78]
styrene–butadiene rubber (SBR)	38	-	-	pore	[79]
Recycled wool based nonwoven material	25	-	-	fiber	[80]
Docosanyl acrylate (DCA) cinamoyloxy ethyl methacrylate (CEMA) or methyl methacrylate (MMA) monomer	-	35	38.8	swelling	[81]
Poly(dimethylsiloxane) Oil Absorbent with a Three Dimensionally Interconnected Porous Structure	9	-	18.7	pore	[82]
Low micronaire raw cotton	30.5	-		fiber	[83]
Cellulose aerogel from paper waste	20.5	-		fiber	[84]
Polyvinyl-Alcohol Formaldehyde sponge	25.9	-	57.6	pore	[85]
Cabot Thermal Wrap (TW)	16	-		pore	[86]
Herein we report high internal phase emulsion (HIPE) xerogels	15.1	-	22.3	pore	[71]
Butyl rubber	23	-	17.8	fiber	[87]
1,3-oxazolidine modified PU	25.06	-	34.04	pore	[88]
Recycled tire rubber	14.78	-	-	swelling	[89]
the hydrogel of chitosan-based polyacrylamide	2.4	-	-	swelling	[90]

Chapter 3

Absorbents Based on Polyolefin Polymers

3.1 Introduction

A wide range of polymer-based sorbents have been discussed in Chapter 2. The melt blown polyethylene and polypropylene pads and booms are used in small scale spilled oil cleanup. Due to high crystallinity, these PP sorbents primarily exhibit an adsorption mechanism with a limited oil sorption capacity and easy oil bleeding. The cross-linked 1-octene/styrene /divinylbenzene terpolymer (x-OS-DVB, Figure 3.1) shows high absorption capacity with low molecular weight hydrocarbons and refined oil products, reaching nearly 40 times that of their weight.[119] In addition, the combination of selective hydrocarbon absorption (without water) and tough mechanical strength offers buoyancy, stability, and easy recovery on water surfaces. In this chapter, we will focus on a systemati study of polyolefin-based networks, including amorphous elastomers and semi-crystalline thermoplastics, and understanding the effects of polyolefin network structure and morphology and how they are relate to absorption kinetics and capacity.

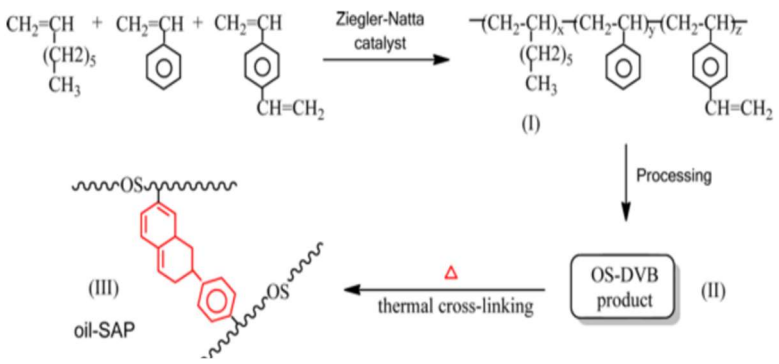

Figure 3-1. Synthesis of crosslinked 1-octene/Styrene/DVB terpolymer.

3.2 Oil Swelling in Polymer Network

During oil absorption in a polymer network, there are two competing forces, including the swelling force caused by the entropy difference between solvent molecules and polyolefin chains and the counter swelling force by the network elasticity. As illustrated in Figure 3.2, the crosslinked polymer chains with a network structure (Figure 3.2a) is expanded (swelled) by oil molecules (Figure 3.2b). The presence of crosslinks affects the swelling capacity and restricts the dissolving of polymer chains into solution. The solubility driving force of the oil molecules with the polymer drags the polymer network to enlargement, but cannot completely spread the polymer chains apart (dissolution) because of the existence of crosslinks. After reaching to the equilibrium state (Figure 3.2c), with two balanced swelling and elasticity forces, the swelled polymer matrix contains a certain amount of oil that is proportional to the degree of swelling.

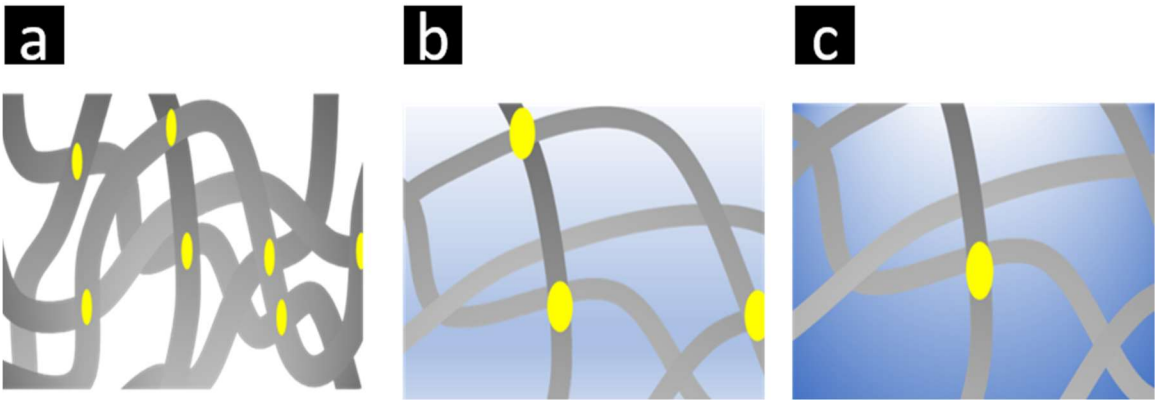

Figure 3-2. Schematic illustration of oil absorption process, including (a) a polymer network with cross-linked polymer chains, (b) the polymer matrix expanded (swelled) by oil molecules, and (c) the fully oil-swelled matrix balanced between elasticity and swelling force

The polymer-solvent interaction parameter χ can be used to explain thermodynamic properties of the polymer in solution. Flory-Huggins proposed the interaction parameter in the lattice model of polymer solutions. The Gibbs free energy change during polymer-solvent mixing can be expressed with the enthalpy (ΔH) and entropy (ΔS) as described in the following relation

$$\Delta G_{mix} = \Delta H_{mix} - T\Delta S_{mix} \quad (3\text{-}1)$$

When mixing with polymer and solvent, the entropy of mixing can be expressed as the following relation

$$\Delta S_{mix} = -k_B(n_1 ln\emptyset_1 + n_2\emptyset_2) \quad (3\text{-}2)$$

Where k_B is the Boltzmann's constant, and $\emptyset_1$ and $\emptyset_2$ are the volume fraction of solvent and polymer, respectively. The volume fractions also can be expressed as the follows relation

$$\emptyset_2 = 1 - \emptyset_1 \frac{w_2\rho_1}{\rho_2 + w_2(\rho_1 - \rho_2)} \quad (3\text{-}3)$$

Where, w_2 is the weight fraction of polymer and ρ_1 and ρ_2 is the density of the solvent and polymer, respectively.

Differentiation of the residual free energy with respect to n_1 yields the residual chemical potential can be expressed in the following relation

$$(\mu_1 - \mu_1^0)^R = (\mu_1 - \mu_1^0) - RT[\ln(1 - \emptyset_2) + \phi_2\left(1 - \frac{1}{x}\right)] \quad (3\text{-}4)$$

where x is the ratio of the molar volume of polymer to that of solvent:

$$x = \frac{\rho_1 M_2}{\rho_2 M_1} \quad (3\text{-}5)$$

M_1 and M_2 are the molecular weight of polymer and solvents.

The interaction parameter χ is defined for this compilation as a reduced residual potential can be expressed in the following relation

$$\chi = \frac{V_0}{kT}(\delta_A - \delta_B)^2 \tag{3-6}$$

As shown in Equation 3-7, the Flory-Rehner equation is used to characterize the polymer network structure with cross-linking density (ρ_c) (Figure 3.3). The calculation is based on the equilibrium swelling network with a suitable solvent, in which the Gibbs free energy of mixing between the solvent and polymer is against the free energy of elastic response from the polymer network. Wherein ν_2 is the volume fraction of the polymer in the solvent, χ_1 is the polymer-solvent interaction parameter, and V_0 is the molar volume of the solvent. Rearranging Equation 3-7 and introducing polymer density (σ_1) give the final expression for the cross-linking density (ρ_c) and molecular weight (M_c) between crosslinks, shown in Equation 3-8.

$$-[\ln(1-\nu_2)+\nu_2+\chi_1\nu_2^2] = V_1\rho_C\left(\nu_2^{1/3}-\frac{\nu_2}{2}\right) \tag{3-7}$$

$$M_c = \frac{-\rho V_s V^{1/3}}{\ln(1-V_r)+V_r+\chi V_r^2} \tag{3-8}$$

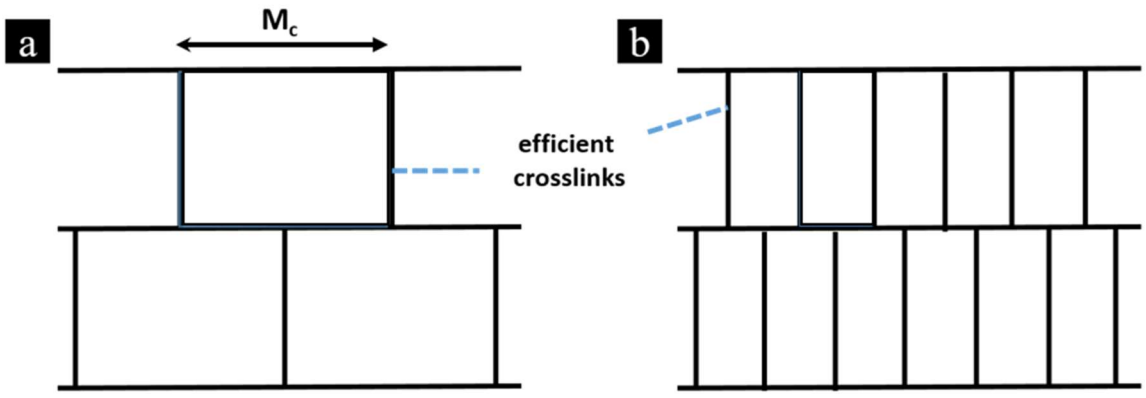

Figure 3-3. (a) Lightly crosslinked polymer, (b) Densely crosslinked polymer.[120]

3.3 Experimental Section

All O_2 and moisture sensitive manipulations were carried out inside an argon filled vacuum atmosphere dry box. 1-decene and DVB were used after distilled to remove the stabilizer and moisture. Toluene was purified with sodium (metal) and used for polymerization. $TiCl_3$.AA, $AlEt_2Cl$, and poly(ethylene-co-1-octene) copolymers (LLDPE in pellet form) with six density grades (Dow Chemical) were used as received. Gasoline and diesel were purchased from a service station of Shell Oil Company. Alaska North Slope (ANS) crude oil was provided by the Bureau of Safety and Environmental Enforcement (BSEE), U.S. Department of the Interior. All ^1H NMR (Bruker AM-300 instrument) spectra were collected on an in chloroform-d at room temperature. The DSC (DSC 4000, Perkin Elmer, USA) used to characterize the thermal properties of the polymers rate of 20 $^{\circ}$C/min under nitrogen.

3.3.1 Preparation of LLDPE Films and Foams

The commercial LLDPE thermoplastics (pellet form) were processed into films and foams. Both compression process and solution casting methods were applied to prepare LLDPE films. The LLDPE compressed film was prepared by compressing LLDPE pellets at 190 °C for 5 min, then cooling to room temperature. In the solution casting process, LLDPE pellets (~5 wt%) were dissolved in toluene solvent under elevated temperature conditions. The homogeneous solution was then cast onto a glass surface. After exposure to air (inside the fume hood) to remove most of the solvent, the polymer film formed was placed in an oven at 70 °C for 24 h. Foams were produced in 316 stainless steel cylinder (50 ml). LLDPE pellets (2 g) were placed in the vessel. Then, the temperature was increased to about 15-20 °C higher than its melting temperature (T_m) and filled with ethane gas at 275 psi. After 1 hour, the vessel was placed in an ice bath (3 °C). The cylinder was then depressurized to atmospheric conditions and cooled to room temperature, and the formed LLDPE was taken out from the cylinder. The resulting porous morphology was stabilized by exposing the resulting foam to air (ambient temperature and pressure). The operation condition can control the foam morphology (cavity size and density).

3.3.2 Synthesis of 1-decene/divinylbenzene (D/DVB) Copolymer

The polymerization reaction was conducted in a 250ml two neck flask. The flask was initially charged with 50 ml of toluene, 10 ml of 1-decene with different concentration of DVB (0.02, 0.2, 0.5, and 1.0 ml) in an argon-filled dry box. The flask was sealed by a stopper then taken out from the dry box and filled with argon gas at room temperature. About 0.1 g of $TiCl_3$(AA) and 1ml of AlCl2Et in 3 ml of toluene were stirred for 20 min then introduced under nitrogen pressure to the reactor to initiate the polymerization. After about 2 h, the termination step was carried out by injecting 100 ml HCl solution (10% diluted in methanol) by syringe into the reactor. The polymer was coagulated and washed completely with methanol and dried under vacuum for about 8 h. About 5.44 g of the D-DVB copolymer was obtained. Its molecular structure was determined by a ^{1}H-NMR spectra. The ^{1}H-NMR spectrum shows the composition of 1-decene/divinylbenzene mole ratio = 97.87/2.38.

3.3.3 Preparation of Crosslinked 1-decene/DVB (x-D/DVB) Network

The resulting D/DVB copolymer was divided into about 1 cm in diameter samples (thickness about 1 cm) and was heated in a furnace at about 220 °C for 2 h to obtain the crosslinked 1-decene/DVB copolymer (x-D/DVB) as shown in Figure 3.4. The x-D/DVB sample was immersed in refluxing toluene for 36 h. After drying at 120 °C in vacuum for 8 h, the insoluble x-D/DVB fraction was weighed to measure the insoluble fraction. The gel content in crosslinked copolymer was determined by dividing the weight of the dried and extracted insoluble x-1-decene/DVB fraction over the weight of the dried D/DVB sample before crosslinking.

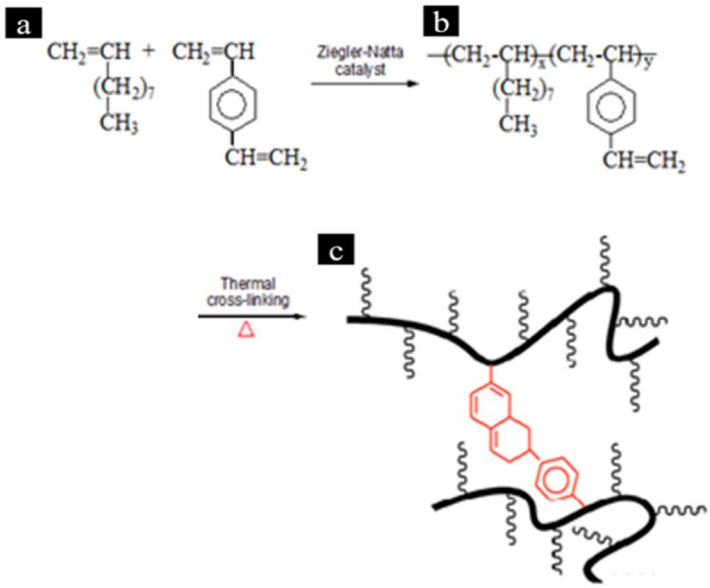

Figure 3-4. Synthesis of 1-decene/DVB copolymer with Z-N catalyst and the subsequent thermal crosslinking reaction to form x-D/DVB network.

3.3.4 Absorption Evaluation

Absorption tests were conducted following the standard method (ASTM F726-06) using various oils. Typically, a piece of polyolefin copolymer with specific weight (W_1) was put into a graduated cylinder. About 100 times the amount of hydrocarbon absorbate was added, then capped with a stopper. After 2 hours at ambient temperature, the free hydrocarbon was poured out of the graduated cylinder and weight (W_2) of absorbed material was determined. Hydrocarbon absorption capacity *(A)* was calculated by the weight ratio between the absorbed oil (W_2-W_1) to the originally unabsorbed material (W_1), using the equation $A(g/g)= (W_2-W_1)/W_1$. In order to study swelling kinetics, the above measurements were carried out from time to time (2 hr and 18 hr).

3.4 Results and Discussion

A systemic study was carried out using a broad range of polyolefin copolymers to understand the effects of the absorbent structure (i.e. composition, morphology, and crosslinking density) on the oil absorption capacity and kinetics. We focused on the two classes of polyolefin materials, including semi-crystalline poly(ethylene-co-1-octene) copolymers (LLDPE thermoplastics) with various melting temperatures and crystallinities and amorphous poly(1-decene-co-divinylbenzene) (D/DVB) copolymers (elastomers). In LLDPE polymers, the partial crystallinity prevents the polymer from dissolving in hydrocarbons. The morphology was further varied by foaming procedures to create the absorbent with various densities, which increases the surface area and shortens the diffusion path.

On the other hand, the integrated DVB units in a set of D/DVB copolymers provide the cross-linking points for the amorphous polymers in forming the network structures. Also, to understand the network structure and the structure-property relationship, the Flory-Rehner theory of swelling was applied to determine the degree of crosslinking and the average molecular weight between two fixed inter-chain links (crystalline domains in LLDPE and cross-linkers in x-D/DVB) in the network structure. The solvent includes pure hydrocarbons (toluene), refined oil products (diesel, and petroleum oil) and ANS crude oil (a complex mixture of hydrocarbons).

3.4.1 Semi-Crystalline LLDPE Copolymers

Semi-crystalline PE and PP polymers with high crystallinity and a high melting temperature are not effective hydrocarbon sorbent materials with the adsorption mechanism. As a result, we chose six poly(ethylene-co-1-octene) random copolymers with low crystallinity and a low melting temperature. These are commercially available LLDPE thermoplastics with narrow molecular weight and composition distributions, prepared by a homogeneous single site constrained geometry complex (CGC) metallocene catalyst.

All received LLDPE polymers were analyzed by ^{1}H-NMR (Figure 3.5a) and DSC (Figure 3.5b) to determine their structure and melting of the semi-crystalline properties. In every ^{1}H NMR spectrum, two chemical shifts at 0.90 and 1.27-1.30 ppm correspond to CH_3 and CH_2 groups, respectively. The peak areas were used to determine the CH_3/CH_2 ratio, and indicated a gradual increase in 1-octene side chain content (Table 3.1). The 1-octene content in the ethylene/1-octene copolymers is in the range of 4.3 to 9.4 mol%. With the systematical increase of 1-octene (side-chain) content, the copolymer systematically reduces its melting temperature and crystallinity. As the 1-octene content increases, the poly(ethylene-co-1-octene) copolymer becomes soluble in hydrocarbon solvents at ambient temperature.

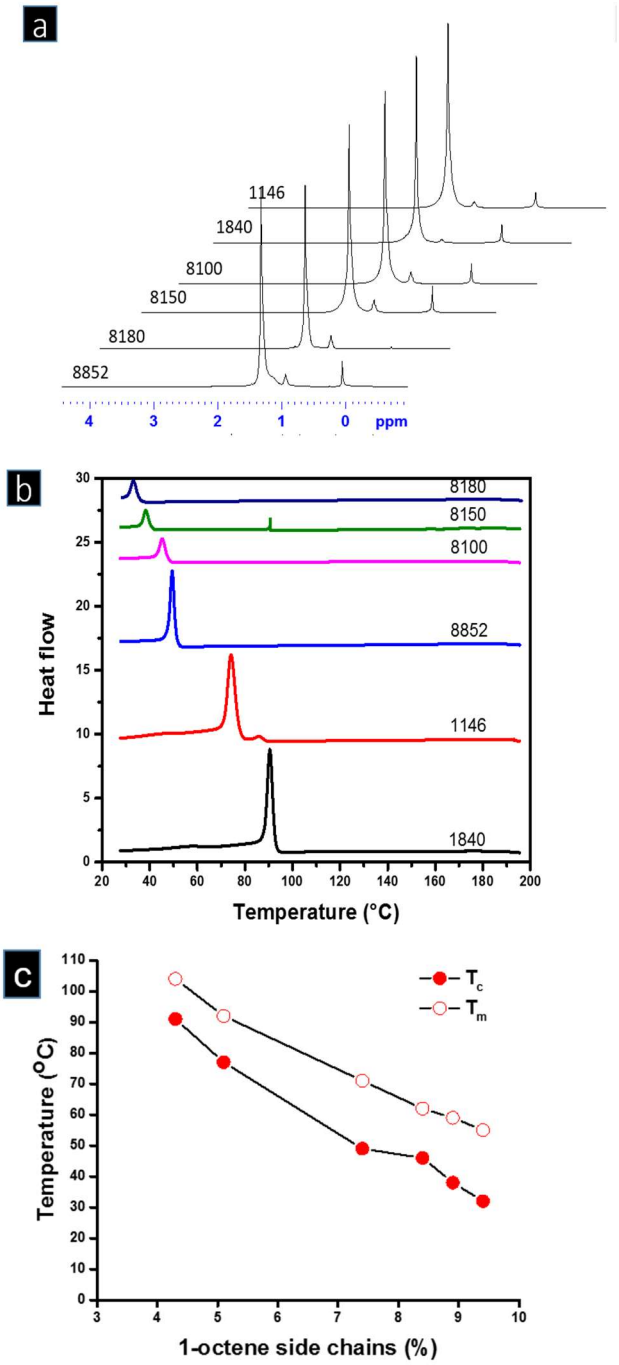

Figure 3-5. (a) ^{1}H NMR and (b) DSC (heating & cooling rate:10 °C/min) spectra of six commercial LLDPE copolymers (c) Tm and Tc as function of 1-octene side chain content.

Table 3-1. Composition and thermal properties of six commercial LLDPE copolymers.

No.	LLDPE samples	Side chain	Density (g/cm^3)	T_m (°C)	T_C (°C)
1	A-1(1840)	4.3%	0.909	104	91
2	A-2(1146)	5.1%	0.897	92	77
3	A-3(8852)	7.4%	0.875	71	49
4	A-4(8100)	8.4%	0.870	62	46
5	A-5(8150)	8.9%	0.868	59	38
6	A-6(8180)	9.4%	0.865	55	32

In addition to the pellet form, these 1-octene/ethylene copolymers were also prepared into films (thickness = 200-300 μm) by solution-casting and melt-compressing processes. They were also converted to foams by a foaming process to reduce further the copolymer density, which not only increases the surface area but also reduces the solvent diffusion tortuous path. Figure 3.6 shows the comparative hydrocarbon absorption kinetics of six different LLDPE pellets (particle size: 4-5 mm) after coming in contact with toluene, diesel, and ANS crude oil for 24 h under ambient condition. Evidently, the absorption capacity of LLDPE pellets with hydrocarbons are relatively small with slow kinetics. In all cases, the absorption capacity of LLDPE pellet consistently shows as inversely proportional to its density and crystallinity. The crystalline domains can not involve the absorption process and lower the overall absorption capacity. The absorption capacity also follows a general trend of toluene > diesel > ANS oil. Flory predicts that smaller molar volume solvent (toluene) have more swelling.

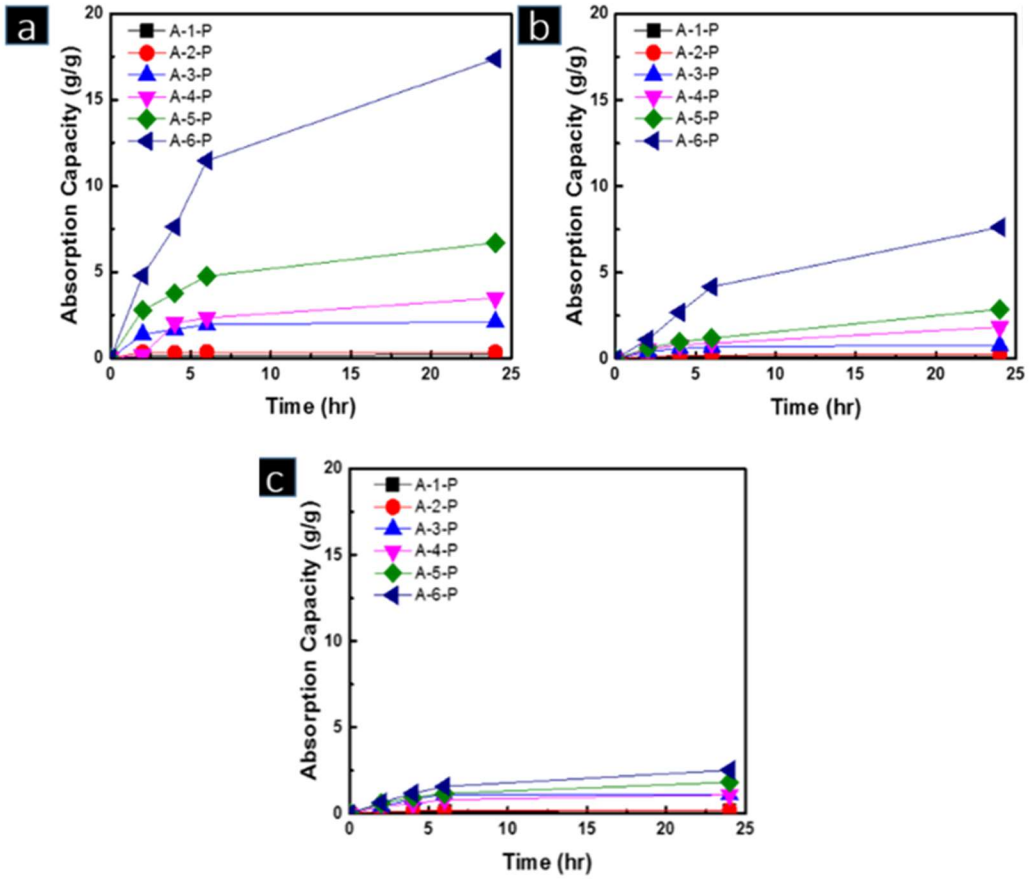

Figure 3-6. Absorption profiles for six ethylene/1-octene copolymer (LLDPE) pellets with (a) Toluene, (b) Diesel, and (c) ANS crude oil.

As we discussed in the previous chapter, crude oil with a complex hydrocarbon mixture is significantly less efficient in all sorption studies. In this case (as shown in Figure 3.6c), all LLDPE copolymers show the absorption capacity < 3 g/g after 24 h. It is worth mentioning that 1-octene comonomer content affects the absorption capacity in the LLDPE copolymer system for various solvents and the refined oil products (Figure 3.6a and 3.6b). The copolymer with less than 9 mol% 1-octene content (T_m >62 °C and crystallinity >20%) absorbs a very small amount of hydrocarbon solvents. The combination of some crystalline domains and dense morphology limits the swelling ability of the polymer, even containing >80% amorphous phase. In contrast, the A-6-P pellet, with the lowest melting temperature and crystallinity, shows a significant hydrocarbon absorption capacity, especially on low molecular weight organic solvents (>17 g/g on toluene). However, its crude oil absorption capacity is relatively low (< 3 g/g).

Overall, the pellet form of LLDPE copolymers is not an effective hydrocarbon absorbents. Although there is limited absorption capacity in this semi-crystalline morphology, these LLDPE copolymers are a good sample set for systematically studying the effect of morphology on absorption performance. It is interesting to consider methods to maximize the absorption kinetics and capacity by shorten the diffusion length and improving the surface area.

The same set of commercial LLDPE polymers were processed into films (A-x-P) with a film thickness in the range of 200-300 μm by high pressure melt-pressing method. Figure 3.7 shows their absorption profiles with ANS crude oil for 24 hours at ambient temperature. Comparing with the results in Figure 3.7c, the new oil absorption profiles show significant improvement, especially for the A-6 LLDPE copolymer with lowest density and crystallinity. The combination of shortened diffusion path length and high free volume in A-6 sample offers fast absorption kinetics and the overall absorption capacity of ANS crude oil is about 11 times of its own weight.

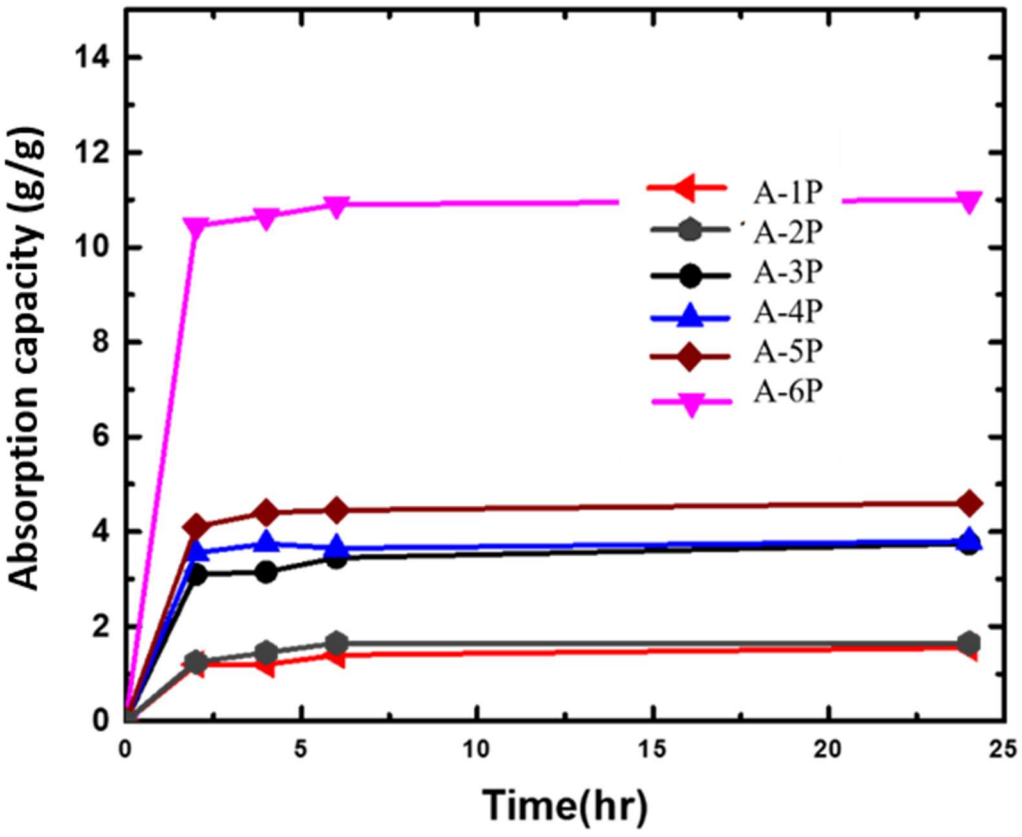

Figure 3-7. Absorption profiles for 6 ethylene/1-octene copolymers pressed films with ANS crude oil.

The same set of commercial LLDPE polymers were also processed into films (A-x-F), with similar film thickness in the range of 200-300 μm, by solution casting method. The solvent evaporation temperature at 20 °C is below the melting temperature of LLDPE copolymers, the formed polymer films shall be less dense than those obtained by the melt-pressing method. Figure 3.8 shows their absorption profiles with toluene, diesel, and ANS crude oil for 24 h at ambient temperature.

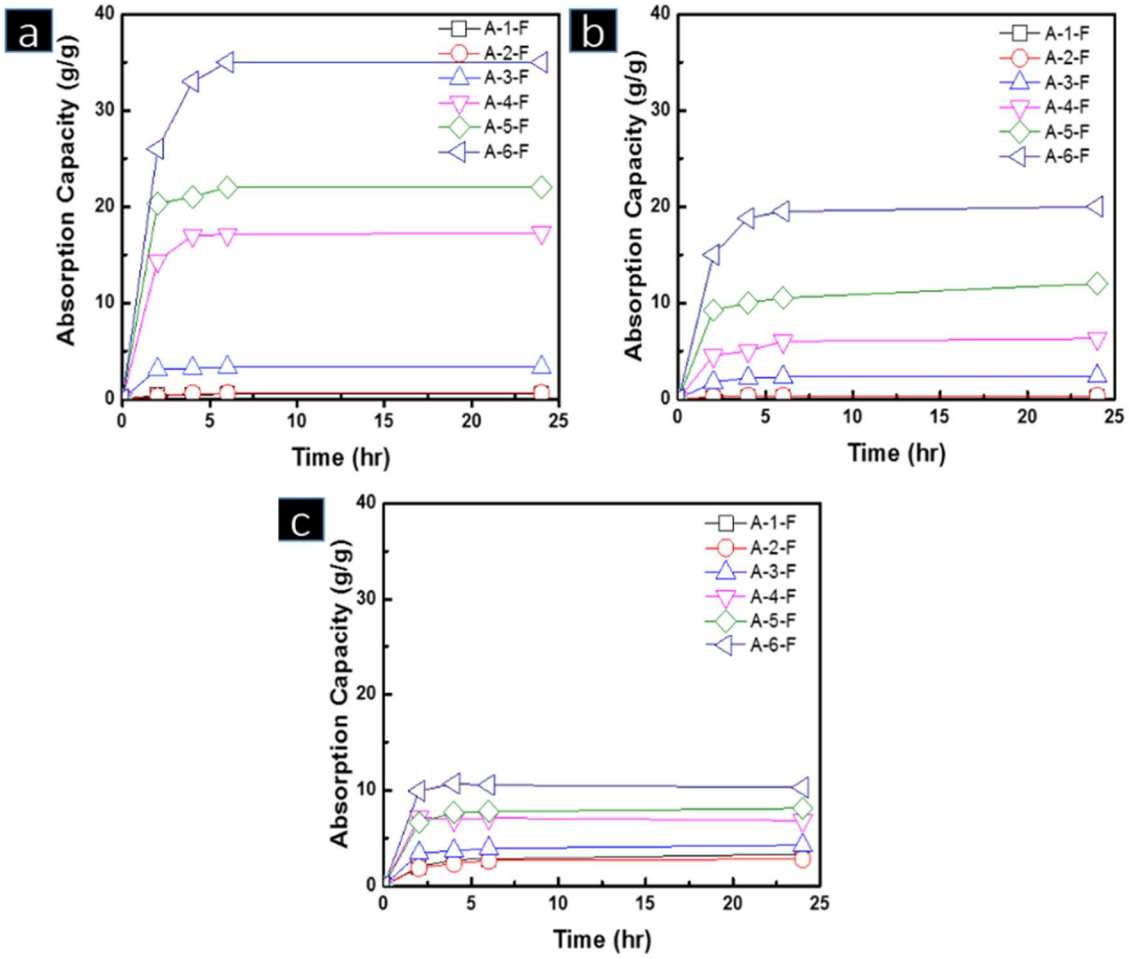

Figure 3-8. Absorption profiles for six ethylene/1-octene copolymer casting films with (a) Toluene, (b) Diesel, and (c) ANS crude oil.

All the LLDPE films show significantly fast kinetics, reaching the maximum oil absorption capacity in less than 4 h. All of them, except two densest LLDPE polymers (A-1F and A-2F), show significantly higher hydrocarbon absorption capacity than their corresponding pellet forms. Again, the A-6F with the lowest density (0.865 g/cm^3) and thickness ~250 μm, shows the highest absorption capacity, about 35 times for toluene, 20 times for diesel, and 10 times for *ANS* crude oil. The general absorption capacity follows the general trend with toluene>diesel>*ANS* crude oil. Also, the resulting hydrocarbon-swelled LLDPE films exhibit excellent mechanical strength and hydrocarbon (oil) retention, which are suitable for hydrocarbon (oil) storage and recovery applications.

Note that a small density difference (0.909 g/cm^3 in A-1 vs. 0.865 g/cm^3 in A-6) in the LLDPE films has a profound effect on their absorption capacities. In the A-6F, the combination of high side chain content (9.4 mol%), low crystallinity (16%), and small crystal size (T_m=55 °C) must spontaneously form the continuous channels between the polymer chains, with higher free volume. This low-density morphology offers the favorable diffusion path and interaction with hydrocarbon molecules.

Compared to the melt-blown polypropylene sorbent, which shows about 10 times sorption capacity and adsorption mechanism with easy oil bleeding issues, this inexpensive LLDPE A-6 film demonstrates significantly better performance. The results from the LLDPE film study have encouraged us to explore further modification of polymer morphology, reducing the bulk density and increasing the specific surface area.

The open-cell foam shall offer an easy flow of the hydrocarbon liquid through the entire polymer matrix. The LLDPE pellet was first swelled with hexane solvent (foaming agent), then the temperature was increased to about 15-20 °C higher than its T_m before pulling the vacuum to foam the polymer matrix. The resulting porous morphology was stabilized by exposing the resulting foam to air (ambient temperature and pressure). The foam morphology (bubble size and density) can be controlled by the foaming agent and operation condition. Preparing LLDPE foams with a density more than 10 times smaller than those of starting LLDPE pellets is reproducible.

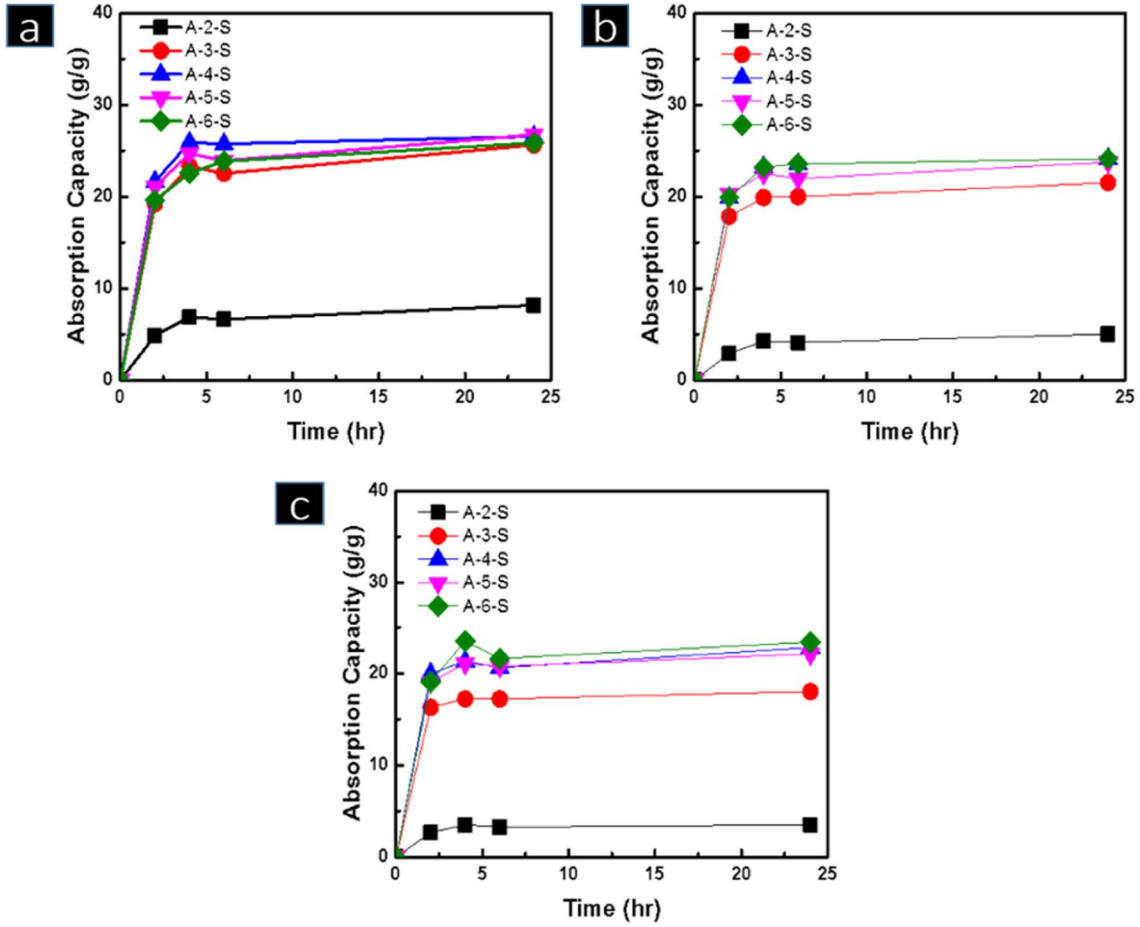

Figure 3-9. Absorption profiles for six LLDPE casting foams with (a) toluene, (b) diesel, and (c) *ANS* crude oil.

Figure 3.9 compares the absorption profiles of toluene, diesel, and *ANS* crude oil with five resulting LLDPE foams that have a similar density (~0.1 g/cm^3). Except, A-2S with relatively high crystallinity and Tm, all other LLDPE foams show a marked improvement in both absorption capacity and kinetics. The A-6S foam saturated with toluene become too weak to be fully recovered, resulting in a slightly reduced absorption capacity. The absorption profiles also merged into a similar pattern with fast kinetics, reaching about 20 times the absorption capacity in 2 h and have been fully saturated within 5 h.

It was a pleasant surprise to have observed similar profile patterns independently between three very different hydrocarbons that include pure solvent (toluene), refined oil product (diesel), and complex crude (*ANS* oil). The results indicate the importance of reducing the diffusion path into the polymer matrix and high surface area for absorbing the viscous and complex mixture of hydrocarbons, especially for complex and viscous hydrocarbons.

This is the first experimental result to demonstrate the absorbent with >20 times the crude oil absorption capacity, without the requirement of diluting crude oil with solvents shown in several papers. As expected, LLDPE does not absorb aqueous solutions. The resulting A-4S, A-5S, and A-6S foams (with low cost and easy processing) shall be appropriate for oil spill recovery and cleanup that has been a challenging technology for decades. It is important further to investigate the correlation between foam density (morphology) and hydrocarbon absorption capacity. LLDPE (A-5 copolymer) was then chosen to prepare a series of foams with various bulk density.

As summarized in Table 3.2, a series of A-5S with the density from original 0.868 to 0.081 g/cm^3 were compared with the corresponding A-5P and A-5F forms. The hydrocarbon (oil) absorption capacity and kinetics are strongly influenced by the porous morphology, the lower material density, the higher absorption capacity. In the A-5-S6 sample, the density was reduced to less than one-tenth of the original bulk density, and this foam shows very high absorption capacity with all hydrocarbons. Comparing ANS crude oil absorption capacity in the same LLDPE (A-5) copolymer but three different forms, i.e. pellet (A-5-P), film (A-5-F), and foam (A-5-S6), the experimental results clearly indicate the advantage of porous morphology, in particular for absorbing the complex crude oils.

Table 3-2. Solvent and oil absorption capacity of the LLDPE foams with various densities.

Sample	LLDPE foam density (g/cm3)	Adsorption results (weight times after 24 h)		
		Toluene	diesel	ANS oil
A-5-P (pellet)	0.868	6.69	2.87	1.82
A-5-F (film)	0.868	21.8	11.1	7.92
A-5-S1	0.405	14.7	18.5	11.3
A-5-S2	0.254	16.8	21.3	14.2
A-5-S3	0.177	18.7	22.7	16.8
A-5-S4	0.143	20.2	23.8	18.9
A-5-S5	0.122	21.2	24.2	20.2
A-5-S6	0.081	30.2	33.8	26.6

3.4.2 Amorphous Polyolefin Copolymer Networks

In searching for the hydrocarbon super-absorbents, we have also studied amorphous polyolefins, without any crystalline domains that prevent polymer dissolution but also reduce the overall absorption capacity. The amorphous polyolefins were crosslinked to create an insoluble polymer matrix. Due to the fact of the absorption capacity inversely proportional to the crosslinking density, we were targeting on the amorphous network with a very low crosslinking density. We employed 1-decene monomer[121] that has a comparative comonomer reactivity with divinylbenzene (DVB) cross-linker[136] during the *Ziegler-Natta* catalyst mediated copolymerization, which forms high molecular weight polymer chain with a uniform copolymer structure, i.e. narrow molecular weight and composition distributions. The combination is essential in forming a complete network structure with a very low DVB crosslinks content. In addition, poly(1-decene) is a polymer with high entangle molecular weight and spontaneously forms low density material with high free volume, due to the long side chain in each monomer unit. They are also very beneficial in crosslinking reaction and absorption kinetics (discussed later). Furthermore, this research project is also benefited from a new polyolefin crosslinking chemistry developed in our group. The polyolefin containing DVB units effectively engage a thermal cyclo-addition reaction between two DVB units to form crosslinked network at >200 ºC. The process involves no external chemical and produces no by-product.

In a typical copolymerization, a specific monomer mixture was introduced into a reactor containing *Ziegler-Natta* catalyst and toluene solvent. The polymerization was carried out under an argon atmosphere with constant agitation. After certain reaction time and a

specific reaction temperature, the reaction was terminated by adding isopropanol; then the coagulated polymer was washed, dried, and weighed. All resulting copolymers were examined by ^{1}H NMR and GPC to determine their copolymer compositions and molecular weights. Most of the polymers were then thermally crosslinked at 220 °C to form the corresponding network structures.

Table 3.3 presents the polymerization conditions and results, as well as the subsequent thermal cross-linking efficiencies based on the gel contents. The traditional *Ziegler-Natta* catalyst shows an effective incorporation of 1-decene and mono-enchainment of DVB to form poly(1-decene-co-divinylbenzene) (D/DVB) copolymers with various DVB cross-linker contents and excellent catalyst activity in all copolymerization runs.

Table 3-3. Copolymerization condition and results between 1-decene and DVB comonomer.

Run	Polymerization condition			Polymerization Results		
	1-decene/DVB (ml/ml)	Temp/time (°C)	Yield (%)	Density (g/cm^3)	1-decene/DVB (mol%)	X-linking (%)
B-1	10/0.5	25/3	69	0.872	97.87/2.13	100
B-2	10/0.3	25/3	90	0.872	97.89/2.11	100
B-3	10/0.2	25/3	95	0.872	98.06/1.94	100
B-4	10/0.1	25/3	91	0.872	98.66/1.34	100
B-5	10/0.05	25/1	84	0.872	99.34/0.66	94
B-6	10/0.02	25/1	92	0.872	99.4/0.6	93

Figure 3.10 shows a typical ^{1}H NMR spectrum of the 1-decene/DVB copolymer (B-1). There is a band of aliphatic proton chemical shifts between 0.9 and 1.6 ppm, corresponding to CH_2 and CH in the polymer backbone and side chains. We can also observe 5.2 and 5.7 ppm ($CH=CH_2$) and 6.7 ppm ($CH=CH_2$), corresponding to the vinyl groups in the pendent styrene groups (after mono-enchainment of DVB units). There is an aromatic (C_6H_4) proton band between 6.9 and 7.4 ppm. The peak intensity indicates that the mole ratio of vinyl group to phenyl group is near unity. All resulting D/DVB copolymers were completely soluble in common hydrocarbon solvents, such as toluene, at ambient temperature.

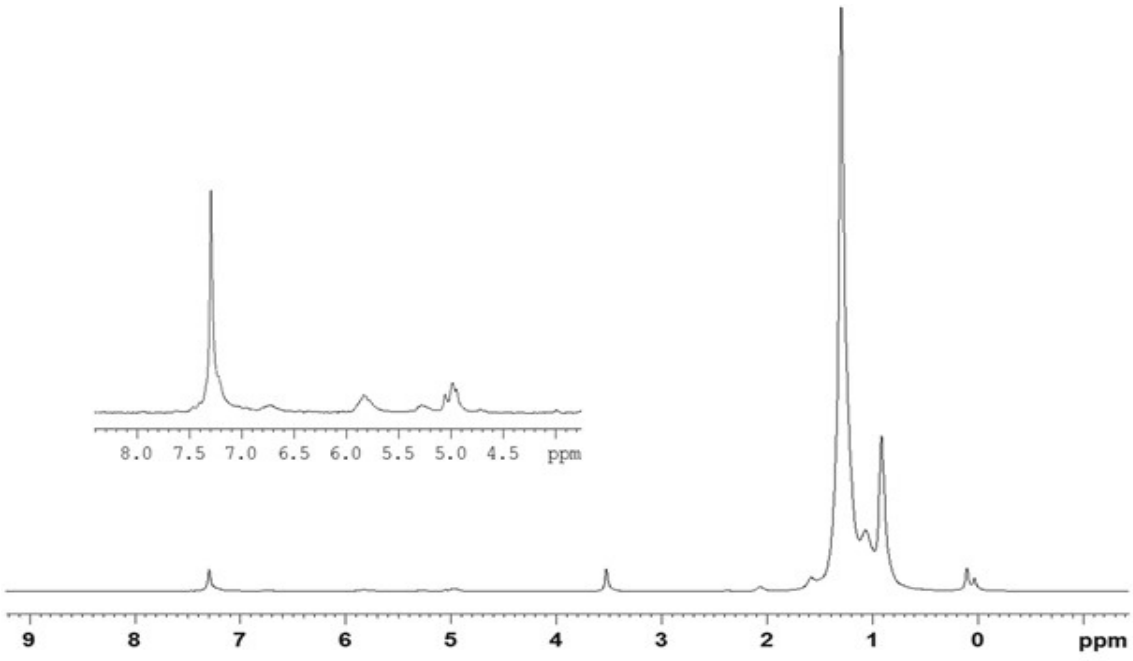

Figure 3-10. ^{1}H-NMR spectrum of 1-decene/DVB copolymer (B-1).

The resulting D/DVB copolymer solids were heated at 220° C under argon for 2 h to form the corresponding cross-linked x-D/DVB copolymer network. They were subjected to a vigorous solvent extraction by refluxing toluene for 36 h to examine any soluble fraction that was not fully crosslinked. As shown in Table 3.3, most samples with >1 mol% DVB content show no detectable soluble fraction, indicating an efficient crosslinking reaction to form a complete network structure. It is interesting to note taht in most known network systems the crosslinker contents are usually significant higher than 1 mol% level. It is also very difficult to observe a complete crosslinked network, without any soluble fraction. In addition to the effective thermal crosslinking reaction, it is essential to have the prepolymer (D/DVB copolymer) with high molecular weight and narrow molecular weight and composition distributions. Two specimens (runs B-5 and B-6) with very low crosslinking density show minor weight loss, which may be partially due to the very soft gel particles that cause some fragmentation and loss during the extraction process.

Overall, it implies that the thermally-induced Diels-Alder [2+4] cycloaddition reactions happened between two pendent styrene units from two adjacent polymer chains under the solid-state conditions.[124,125] The long entangle molecular weight of poly(1-decene), minimized the possible intra-chain cycloaddition reactions between two adjacent DVB units in the same D/DVB polymer chain. The narrows composition distribution and high DVB reactivity shall also increase the crosslinking efficiency and reduce the unreacted DVB units.

Figure 3.11 compares the kinetic absorption profiles of all x-D/DVB amorphous networks with three representative hydrocarbons, i.e. toluene, diesel, and ANS crude oil (complex mixtures). Figure 3.12 compares the absorption capacity results of B-6 sample with various hydrocarbons after coming in contact for 24 hours.

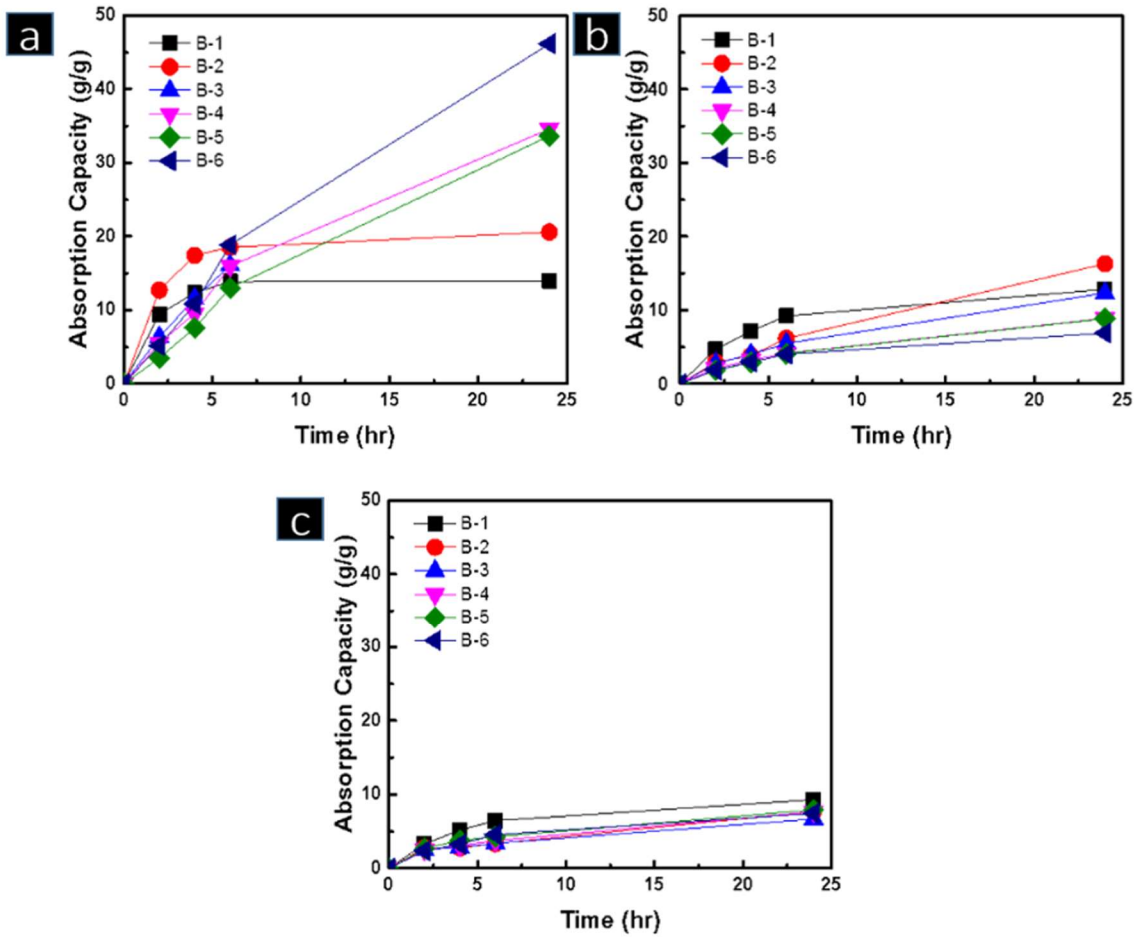

Figure 3-11. Absorption capacities of 1-decene/DVB copolymer with (a) toluene (b) diesel (c) ANS crude oil.

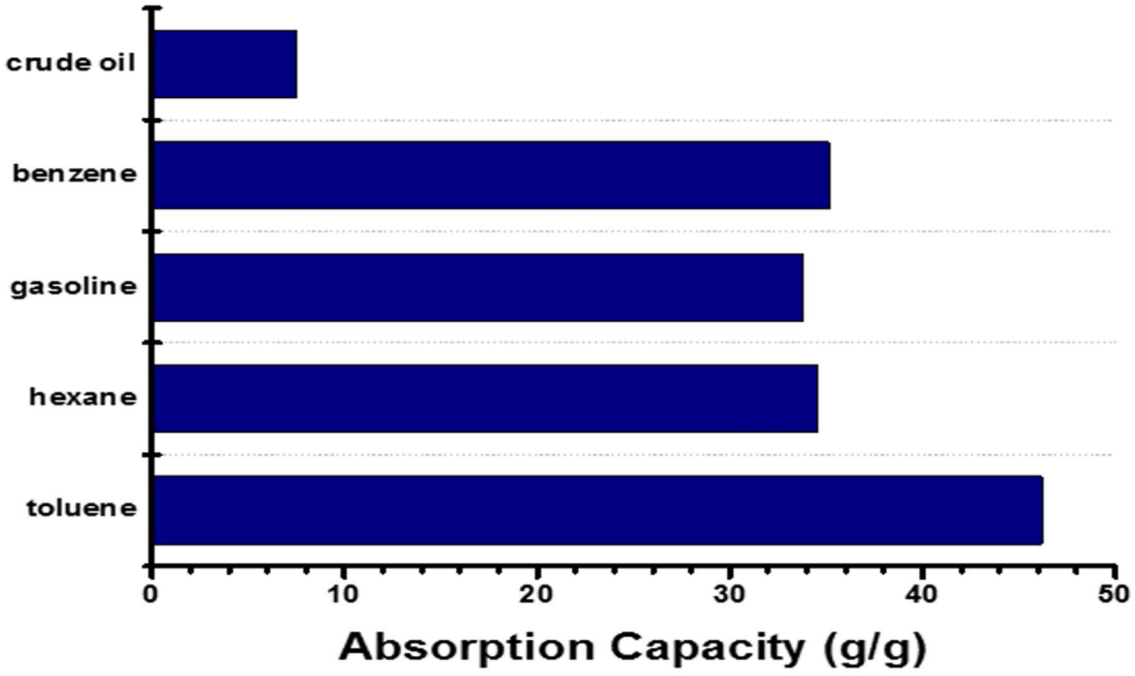

Figure 3-12. Absorption efficiency of 1-decene/DVB copolymer (B-6 sample) after 24 h.

The absorption behaviors are very different between pure organic solvents and complex hydrocarbon mixtures. Toluene is a good solvent and can effectively migrate into the amorphous network structure. The absorption capacity is inversely proportional to the cross-linking density, and the absorption capacity can reach to >40 times for the most lightly cross-linked x-D/DVB copolymer (sample B-6).

On the other hand, in the case of both diesel and ANS oil cases, the absorption profiles do not follow the cross-linking density, and all curves nearly merge into one during the ANS oil absorption, indicating the diffusion difficulty in the dense morphology with a long diffusion path. When comparing the absorption profiles in Figure 3.6 and Figure 3.11, both involve similar dense particle forms but different morphologies (semicrystalline LLDPE vs. amorphous x-1-decene/DVB networks). The general slow absorption kinetic patterns are very similar in all three representative hydrocarbons, but the amorphous x-D/DVB network shows higher absorption capacity than the semicrystalline LLDPE.

Evidently, the crystalline domains in LLDPE cannot contribute to the absorption activity and reduce the overall capacity. Unfortunately, the combination of low-Tg amorphous (soft) material and naturally tacky property of x-D/DVB properties does not allow us to prepare the corresponding film or foam absorbents, following the same strategy used in the semicrystalline LLDPE cases.

3.4.3 Calculation of Network Structures

The experimental results clearly show a complex structure-property relationship in the polyolefin-based network system with a relatively weak absorbent-absorbate interaction and strong morphology effects. As shown in Equations 3-7 and 3-8, Flory-Rehner equation is commonly used to characterize the polymer network structure with cross-linking density (ρ_c) and average molecular weight (M_c) between two crosslinks. The calculation is based on the equilibrium swelling network with a good solvent, in which the free energy of mixing between the polymer and solvent is against the free energy of elastic response from the polymer network.

Based on the experimental results in Figure 3.12, toluene (with molar volume V_1=106.3 $cm^3 \cdot mol^{-1}$) is a good solvent for x-D/DVB copolymers. The polymer volume fraction (υ_2) in the equilibrium toluene-swollen network can be computed by the absorption capacity with the mass densities of the polymer (σ_1=0.872 g/cm^3) and solvent (σ_2=0.867 g/cm^3). If one knows the Flory χ_1, the values of ρ_c and Mc can be determined.[126] However, the determination of the χ_1 value, including both entropy (χ_S) and enthalpy (χ_H) contributions, is far from perfect.

For the x-D/DVB/toluene interaction, the χ_H value is related to the heat of mixing and can be calculated by $\chi_H = (V_1/RT)(\delta_s-\delta_p)^2$, wherein the solubility parameter of toluene δ_s= 18.2 $Mpa^{1/2}$ and solubility parameter of poly(1-decene) δ_p= 16.6 $Mpa^{1/2}$.[127] However, the χ_S entropy parameter, associated with the dispersion forces, is a mean semi-empirical value 0.34 (with the largest deviation of 0.15) in the nonpolar-nonpolar system. The branched polymer structure usually possesses a considerably lower χ_S value. In this highly branched

D/DVB copolymer structure, we adopted the low end of χ_S= 0.19 with the calculated χ_1 =0.31 that is inconsistent with the reported Flory interaction parameter in other polyolefin-toluene systems.[123]

Table 3.4 summarizes the estimated ranges of the χ_1 parameter using $\chi_1 = \chi_S + (V_1/RT)(\delta_s-\delta_p)^2$ with the range of χ_S values between 0.19 and 0.34. However, ρ_c, M_c and the corresponding 1-decene units between two crosslinks are calculated based on the χ_1=0.31 value. The experimental results in Table 3.4 indicate that only a small fraction of DVB units (35% in B-1 and 18% in B-6) in the D-DVB copolymers involve the interchain crosslinking reactions, and the crosslinking efficiency decreases with the decline of the DVB crosslinks content in the D-DVB copolymer.

Table 3-4. Calculated ρc and Mc Values in the Toluene-Swollen x-D/DVB Networks

Run	υ_2 value	χ_1 range	ρ_c (x10^{-6} mol/cm^3) [a]	M_c (x10^3 g/mol)[a]	1-decene units/ crosslink[a]
B-1	0.0663	0.31-0.46	23.4	37	264
B-2	0.0460	0.31-0.46	12.0	72	514
B-3	0.0447	0.31-0.46	11.4	76	730
B-4	0.0322	0.31-0.46	6.39	136	971
B-5	0.0298	0.31-0.46	5.58	156	1114
B-6	0.0224	0.31-0.46	3.39	256	1828

Figure 3.13 plots the toluene absorption capacity as a ρ_c and the M_c between two crosslinks. The absorption capacity exponentially decreases with the increase of crosslinking density and is linearly proportional to the increase M_c. It is important to note the relatively low crosslinking density in most cases, especially for the B-6 sample with an average of only four crosslinks per polymer chain and about 1828 repeating 1-decene units between two crosslinks. The combination of high polymer molecular weight and the uniform distribution of the DVB comonomer units are essential in forming this highly swellable (but not soluble) network structure with the lowest crosslinking density possible. The B-6 sample may reach the optimal x-D/DVB network structure that can absorb toluene (good solvent) up to about 43 times its weight at ambient temperature.

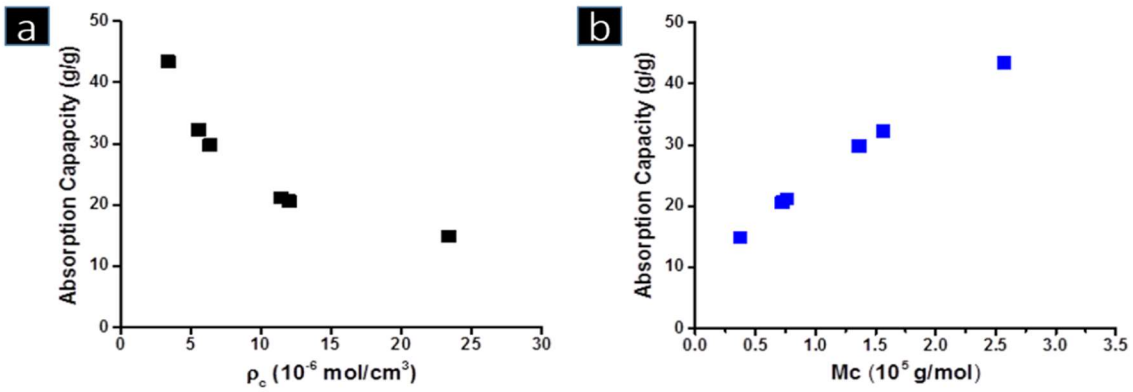

Figure 3-13. The plots of toluene absorption capacity vs. (a) crosslinking density (ρ_c) and (b) the average molecular weight (M_c) between two crosslinks in the x-D/DVB networks.

It is of benefit to extend this network structure calculation to the semi-crystalline LLDPE polymer system, in which each crystalline domain can serve as a crosslinking point. As discussed, the non-swellable crystalline domains maintain the structure integrity while allowing the amorphous domains to be swollen by a good solvent, such as toluene. The combination of the equilibrium toluene absorption capacity shown in Figure 3.14 and the density of polymer (σ_1) and toluene (σ_2=0.867 g/cm^3) allows us to determine the υ_2 value. With the reported χ_1 =0.34 for the LLDPE-toluene interaction parameter,[55] we apply the same Equations 3-7 and 3-8 to estimate the density of crystalline domains and the average molecular weight between two crystalline domains in the LLDPE polymers. The results are summarized in Table 3.5, and Figure 3.14 plots the absorption capacity vs. crystalline domain density (ρ_c) and the average molecular weight (M_c) between two crystalline domains.

Table 3-5. Calculated ρ_c and Mc Values in the Toluene-Swollen LLDPE Copolymer

Run	σ_1 (g/cm^3)	V_1 (cm^3/mol)	υ_2 value	χ_1 value	ρ_c (x10^{-6} mol/cm^3)	M_c (x10^3 g/mol)
A-1	0.909	106.3	0.67	0.34	4982.7	0.18
A-2	0.897	106.3	0.62	0.34	3759.5	0.24
A-3	0.875	106.3	0.23	0.34	252.8	3.46
A-4	0.870	106.3	0.05	0.34	12.1	71.64
A-5	0.868	106.3	0.04	0.34	8.1	106.87
A-6	0.865	106.3	0.03	0.34	4.8	177.48

As expected, the relatively high crystallinity (36%) in the A-1 sample results in high ρ_c and low M_c values, indicating a tight network structure with low swelling capacity. With the systemati decrease of crystallinity in LLDPE samples, the material becomes softer (expandable) with the reduction of non-swellable domains, and the increase of M_c molecular weight in the amorphous phase. Evidently, the A-6 sample may reach to the structure limit, in which the 12% crystallinity still can provide the absorbent material integrity while allowing toluene to swell in its matrix to the maximum capacity (35 times by weight) at ambient temperature.

In fact, both ρ_c and M_c values approach to similar values in both A-6 and B-6 samples, along with the toluene absorption capacity (35 vs. 43 times). Considering the size and volume fraction of crystalline domains in LLDPE is always larger than the those of DVB crosslinking units in x-D-DVB, it is logical to expect that the amorphous polymer will always exhibit higher absorption capacity with a suitable solvent under an equilibrium condition.

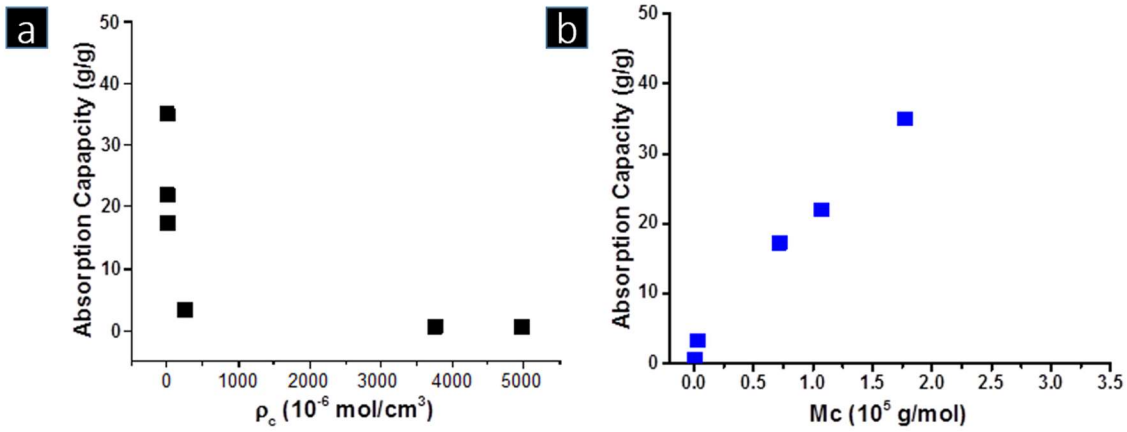

Figure 3-14. The plots of toluene absorption capacity vs. (top) crystalline domain density (ρ_c) and (bottom) the average molecular weight (M_c) between two crystalline domains in LLDPEs.

3.5 Conclusions

A systematic study has been conducted to understand the hydrocarbon absorption in the polyolefin-based polymer networks, which involves a series of semi-crystalline LLDPE thermoplastics and amorphous x-D/DVB elastomers with various adsorbates, from pure solvents, refined oil products, to crude oil. Although LLDPE copolymer has no chemical crosslinking unit, it exhibits similar network swelling behaviors with hydrocarbons. The crystalline domains provide the structural junctions between polymer chains in forming the network and the amorphous domains allow the solvent to swell to expand its matrix.

Flory-Rehner polymer swelling theory was applied to both systems to determine the network structures, i.e. crosslinking (or crystalline domain) density (ρ_c) and average polymer molecular weight (M_c) between two crosslinks (or crystalline domains). With the toluene (good solvent) condition, we observed the equilibrium absorption capacity of 35 and 43 times of the polymer weight for LLDPE and x-D/DVB systems, respectively. The slight difference may be because LLDPE contains some non-swellable crystalline domains. Overall, the key factor impacting the absorption capacity is the crosslinking density (ρ_c) and the associated average molecular weight (M_c) between two crosslinks. However, the trend does not follow with more complicated hydrocarbon mixtures, especially crude oils. Most of ANS oil absorption curves are collapsed into a low absorption profile, with <10 times absorption capacity. In addition to the loose three-dimensional (3D) molecular structure, the polyolefin absorbent requires a specific morphology with high surface area and small oil diffusion path for reaching the equilibrium absorption condition. By

fabricating a specific low-density LLDPE foam, for the first time, we have observed a crude oil absorption capacity >26 times at ambient temperature.

Chapter 4

Interpenetrating Polyolefin Networks as Innovative Crude Oil Cleanup Absorbents

4.1 Introduction

Many high surface area adsorbents, such as aerogel[129], zeolites[130], spongy type graphene[131] and natural adsorbents[82], have been investigated to enhance oil adsorption properties. With surface modification, some surface modified porous adsorbent materials, with high porosity, large surface area, and hydrophobicity and oleophillicity surfaces, have shown remarkable improvement in oil adsorption capacities. Unfortunately, they also showed some deficiency in oil/water separation and poor efficiency for highly viscous oils. Crude oil can penetrate into a macro or microporous channels, they also tend to clog pores in the outer layer so no further adsorption can happen[132]. Furthermore, even if they are effective in absorbing spilled oil in on the ocean, the absorbents can be carried away and dispersed by ocean tides, and thus it is difficult to collect all of them from the surface of sea water and shorelines.

On the other hand, the polymeric absorbents, including some hydrophobic polymers discussed in Chapter 2 and polyolefins discussed in Chapter 3, are based on a random copolymer network structure. Both aliphatic and aromatic hydrocarbon monomer units are randomly distributed along the polymer chains. A small amount of crosslinkers or crystalline domains are also incorporated in the polymer chain to form a network structure that allows the polymer to swell with the oil (hydrocarbons), without dissolving the polymer chains in the solution. With low molecular weight absorbates (solvents and oil

refined products), the oil absorption capacity (swelling-ability) can be very high (>40 times of polymer weight) and is reversely proportional to the crosslinking density. However, the trend does not follow with more complicated hydrocarbon mixtures, especially crude oils.

The experimental results (Chapter 3) clearly demonstrate that absorption performance is favorable to the polymer morphology with high surface area and short oil diffusion path. In the semi-crystalline polyolefin cases, such as LLDPE thermoplastics, the crystalline domains allow the formation of stable porous morphology that significantly enhances the oil diffusion. The absorption capacity and kinetics become less dependent on the oil types. However, the crystalline domains also reduce the overall absorption capacity. The best LLDPE foam (sample A-5-S6 in Table 3.2) shows ANS oil absorption capacity of >26 times of the polymer weight. On the other hand, the low-Tg amorphous x-D/DVB elastomers with very low crosslinking density do not allow us to prepare a stable porous foam structure. Although they show excellent absorption capacity (>40 times) with low molecular weight organic solvents and refined oil products, they exhibit poor ANS crude oil absorption performance (<10 times). It is logical to think the suitable ANS absorbent will possess the combination of amorphous morphology and porous morphology. In this Chapter, I will discuss a new polyolefin absorbent material that is a mixture of both semicrystalline LLDPE thermoplastic and amorphous D/DVB elastomer, with an interpenetrated polymer network (IPN) structure. This IPN structure contains two independent but interpenetrated (physical interconnection) LLDPE (rigid) and x-D/DVB (soft) networks. The molecule-scale connectivity offers new polyolefin material with uniform morphology and advantages of multiple physical properties and functions.

4.2 Interpenetrating Polymer Network (IPN)

The interpenetrating polymer network (IPN) has been applied to Hydrogels that have acrylic and methacrylic polymer backbones prepared by free radical mediated polymerization process. However, this IPN structure is new to polyolefins (Petrogels) prepared by transition metal coordination polymerization, due to the chemical difficulties. Some hydrogens with IPN structures are commonly used in drug control delivery[133–137] and biomedical applications.[138–140] IPN structure contains two individual polymer networks; they are independent but interpenetrated each other (physical interconnection). The molecule-scale connectivity offers the materials with uniform morphology and advantages of manipulating the materials physical properties and functions, which can significantly improve the mechanical properties and overcome some limitations of individual polymers[141].

As discussed, both polyolefin semicrystalline and amorphous random copolymer network systems show limitations in absorbing ANS crude oil. In this study, we have further investigated Petrogel molecular structure from a random copolymer network to an interpenetrated polymer network (i-Petrogel). The new i-Petrogel structure contains two independent polyolefin networks, including a rigid polyolefin network and a soft polyolefin network, and the polymer chains in two networks are intertwined and uniformly distributed in the whole interpenetrated network structure, as illustrated in Figure 4.1. Each polyolefin network is formed by one or more olefinic monomers with a high affinity for a target hydrocarbon, or mixture of hydrocarbons, and either crosslinking units or crystalline domains so that the polyolefin does not dissolve in the target hydrocarbon. The preparation

of polyolefin IPN structure is greatly benefited from a new polyolefin crosslinking chemistry developed in our group. In this chemical scheme, divinylbenzene (DVB) comonomers can be homogeneously incorporated along the polyolefin chain with mono-enchainment fashion, and the resulting polyolefin copolymer containing DVB units is completely soluble and melt-processible. Upon heating to >200 ºC, the resulting pendent styrene groups along polyolefin chain effectively engage a cyclo-addition reaction between two DVB units to form crosslinker units. The process involves no external chemical and produces no by-product.

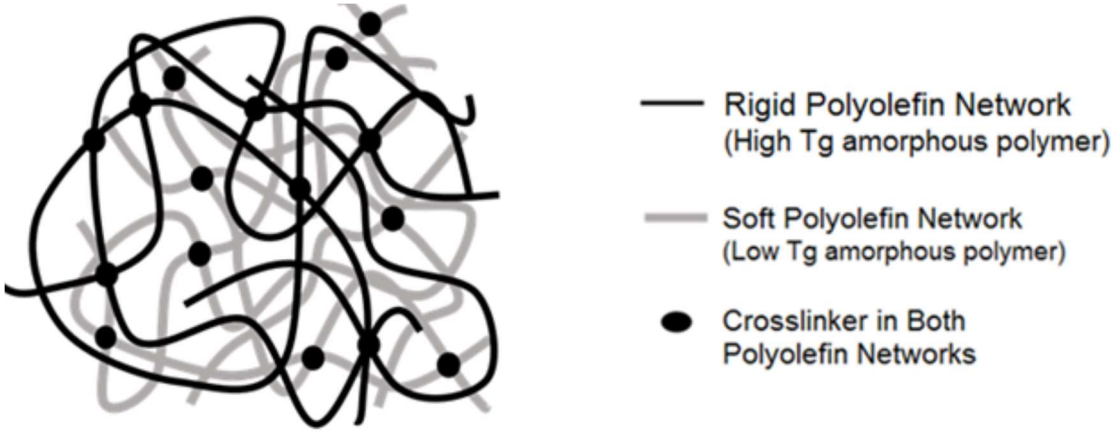

Figure 4-1. Structural illustration of interpenetrated polymer network (i-Petrogel).

In the broad description of new polyolefin IPN structure, the soft polyolefin network is an amorphous polyolefin copolymer with a low Tg of less than about 10°C and high free volume (due to side chains and/or pendant groups from monomer units) and a network structure (due to the cross-linking in its matrix). The rigid polyolefin is either a cross-linked amorphous polyolefin with a high Tg of more than about 50°C and a network structure (due to the cross-linking in its matrix) or a semi-crystalline polyolefin thermoplastic and a network structure (due to some insoluble crystalline domains in its matrix). The polyolefin IPN material shown in Figure 4.1 is completely insoluble in any hydrocarbons under ambient conditions and can be processed into film and foam structures with high surface area such that it reduces absorbate (hydrocarbon) diffusion path into the matrix. During absorbing hydrocarbons, the matrix swells its volume to form a hydrocarbon-polyolefin composition (i.e., gel). The combination of high affinity between the hydrocarbon and/or polymer and/or side chains or pendant groups off of the backbone of polyolefin and the open morphology with high surface area for shortening absorbate diffusion path enhances the hydrocarbon absorption capacity and kinetics, especially in the cases of absorbing viscous hydrocarbons and crude oils with high molecular weights and complex mixtures.

The major reason for developing this IPN structure is related to the preparation of foam materials with porous morphology and high surface area for all polyolefin absorbents. Both amorphous 1-decene/DVB and 1-octene/styrene/DVB elastomers show excellent absorption capacity for solvents and refined oil products but exhibit difficulty for viscous crude oils. Unfortunately, they cannot form a stable foam product, due to low crosslinking density. In the following sections, I will focus on a specific polyolefin IPN structure that contains an amorphous (low Tg) x-D/DVB elastic network and a rigid semi-crystalline

LLDPE thermoplastic network, in which both polymer chains are interpenetrated and uniformly distributed in the whole network structure. In this IPN structure, the rigid polymer segments with continuous molecular structure offer the rigid framework to support (stabilize) the porous morphology of soft polyolefin elastomer network with a very low Tg and a very low crosslinking density.

4.3 Experimental Section

Figure 4.2 illustrates the typical reaction scheme to prepare an IPN i-Petrogel material, containing an amorphous (soft) x-D/DVB elastic network and a semi-crystalline (rigid) LLDPE thermoplastic network.

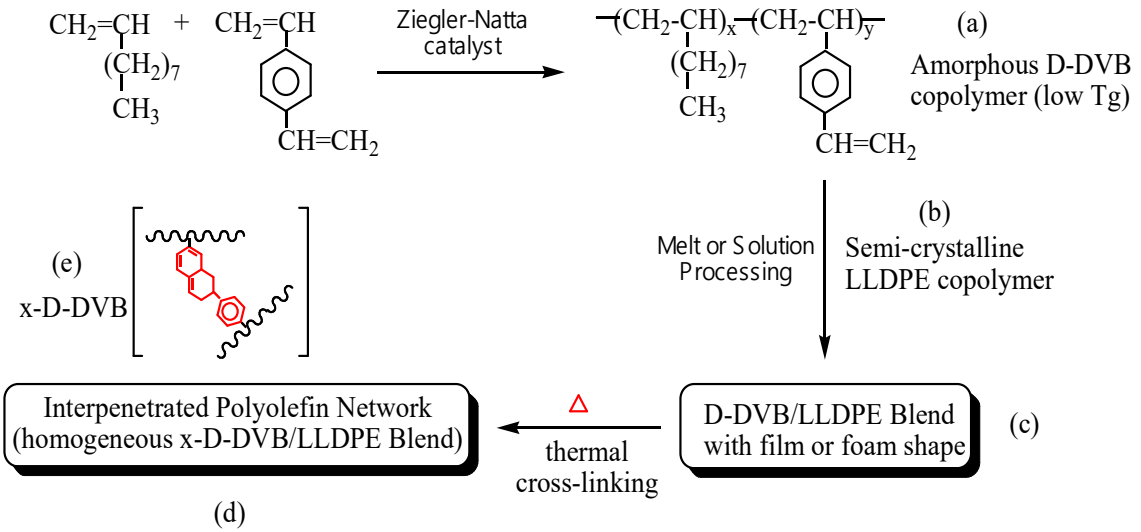

Figure 4-2. Schematics illustration of synthesis of i-Petrogel.

4.3.1 Preparation and Characterization of x-D/DVB Copolymers

The cross-linkable polyolefin elastomer is prepared using a heterogeneous Ziegler-Natta catalyst (i.e. $TiCl_3$(AA)/$AlCl_2Et$; where AA represents an activated by aluminum metal). This traditional Ziegler-Natta catalyst shows effective incorporation of 1-decene monomers and mono-enchainment of DVB at ambient temperature to form poly(1-decene-co-DVB) copolymer with high molecular weight (M_w>330,000 g/mol). The resulting D-DVB copolymers are completely soluble in common organic solvents, such as hexane and toluene.

Figure 4.3 shows the ^1H NMR spectrum of a D/DVB copolymer containing 4 mol% of DVB units. In addition to a chemical shift at 0.8 ppm, corresponding to CH3 in the 1-decene units, and a band between 0.9 and 1.7 ppm, corresponding to CH_2 and CH in the polymer backbone, there are three bands around 5.2 and 5.7 ppm ($CH=CH_2$) and 6.7 ppm ($CH=CH_2$); and an aromatic proton band between 6.9 and 7.4 ppm (C_6H_4). The integrated intensity ratio between all three vinyl protons and the four phenyl protons determine the vinyl/phenyl mole ratio, which is near unity. The experimental results confirm the mono-enchainment of DVB comonomers in forming the processible D/DVB copolymer (a).

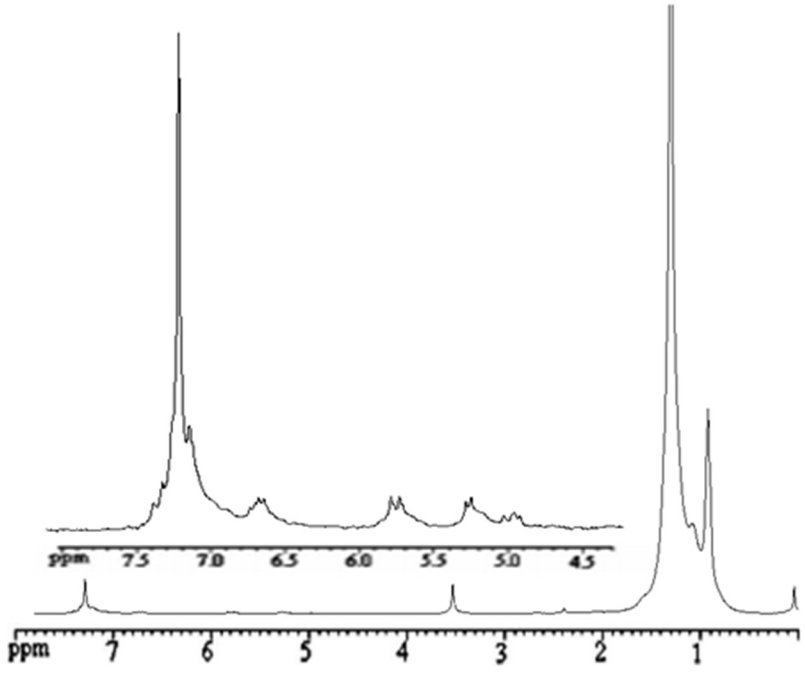

Figure 4-3. ^{1}H NMR spectrum of a soft D/DVB copolymer containing 4 mol% of mono-enchained DVB units.

Table 4.1 summarizes the copolymerization conditions and results of D/DVB copolymers. Evidently, Ziegler-Natta catalyst shows an effective incorporation of both high aliphatic (1-decene) and aromatic (divinylstyrene) monomers and mono-enchainment of DVB monomer to form D/DVB copolymers with random copolymer structures. Although aliphatic monomers usually exhibit higher reactivity than the aromatic styrene monomer in heterogeneous Ziegler-Natta copolymerization, GPC and DSC results demonstrate all copolymers have high molecular weights and rather narrow composition distributions. All copolymerization reactions between 1-decene and DVB monomer show excellent catalyst activity. As will be discussed later, the resulting D/DVB copolymers are used for constructing IPN networks.

Table 4-1. Condition and results of preparing D/DVB copolymers using Ziegler-Natta catalyst.

Run	Polymerization conditions			Polymerization results		
	1-decene (ml)	DVB (ml)	Temp/Time (°C/hr)	Yield (%)	D/DVB (mol%)	x-linking (%)
1	10	0.5	25/3	69	97.87/2.13	100
2	10	0.3	25/3	90	97.89/2.11	100
3	10	0.2	25/3	95	98.06/1.94	100
4	10	0.1	25/3	91	98.66/0.34	100
5	10	0.05	25/1	84	99.34/0.66	94
6	10	0.02	25/1	92	99.40/0.60	93

4.3.2 Preparation and Characterization of x-D/DVB/LLDPE IPN absorbent

The resulting soft D/DVB copolymer was mixed with semi-crystalline LLDPE copolymer in solution or melt, then processing to form films, as illustrated in Figure 4.4.

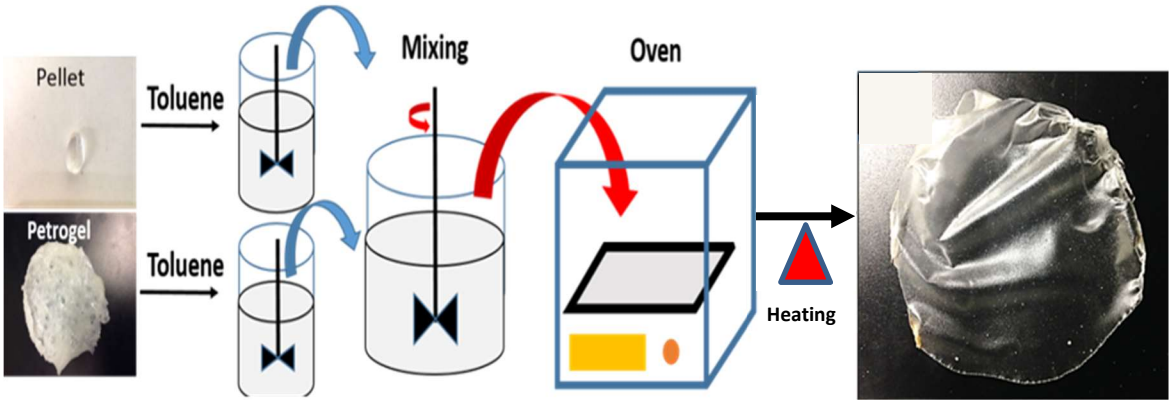

Figure 4-4. Preparation of i-Petrogel by a solvent evaporation process.

Upon thermal heating and then cooling down to ambient temperature, the polymer films become a completely insoluble interpenetrated polyolefin network material that contains two independent networks, including a thermally-crosslinked x-D/DVB network and a semi-crystalline LLDPE network with both polymer chains intertwined and uniformly distributed in the whole interpenetrated network structure. Both processing and thermal crosslinking reaction can happen in one step. Heat treatment is usually part of the processing procedure, the crosslinked x-D/DVB network structure was formed by engaging in a Diels-Alder [2+4] inter-chain cycloaddition reaction between two pendent styrene units in the adjacent D/DVB polymer chains. This solid-state crosslinking reaction is very effective and without by-products, which eliminates the need for expensive solution-removal of hydrocarbon-soluble fraction shown in many prior arts, in which the

crosslinking reactions were usually carried out in dilute solutions with considerable amount of intra-chain coupling reaction. On the other hand, the mobile LLDPE polymer chains in solution or melt spontaneously form a strong and tough network structure during solvent evaporation or cooling, respectively. Some portion of LLDPE polymer chains form crystalline domains (physical crosslinkers) for creating an independent but intertwined network structure.

The i-Petrogel shows significantly higher elongation and tensile strength than the corresponding polymer blend. Figure 4-5 compares the stress-strain curves of an i-Petrogel film with 1:1 weight ratio between x-D/DVB and LLDPE networks and a poly(1-decene)/LDPE film, prepared under similar film process conditions. As prepared sample without DVB crosslinker showed low tensile strength about 1.4 Mpa and the elongation to break was low (about 550 %). On the other hand, the i-Petrogel film shows more than double mechanical strength and elongation.

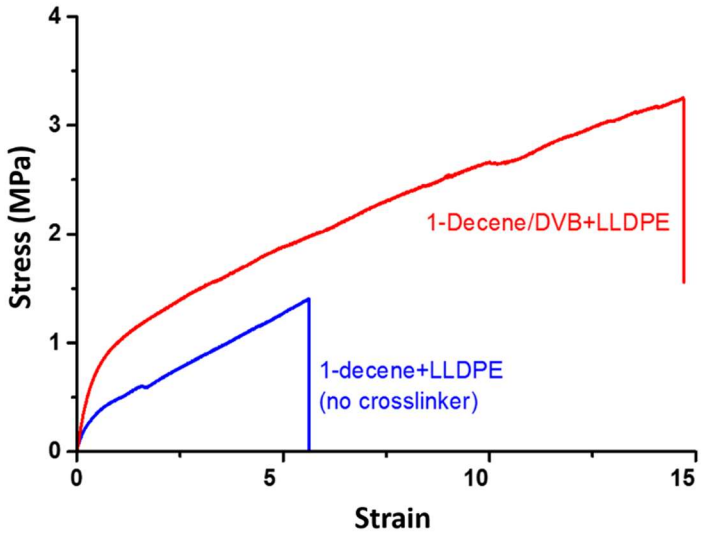

Figure 4-5. Stress-strain curves for i-Petorgel (Red) and two copolymer blend (blue).

Figure 4-6 shows the TEM micrograph of the x-D/DVB/LLDPE IPN film that was stained by RuO_4 to enhance the image of DVB crosslinkers. The homogeneous distribution of DVB units indicates that the polymer chains in the x-D/DVB network and the semi-crystalline LLDPE network are intertwined and homogeneously distributed in the interpenetrated polyolefin network structure. With the presence of semi-crystalline LLDPE thermoplastic, the resulting i-Petrogel is tough and not sticky and has the mechanical strength to form various structures and morphologies (i.e. films, foams, powders, etc.). The property can be easily tuned by the mixing ratio between D/DVB and LLDPE copolymers, as well as the DVB (crosslinker) content in D/DVB copolymer. To assess factors that control crude oil absorption capacity and kinetics, we have prepared several i-Petrogel with various compositions and morphologies and evaluated their performance with Alaska North Slope (ANS) crude oil.

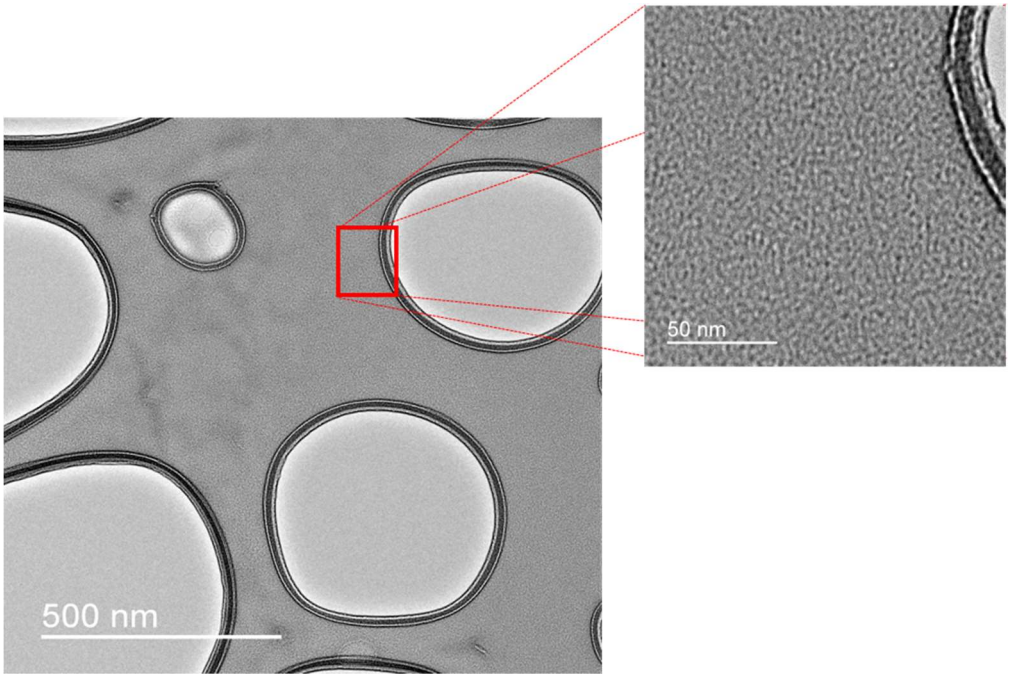

Figure 4-6. TEM micrograph of the x-D/DVB/LLDPE IPN film.

4.3.3 Evaluation of Crude Oil Absorption Performance with i-Petrogels.

All i-Petrogel samples were processed into film forms, with the thickness between 0.20 and 0.30 mm, and the absorption tests were conducted under similar experimental conditions at 25 or 0 ºC, following ASTM F716-09 (type II loose absorbent procedure). The absorption capacity was determined by measuring the weight ratio W_t-W_0/W_0 between the absorbed oil to the original dried absorbent, wherein W_0 is the initial weight of the absorbent sample and W_t is the total weight of absorbent-hydrocarbon gel after 24 hours as shown in Figure 4.7 .

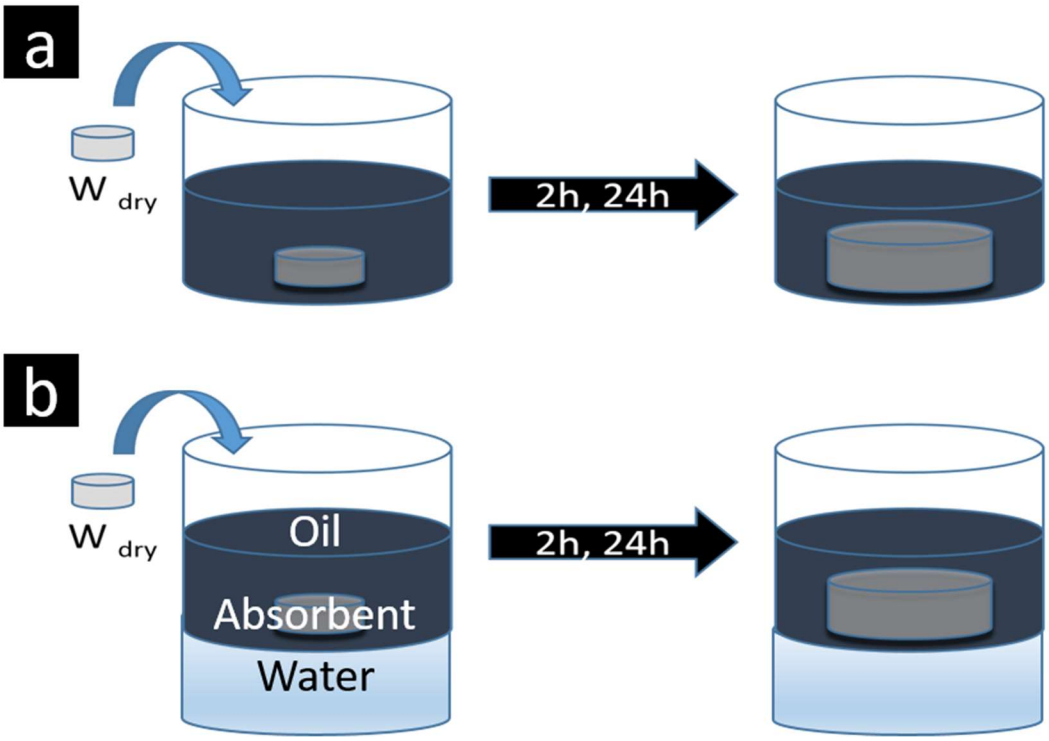

Figure 4-7. Oil absorption evaluation of (a) oil without water and (b) oil on the watr.

4.4 ANS oil absorption Capacity and Kinetics

As discussed, the strong correlation between Petrogel porous morphology and the ANS oil absorption capacity prompts us to design the new i-Petrogel molecular structure. The focus is not only to find the most suitable i-Petrogel composition that provides high oil absorption capacity (interaction issue) but also the foaming ability (kinetic issue). Figure 4.8 shows ANS oil absorption profiles for four dense i-Petrogel absorbents that are prepared by melt-compressed method (80 °C, 7.7 ton for 10 min) with different weight ratios between LLDPE and 1-decene/DVB (2/1, 1/1, 1/2, 1/3, and pure LLDPE), respectively. The 1-decene/DVB copolymer contains 0.2 mol% DVB concentration.

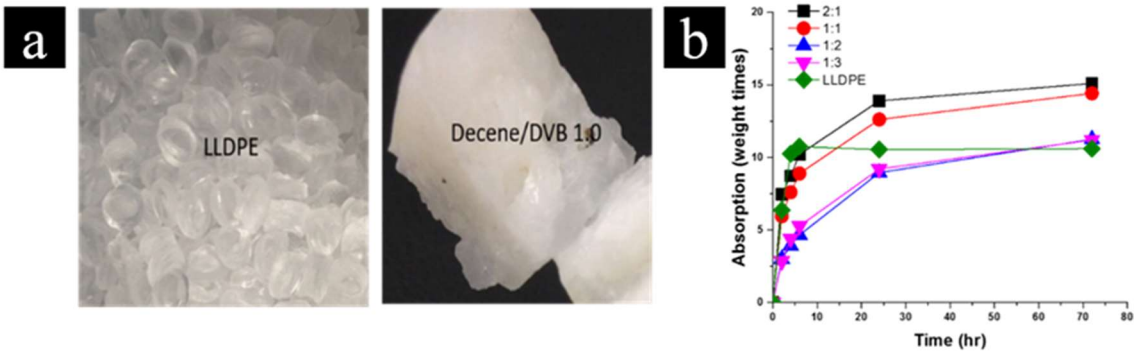

Figure 4-8. (a) photo images of LLDPE pellet and 1-decene/DVB copolymer, (b) ANS oil absorption profiles of several melt compressed IPN films with various D/DVB and LLDPE weight ratios.

The LLDPE film shows rapid ANS oil absorption kinetics, reaching more than 11 times of the polymer weight in less than 2 hours (Figure 4.8b). However, the overall absorption capacity of LLDPE film was not increased with time (72 h). Two i-Petrogel absorbents, with 2/1 and 1/1 weight ratios between LLDPE and 1-decene/DVB, reach 15 times after contacting with ANS oil for 72 h. However, the i-Petrogels with 1/2 and 1/3 weight ratios reach only to 10 times oil absorption capacity. These experimental results show that the oil absorption capacity could be affected by the mixing ratio of two polymers. However, the dense morphology of IPN structure is still not effective in the recovery of crude oil spills.

Figure 4.9 shows the ANS oil absorption curves (absorption capacity vs. time) for the corresponding solution-casted LLDPE/x-D/DVB interpenetrated networks (i-Petrogel samples) and the corresponding LLDPE sample at 25 and 0 °C conditions. Comparing with the dense melt-compressed samples (Figure 4.9), all the corresponding solution-casted i-Petrogel samples perform significantly better oil absorption capacity and kinetics. They also show remarkably better ANS oil absorption capacities and kinetics than the corresponding individual aliphatic (soft) and aromatic (rigid) polymer networks. All three i-Petrogel absorbents almost reach to the saturation level in 2-3 hours. It is interesting to note that he D/DVB copolymer with 0.2 mol% DVB cross-linker content was used to minimize the crosslinking density but maintain a complete crosslinked x-D/DVB (0.2) network structure (no observable soluble fraction after extensive toluene extraction).

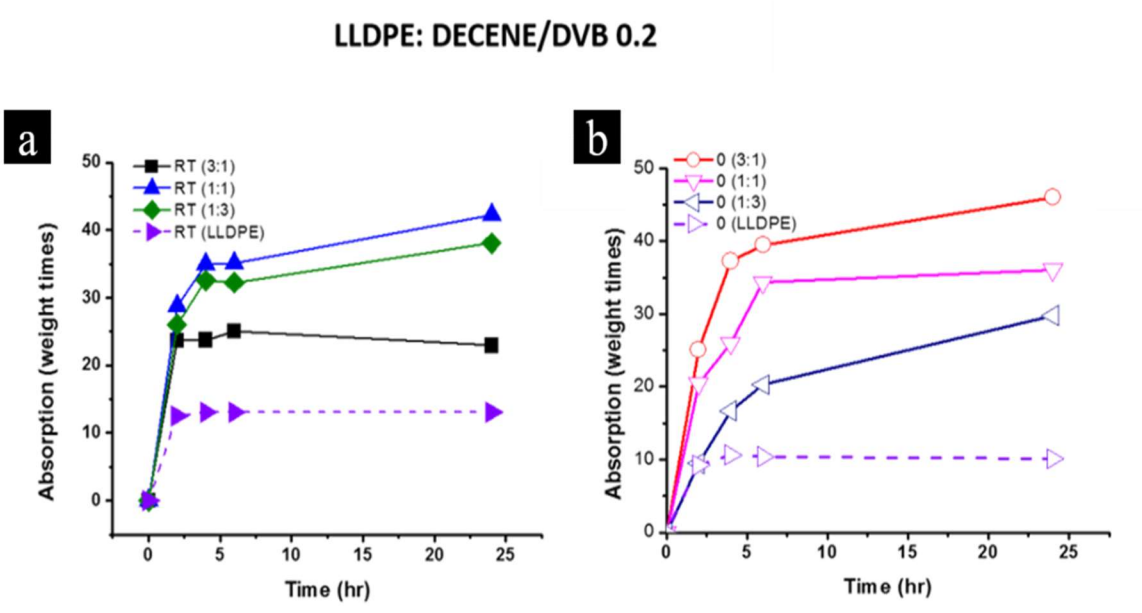

Figure 4-9. ANS crude oil absorption capacity of three different i-Petrogel samples and LLDPE film at (a) 25 °C and (b) 0 °C.

At ambient temperature (Figure 4. 9a), all three i-Petrogel-0.2 materials performed rapid ANS oil absorption kinetics, reaching more than 20 times the polymer weight in less than 2 hours. The i-Petrogel-0.2 with 1/1 wt. ratio reached 42 times after contacting with ANS oil for 24 hours. Furthermore, it is very interesting to observe the results (Figure 4.9b) when the ANS oil absorption is carried out at 0 ºC. The i-Petrogel-0.2 with 1/1 wt. ratio reached 35 times, and the i-Petrogel-0.2 with 3/1 wt. ratio reached 45 times the oil absorption capacity. All of them became highly oil-swelled soft gels. It is interesting to note that the differences between the three absorption profiles may be associated with the recovery of the resulting i-Petrogel-0.2/ANS oil gel. Some of them, especially the 1/3 sample, after absorbing a large quantity of ANS oil became too soft to fully recover (isolated) from the water surface. After contact with ANS oil for 24 hours, the LLDPE/x-D/DVB (1/1 ratio) IPN material reaches to 42 and 37 times at 25 and 0 ºC, respectively.

The attempt of using D/DVB copolymer with 0.02 mol% DVB cross-linker units in the i-Petrogel-0.02 IPN structure experienced some difficulty. Figure 4.10 shows the ANS oil absoption profiles of the solution-cased i-Petrogel-0.02 absorbents, involving x-D-DVB copolymer with 0.02 mol% DVB cross-linker units and the same three different compositions 3/1, 1/1, and 1/3 weight ratios between LLDPE and x-D/DVB (0.02) networks. The inconsistent results may be associated the insufficient DVB crosslinker units that result in an incomplete x-D/DVB netwrok structure.

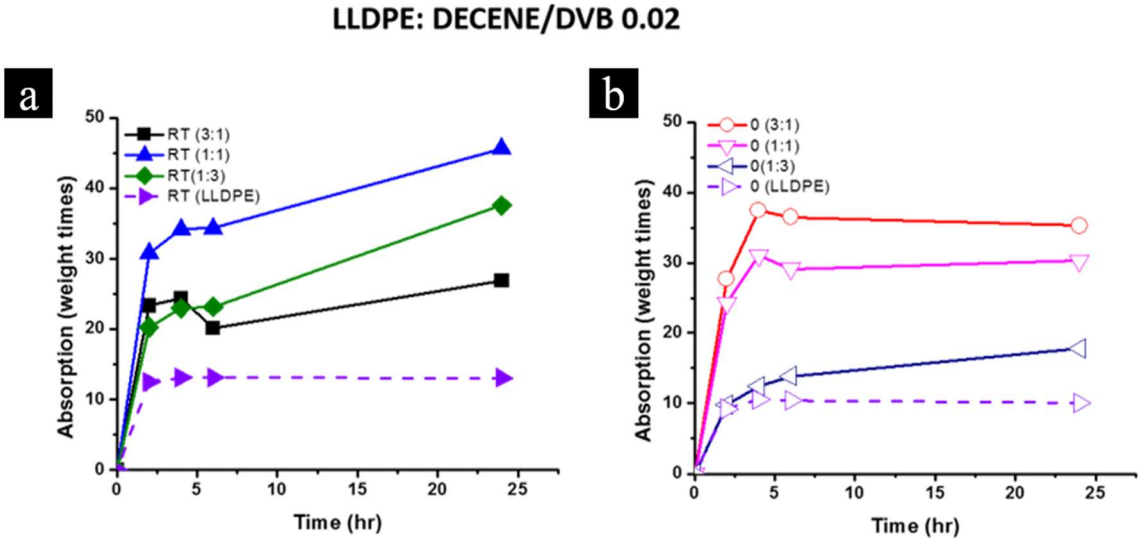

Figure 4-10. ANS crude oil absorption capacity of three different i-Petrogel (0.02 mol% DVB units) and LLDPE film at (a) 25 °C and (b) 0 °C.

4.5 Recovery and Recycling of Oil Absorbed Gel

The collectability of absorbent adducts (with the absorbed oil) is also a critical consideration for the practical recovery of massive oil spillage on the ocean. If the absorbent adducts form small individual patches and can be pushed away by the wind and waves in any directions. It will be very difficult to collect them from the open sea. Ideally, the adducts form a coherent gel structure floating on the water surface with self-supporting network structure that can be mechanically recovered, without leaking oil. In other words, i-Petrogel serves as a temporary oil storage vessel to prevent oil weathering and easy recovery. Figure 4.11 demonstrates the recoverability of i-Petrogel/ANS oil adducts.

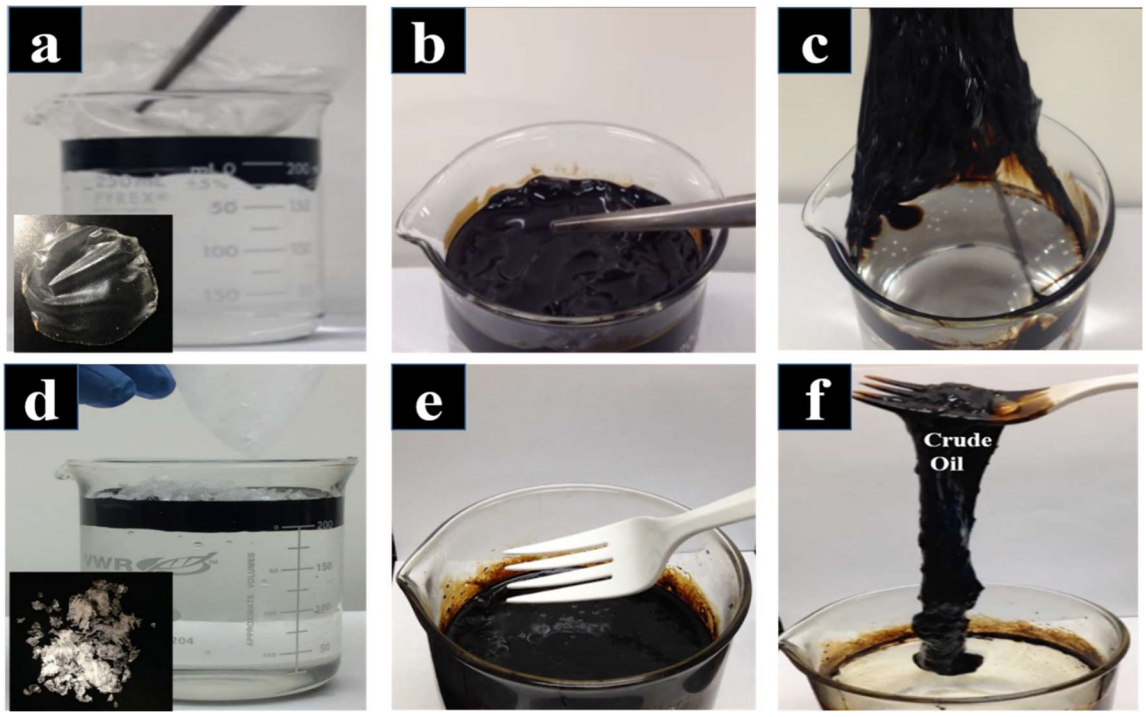

Figure 4-11. (a) i-Petrogel film contacting with ANS oil on water, (b) after 2 h absorption, (c) recovering the adducts by tweezer from the water surface. (d) i-Petrogel flakes contacting with ANS oil on water (e) after 2 h after application, and (f) recovering the adducts by stirring up with a fork.

After we placed the i-Petrogel-0.2 (1 g) in either film or flake forms on the ANS crude oil (30 ml) that is floated on the water surface in a beaker for 2 h, respectively (Figure 4.11 a and d). Oil quickly was absorbed into the i-Petrogel materials, and the color of the film and flakes changed to black. Meanwhile, both absorbents kept thicker and grew to a larger volume (oil swelling). After 2 h, the film surface was wrinkled, while the flake type has a smooth surface (Figure 4.11 b and e). No agitation was applied to pick the film type absorbent from water surface except recovering. In flake form, with little agitation make all absorbent coagulate into one piece of the chunk that can be stirred up at once. Both types absorbents were easily removed from water with a tweezer and a fork while only left clean water in a beaker (Figure 4.11c and Figure 4.11f, respectively).

The recovered i-Petrogel/ANS oil adducts, containing >97 wt.% ANS oil, show no re-bleeding in water. As shown in Figure 4.12, a piece of recovered adducts was immersed in water for more than 10 minutes, without any detection of oil leaking out.

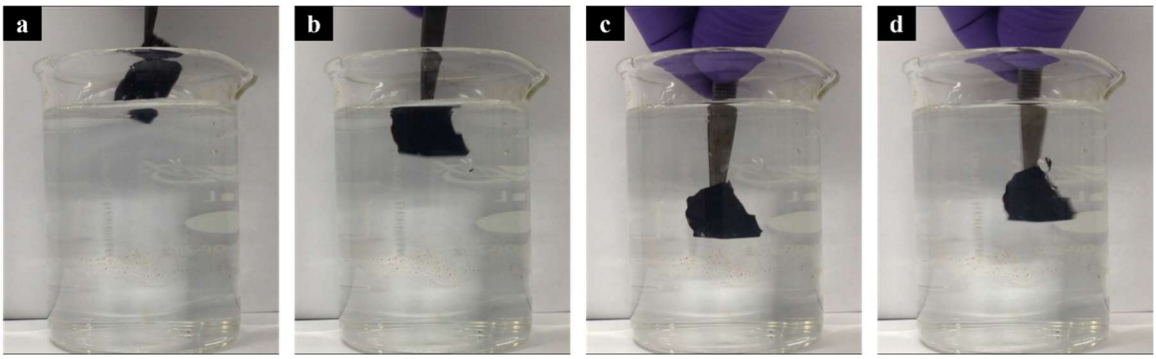

Figure 4-12. A recovered ANS oil absorbed i-Petrogel film was immersed in water.

In addition to effective oil recovery, the resulting i-Petrogel/ANS oil gel (containing no water) can be treated as crude oil, suitable for regular refining processes (distillation and cracking). In fact, the recovered gel has a composition similar to the original crude oil (with only few % of i-Petrogel). During refining the gel, the minor component of the gel, which is the polyolefin interpenetrated network can be thermally decomposed back to small liquid hydrocarbon molecules without residue. Figure 4.13 shows a TGA (Thermogravimetric Analysis) curve of an x-D/DVB/LLDPE (1/1 weight ratio) interpenetrated polyolefin network material that can be thermally decomposed back to small hydrocarbon molecules without residue well below the typical crude oil refining temperature. Therefore, there would be little to no solid waste disposal.

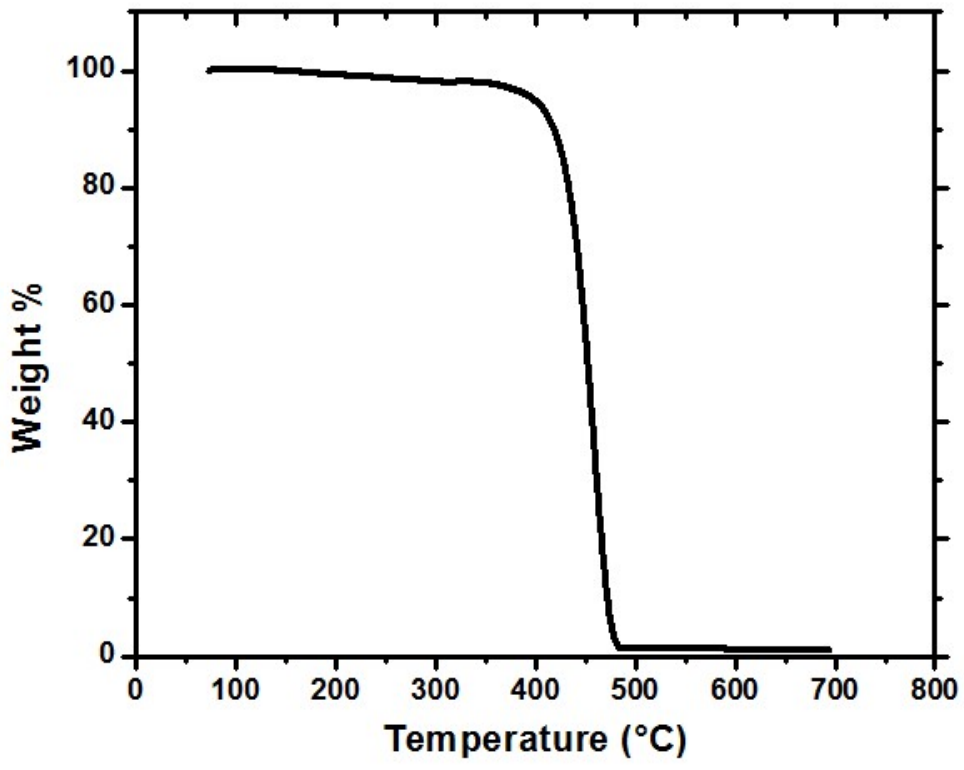

Figure 4-13. TGA curve of x-D/DVB/LLDPE (1/1) IPN material.

Figure 4.14 shows GC-Mass spectra of two resulting i-Petrogel-0.2 and i-Petrogel-0.02 (1:1 weight ratio) gels (after fully absorbing ANS oil) with ANS oil itself. Table 4.2 summarizes the chemical species with the GC retention time. It is fascinating to study the effect of i-Petrogel absorbent to the refining capability of the recovered ANS oil. All three GC-Mass spectra are almost indistinguishable. They are the same ANS oil mixture, and the couple percentage of i-Petrogel polymer in the gel mixture can be completely thermal-decomposed to liquid hydrocarbon (oil) molecules. The combination of this i-Petrogel thermal degradation property and its selective oil absorption capability (without water) is unique, which offers an oil spill recovery process without secondary pollution due to the disposal of recovered oil/water mixtures and solid wastes. It saves the environment and nature resource.

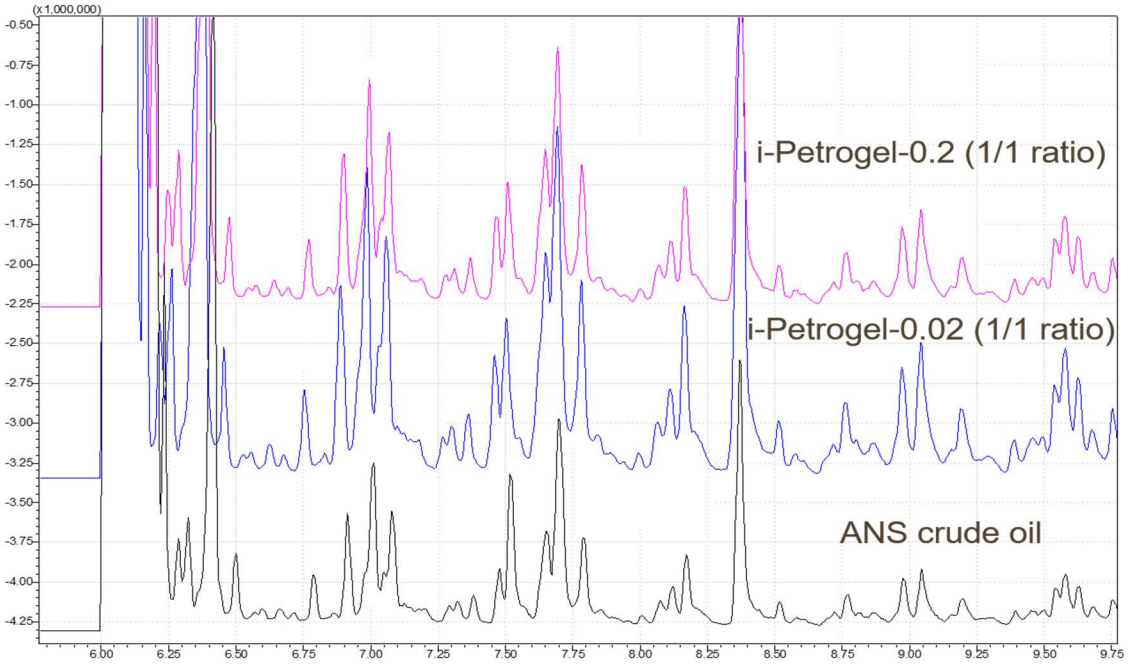

Figure 4-14. GC-Mass spectra of i-Petrogel-0.2 (1/1 wt. ratio)/ANS oil (pink), i-Petrogel-0.02 (1/1 wt. ratio)/ANS oil (blue), and ANS oil (black). The sample was ramped from 25 to 600°C in helium at a heating rate of 10 °C/min.

Table 4-2. List of components of a refined ANS oil identified by gas chromatography/mass spectrometry.

Ret. Time	Name	Ret. Time	Name	Ret. Time	Name
6.234	Cyclohexane, 1,4-dimethyl	7.08	Cyclohexane,1,1,2-trimethyl	8.371	Nonane
6.286	Cyclohexane, methyl-	7.478	1-Octene,4-methyl-	9.046	Tridecane, 3-methyl
6.323	Cyclepentane, 1-ethyl-2-meth	7.52	Ethylbenzene	10.286	Nonane
6.416	Octane	7.654	Octane,2-methyl-	11.986	Nonane
6.5	Cyclohexane, 1,4-dimethyl	7.7	Benzene, 1,2-dimethyl	13.525	Nonane
6.914	Heptane, 2,6-dimethyl-	7.791	Heptane,2,5-dimethyl	15.009	Octane, 2,7-dimethyl
7.01	1-Pentene, 3-ethyl-2-methyl	8.173	Benzene, 1,2-dimethyl		

4.6 Conclusion

In this Chapter, we have discovered a new chemical route to prepare polyolefin interpenetrated network. This invention is benefited from our new crosslinking chemistry that incorporates DVB crosslinker units into polyolefin chain via mono-enchainment manner, and the resulting pendant styrene units involve a facile thermal crosslinking reaction between two pendent styrene units to form network structure. With the available polyolefin crosslinking mechanism, we have systematically investigated a new class of i-Petrogel oil-superabsorbent polymer (oil-SAP) that contains two interpenetrated and connected x-D/DVB (soft) and LLDPE (rigid) polymer networks. We have successfully identified the most suitable i-Petrogel (0.2) composition with 1/1 weight ratio between x-D/DVB elastomer with 0.2 mol% DVB crosslinker and LLDPE (rigid) polymers. This oil-SAP shows fast ANS oil absorption kinetics and reaches the absorption capacity to 42 and 35 times of its weight after contacting with ANS oil for 24 h at 25 °C and 0 °C, respectively. Also, the resulting i-Petrogel (0.2)/ANS oil mixture (soft gel) contains no water, but floating on the water surface for easy recovery. The GC-Mass results indicate a complete absorption spectrum of all ANS hydrocarbon molecules by i-Petrogel (0.2), and the recovered i-Petrogel (0.2)/ANS oil mixture (soft gel) can be refined as the regular ANS oil. All the combined experimental results indicate that this i-Petrogel (0.2, with 1/1 weight ratio) shall be suitable for absorbing ANS oil under Alaska arctic condition.

Overall, the cross-linked polyolefin interpenetrated network materials exhibit a combination of benefits in oil recovery and cleanup, including (i) high oil absorption capability, (ii) fast kinetics, (iii) easy recovery from water surface, (iv) little to no water absorption, (v) minimal waste in natural resources, and (vi) cost effective and economic feasibility. All of these advantages indicate the potential impact on recovering oil spillage on the sea and providing temporary storage to prevent the spilled oil evaporated, emulsified, or spread to the shoreline by wind and waves. In addition, the flake form of i-Petrogel could be deployed (spreading) from a drone or airplane to save the precise time to minimizing the weathering process on the spilled oil. The combination of excellent mechanical strength and superoleophilicity assure its structure integrity, it shall be stable under severe weather conditions and recovery from the water surface by the available rotary drum-skimmer.

Chapter 5
Scaling-up and Field Testing of i-Petrogel Absorbent for Crude Oil Spillage

5.1 Introduction

As discussed, the discovery of an effective and practical method for oil spill recovery and cleanup is both scientific challenge and societal and industrial importance. A great deal of research efforts has been devoted in developing new sorbent materials with some success.[142–147] However, they are still far from the practical application for large-scale crude oil spillage in the open waters. Few of them had ever been scaled up for field tests.[143–146] The technology implementation commonly requires many optimizations in chemistry, processing, performance, and cost. It is essential to understand the kinetics, thermodynamics, and product properties to minimize the difference between lab and industrial scale productions.[154–156] With some practical and commercial interest in our i-Petrogel technology, we decided to demonstrate its large-scale production and field tests, to evaluate its suitability in the large-scale oil spillage applications.

As shown in Chapter 4, we have identified two suitable i-Petrogel-0.2 materials with 3/1 and 1/1 weight ratios between rigid LLDPE and soft D/DVB copolymer, which form an IPN network structure. In addition to learning the material scale-up process and conditions, the main objective was to prepare 25 pounds of two i-Petrogel absorbents for an operational evaluation at the Ohmsett facility, which was conducted by DOI and BSEE. As discussed, the preparation of i-Petrogel material involves two steps, including the first step of preparing both rigid and soft polyolefin polymers and then investigating the reactive-compounding process with a specific composition of two polymers and *in situ*

thermal-crosslinking reaction to form the desired i-Petrogel product with an interpenetrated polymer network. To carry out this polymer scale-up task, we first installed a pilot plant polymerization unit with the equipment for handling air-sensitive chemicals (catalysts and purified monomers). As shown in Figure 5.1, this system is centered at an autoclave (1 gallon) reactor with control units for chemical feeding, heating/cooling, and agitation. A drybox (with an inert atmosphere) was also deployed to prepare catalyst and purify monomers. With this complete system, we routinely produced about few pounds of polymer in each reaction cycle. This system can make 2-3 runs per day based on the availability of purified chemicals. In addition, a mixer (50 liters) was also installed for solution-mixing between LLDPE and D/DVB copolymer.

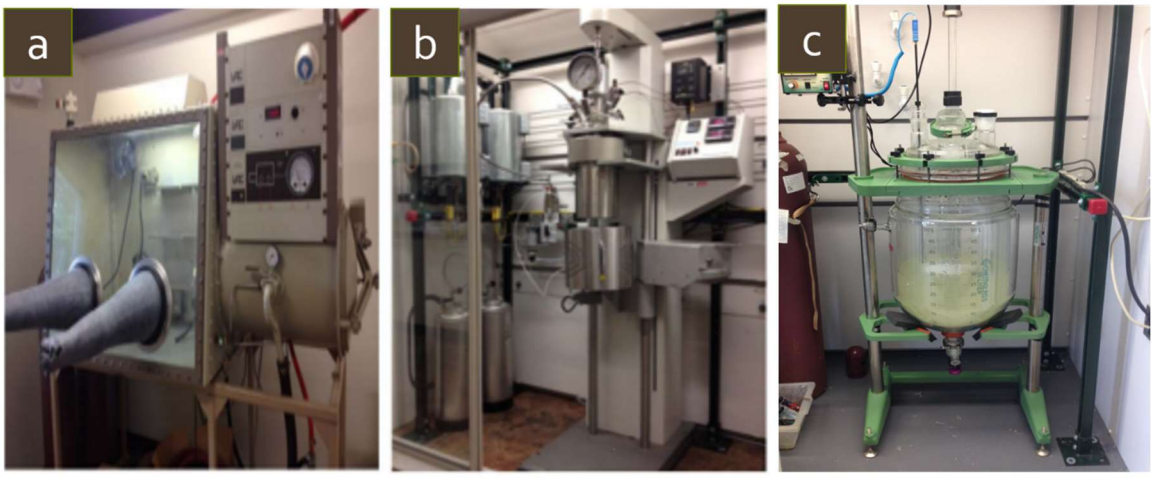

Figure 5-1. Images of (a) A dry box with inert atmosphere, (b) an 20 L pilot polymerization unit, and (c) a 50-liter mixer for scale-up.

5.2 Preparation and Characterization for Large Scale Production and Application

The first step involves heterogeneous $TiCl_3$.AA/Et_2AlCl catalyst mediated copolymerization reaction between 1-decene and DVB comonomer to prepare D/DVB copolymer. In addition to polymer productivity, it is essential to obtain high molecular weight polymer with narrow composition distribution for effective crosslinking reaction, which are influenced by the polymerization condition, such as temperature, catalyst concentration, and reaction time. The polymer molecular weight can drop with the increase of reaction temperature due to the dominance of the chain transfer reaction during polymerization.[157] Furthermore, a lab scale formula directly transforms to pilot plant is rarely feasible, due to heat dispersion, impurity content, etc. It is necessary to optimize the reaction temperature and catalyst concentration to achieve the desirable copolymer structure. Table 5.1 summarizes three pilot reaction runs with reduced catalyst concentration, 25%, 50%, and 75 % of the control lab scale run. This study is concentrated on the effect of catalyst concentration to polymer conversion rate and the amount of heat evolved during the reaction.

Table 5-1. The reaction conditions in three pilot scale-up reactions and one control run.

	Ratio	$TiCl_3$.AA	$Al(C_2H_5)_3$	1-Decene	DVB	Reaction Temp.
Run-1	Lab scale	0.1 g	0.8 ml	100 ml	0.2 ml	42 °C
Run-2	75%	15 g	120 ml	2.5 L	5 ml	60 °C
Run-3	50%	10g	80 ml	2.5 L	5 ml	62 °C
Run-4	25%	5g	40 ml	2.5 L	5 ml	45 °C

Figure 5.2a shows the reaction temperature for each reaction run, which was sharply increased for 1 h before reaching to the steady state. It was well known that the high internal temperature reduces polymer molecular weight but increase the copolymer incorporation and homogenity.[158] The temperature usually raised linearly with catalyst concentration. However, for R50 (62 °C) and R75 (60 °C) did increase similarly with increasing time, because the initial temperature of R75 (19 °C) was slightly lower than R50 (22°C). Thus, it is understandable that temperature at R50, R75 were reached a similar temperature. The typical conversion rate of 1-decene/DVB copolymerization in the lab scale was <70%, The conversion rate for two pilot scale runs reach to more than 80% with less catalyst, indicating higher catalyst activity.

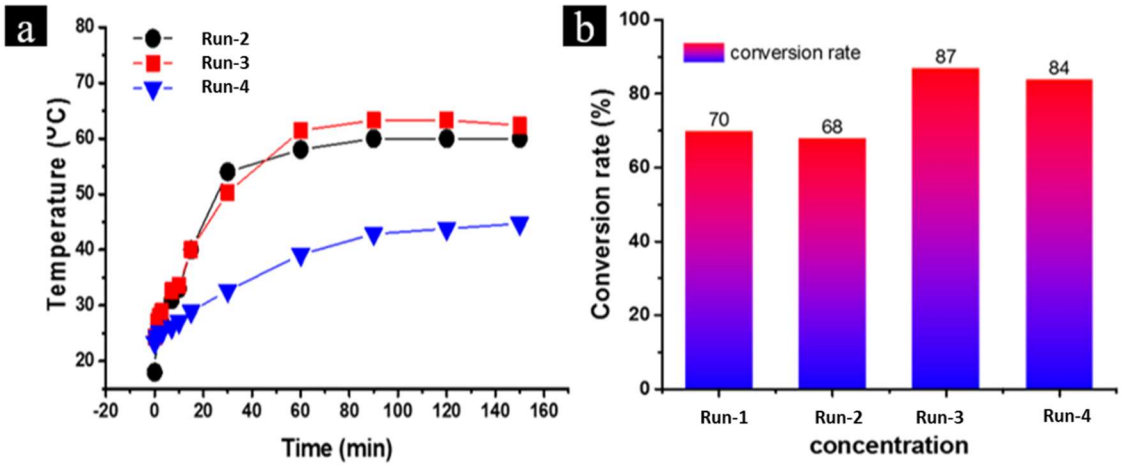

Figure 5-2. Scale up study of 1-decene/DVB copolymerization with different catalyst concentration as a function of (a) reaction temperature and (b) conversion ratio (%).

Figure 5.3a shows the ^{1}H NMR spectrum of a D/DVB copolymer (Run-4). In addition to a chemical shift at 0.8 ppm, corresponding to C**H**$_3$ in the 1- decene units, and a band between 0.9 and 1.7 ppm, corresponding to C**H**$_2$ and C**H** in the polymer backbone, there are three bands around 5.2 and 5.7 ppm (CH=C**H**$_2$) and 6.7 ppm (C**H**=CH$_2$); and an aromatic proton band between 6.9 and 7.4 ppm (C$_6$**H**$_4$). The integrated intensity ratio between all three vinyl protons and the four phenyl protons determine the vinyl/phenyl mole ratio, which is near unity. The experimental results confirm the monoenchainment of DVB comonomers in forming the processible D/DVB copolymer.

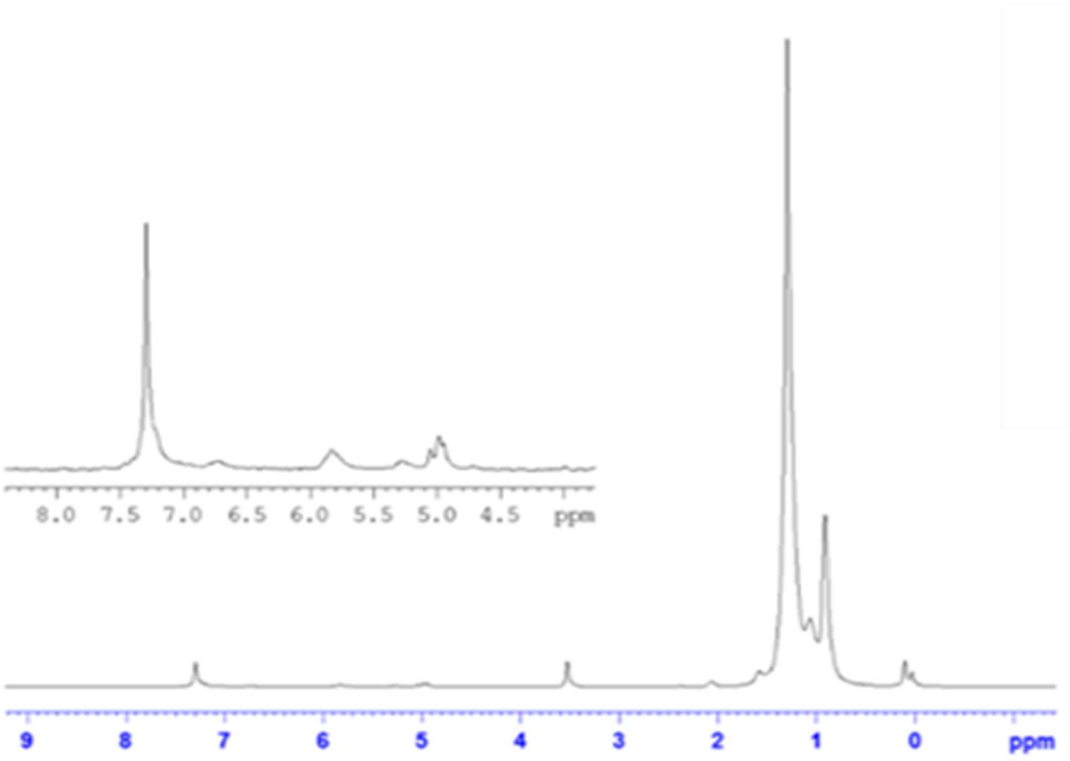

Figure 5-3. Characterization of 1-decene/DVB copolymer with ^{1}H-NMR.

The resulting three D/DVB copolymer samples were used to prepare i-Petrogel flake-form with 1/1 soft/rigid polymer ratio, following the similar processing condition shown in Chapter 4. They were then examined the ANS oil absorption capacity and kinetics. As shown in Figure 5.4, the oil absorption capacity of i-Petrogel (R75%) is 37 times of its own weight after 24 h. Interestingly, the absorption capacity of the i-Petrogel is inversely proportional to the catalyst concentration. The ANS oil absorption capacity of i-Petrogel (R25%) reaches to 43 times, almost the same shown in the lab scale sample. In addition, the absorbed oil/i-Petrogel adducts is also easier to recover by tweezer. Due to higher molecular weight and lower DVB incorporation in the D/DVB copolymer (R25%) that enhances polymer swelling and coagulation.

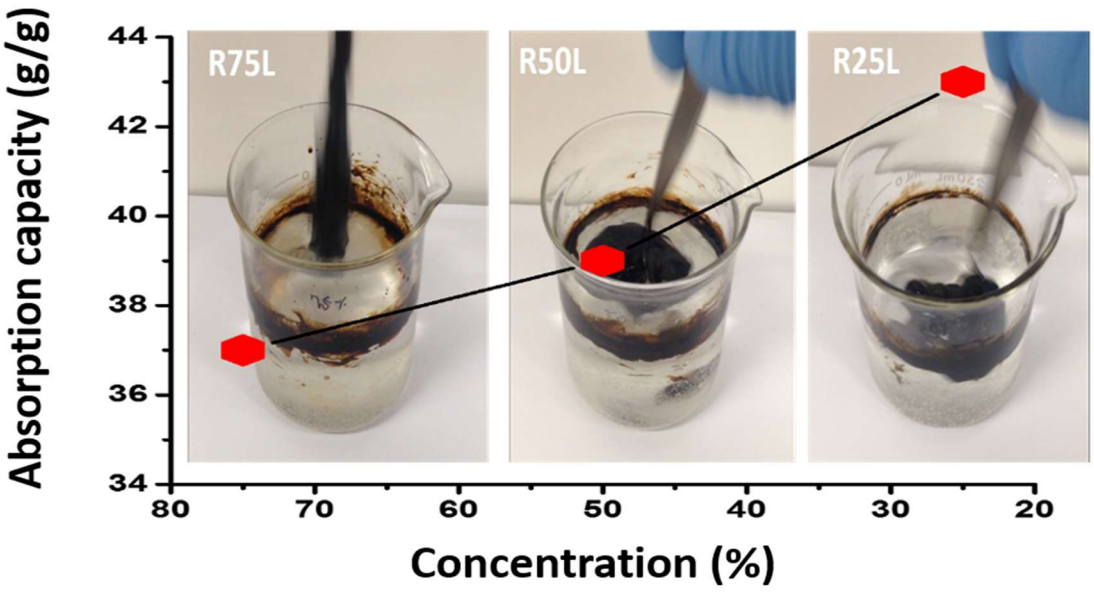

Figure 5-4. Crude oil absorption capacity with different absorbents and images of oil absorbed gel.

5.3 Field Tests

Between October 5-8, 2015, BSEE conducted an operational test at the Ohmsett facility to evaluate oil spill recovery using two scaled-up i-Petrogel absorbents containing 1/1 and 3/1 weight ratio. They are the same i-Petrogel materials showing good ANS oil absorption capacities (Chapter 4). This operational test was performed in two open tanks, containing seawater and the weathered Alaska North Slope (ANS) crude oil, using 20 pounds of i-Petrogel material (10 pounds each). The test focused on oil absorption capacity, recovery of the oil/polymer adducts on water surface by mechanical skimmers, and the ability of the resulting oil/polymer adducts to be pumped into a storage tank.

The main objective was to identify the performance of i-Petrogel absorbent and understand the opportunities and barriers for large scale implementation of i-Petrogel technology in an oil spilled site on an open water surface. For the oil absorption tests, a specified amount (20 gallons) of 10 % weathered Alaska North Slope (ANS) oil was added to a 10’ x 10’ x 3 foot deep portable frame water tank containing seawater (salinity=33ppt). The oil slick was about 8-9 mm thick and the tank was placed in the open air (outdoor). In order to understand the effect of the structure and composition of the materials on the oil absorption and recovery, two i-Petrogel flakes with 1/1 and 3/1 weight ratios between rigid and flexible polymers were evaluated under similar operational conditions. They were sprinkled onto the oil surface in the tank, evenly covering the surface.

During the testing period, the outdoor weather was fair with clear sky and a temperature range between 50 (night) and 75 °F (noon). Both oil and water temperatures were monitored during the tests. At the end of absorption period, we gently agitated the surface with a stick for about 10 min to ensure complete contact between oil and i-Petrogel flakes. Two skimmers were applied, including an Elastec TDS 118 oleophilic drum skimmer and a double diaphragm vacuum pump skimmer to study the recovery operation and efficiency.

Several samples were isolated either directly from the testing surface or from the recovered oil by the skimmer. Figure 5.5 shows several images during the oil absorption operation. First, 3.75 pounds of i-Petrogel with a 1/1 weight ratio, shown in image (a), were uniformly spread onto the surface of 20 gallons of 10% weathered ANS oil (40:1 oil/polymer weight ratio), shown in image (b). The mixed ANS oil/i-Petrogel surface was left overnight (about 18 hours), without agitation (calm winds). After this spontaneous absorption period, the mixture shown in image (c) became a film like gel material with a relatively uniform and bright surface and some swelled gel particles. There is a viscous fluid floating on the water surface that can be physically picked up and recovered by simple sticks or nets. As shown in image (d), they can be effectively recovered by an Elastec TDS 118 oleophilic drum skimmer with various speeds. Although the high drum rotation speed (>20 rpms) increased the recovery rate, it also picked up some water drops along with the recovered ANS oil/i-Petrogel fluid as shown in image (e). It is interesting to note that the viscous ANS oil/i-Petrogel fluid exhibits good adhesion to the HDPE drum surface and also provides a continuous oil/i-Petrogel fluid flow toward the rotating drums during the recovery. As shown in image (f), the recovered ANS oil/i-Petrogel fluid can also be pumped using a centrifugal or double diaphragm pump.

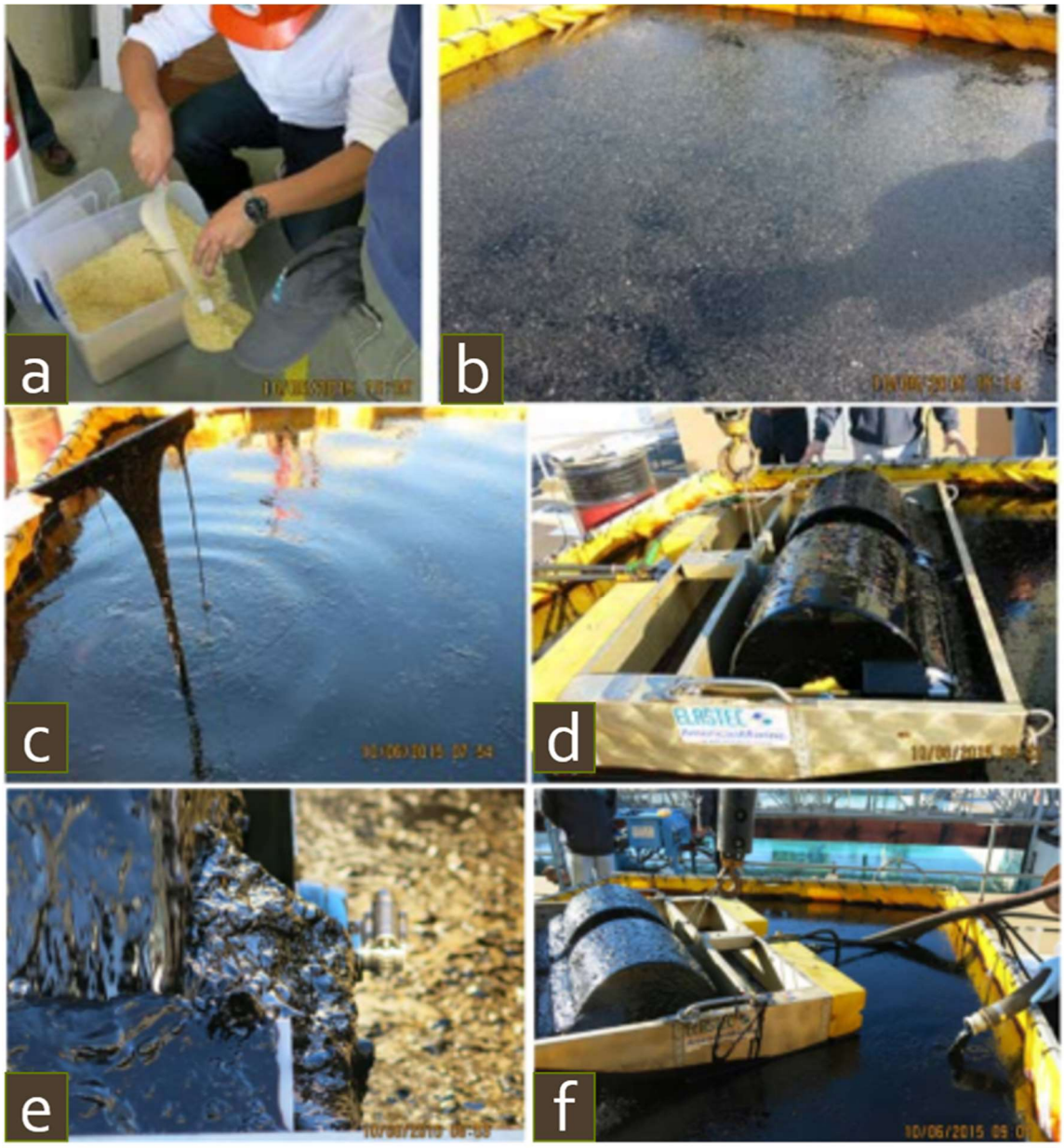

Figure 5-5. (a) The scaled-up i-Petrogel flakes with 1/1 weight ratio, (b) after spreading i-Petrogel flakes onto the oil surface, (c) after 18 hours absorption time, (d) recovery of ANS oil/i-Petrogel fluid by an Elastec TDS 118 oleophilic drum skimmer, (e) the recovered ANS oil/i-Petrogel fluid with high drum rotation speed, and (f) pumping of the recovered ANS oil/i-Petrogel fluid.

Figure 5.6 shows two images during another absorption test with 3:1 weight ratio that was carried out under similar operation in 1/1 weight ratio, except using the i-Petrogel with a 3/1 weight ratio. The same 3.75 pounds of iPetrogel with a 3/1 weight ratio was spread onto the surface of 20 gallons of 10% weathered ANS oil (40:1 oil/polymer weight ratio), and the mixture was left overnight under similar weather conditions. Figure 5./a shows the ANS oil/i-Petrogel surface after 18 hours of spontaneous oil absorption. The resulting ANS oil/i-Petrogel adduct forms cohesive (sheet-like) gel that can be easily picked up and recovered by simple sticks or nets, as shown in Figure 5.6b. However, the recovery by an Elastec TDS 118 oleophilic drum skimmer requires some physical assistance to move the sheet-like ANS oil/i-Petrogel adduct toward the rotating drums. In addition, the recovered viscous adduct also showed some pumping difficulties.

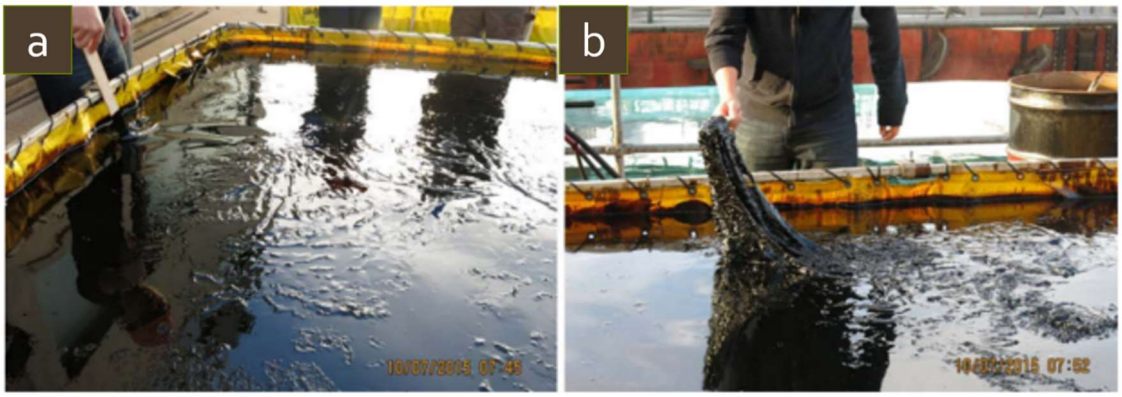

Figure 5-6. The sheet-like ANS oil/i-Petrogel (3/1) adduct, (b) recovery of ANS oil/i-Petrogel sheet by a simple stick.

The same set of the recovered ANS oil/i-Petrogel samples were provided to all three organizations – Penn State, BSEE, and Ohmsett – for further analysis. At Penn State, we focused on the water contents and refinery characteristics of these recovered samples. Water content in the recovered samples were determined by the phase-separated water. As shown in Figure 5.7, the trapped water is slowly phase-separated from the recovered ANS oil/i-Petrogel fluids and they are clearly observed in the bottom of sample and sample bottles. We usually sampled the top layer of the ANS oil/i-Petrogel fluids for all the measurements. The first experiment was conducted by diluting the recovered ANS oil/i-Petrogel sample with dry toluene to reduce the material viscosity. As shown in Figure 5.9, the mixed solution was then placed in a burette for 24 hours to separate the trapped water and remove the contaminated water at the bottom of the burette. The water content in samples were very low (<0.1 wt%). Other samples have significantly higher water content, associated with the drum rotation speed, the viscosity of ANS oil/i-Petrogel fluid, and the setting time. It is interesting to note that some different water content results were observed by the Ohmsett technicians, despite applying a similar measurement method. The deviation may be due to the sampling of experimental specimens from the mixed solutions, not the top of the recovered sample as was done in our case.

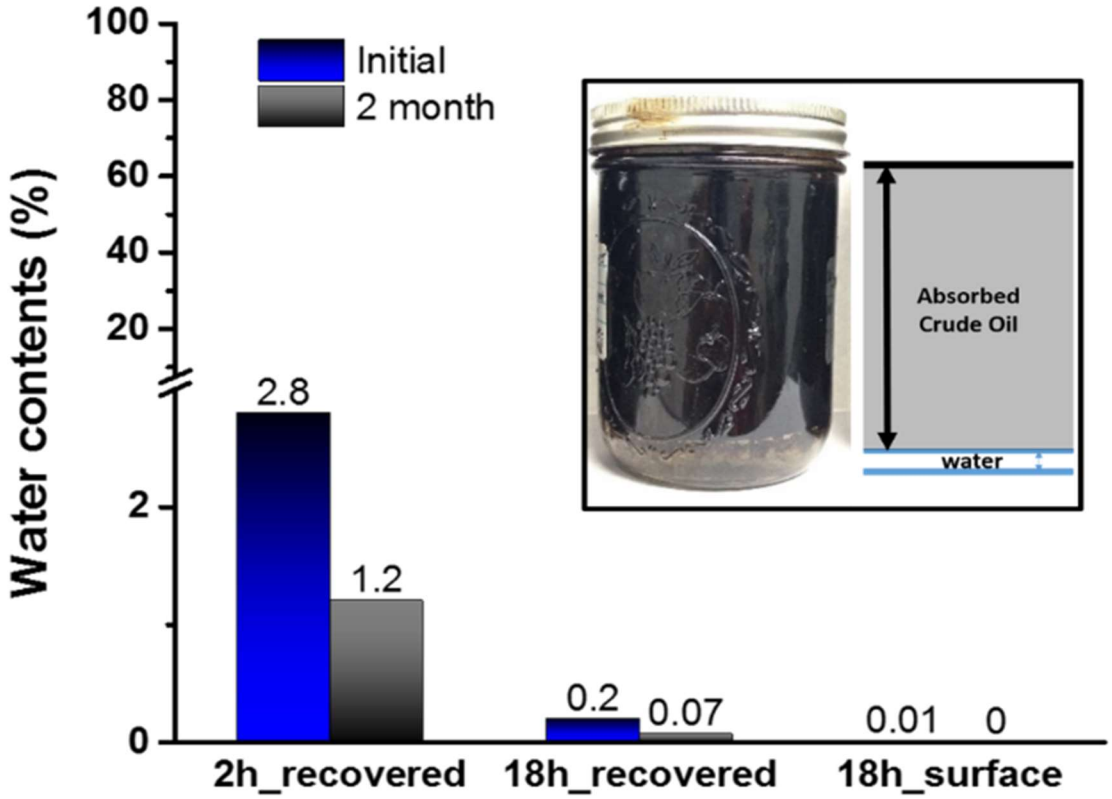

Figure 5-7. Water contents in the recovered samples with the different condition at initial (blue) and after two months (gray) and the 2h-recovered samples after two months (inset).

For comparison, we have also evaluated several commercial oil-sorbents under water sorption conditions at ambient temperature. Figure 5.8 shows the water-sorption profiles for these commercial oil sorbents. It's clear that there are two classes of commercial oil-sorbents in terms of oil/water selectivity (Chapter 2). Both PP fiber (#1) and EPDM Rubberizer (#3) are prepared from pure hydrocarbon polymers with hydrophobicity to prevent water sorption. On the other hand, the recycled cellulose (#2) and two polyurethane foams (#4 and #5) are quite hydrophilic with significant water-sorption capacity, more than 5 times of the polymer weight.

Recovering oil with contaminated water is problematic; it is designed as a pollutant instead of an asset. As discussed, a unique feature of i-Petrogel is its ability for recovery and reuse of the oil/iPetrogel adducts. Because Petrogel doesn't absorb water and is less dense than water, after absorbing ANS oil, the resulting oil/i-Petrogel adducts float on the water's surface and is easy to see and recover. The recovered oil/i-Petrogel adducts contain >97% ANS oil and <3% polyolefin (hydrocarbon polymer). It is very interesting to understand the refining capability of these adducts. They are essentially the same as the ANS oil mixture. The low percentage of i-Petrogel polymer in the gel mixture can be completely thermally decomposed to liquid hydrocarbon (oil) molecules. This combination of i-Petrogel's thermal degradation property and its selective oil absorption capability (without water) is very unique, and may offers an oil spill recovery process without secondary pollution caused by the disposal of recovered oil/water mixtures and solid wastes.

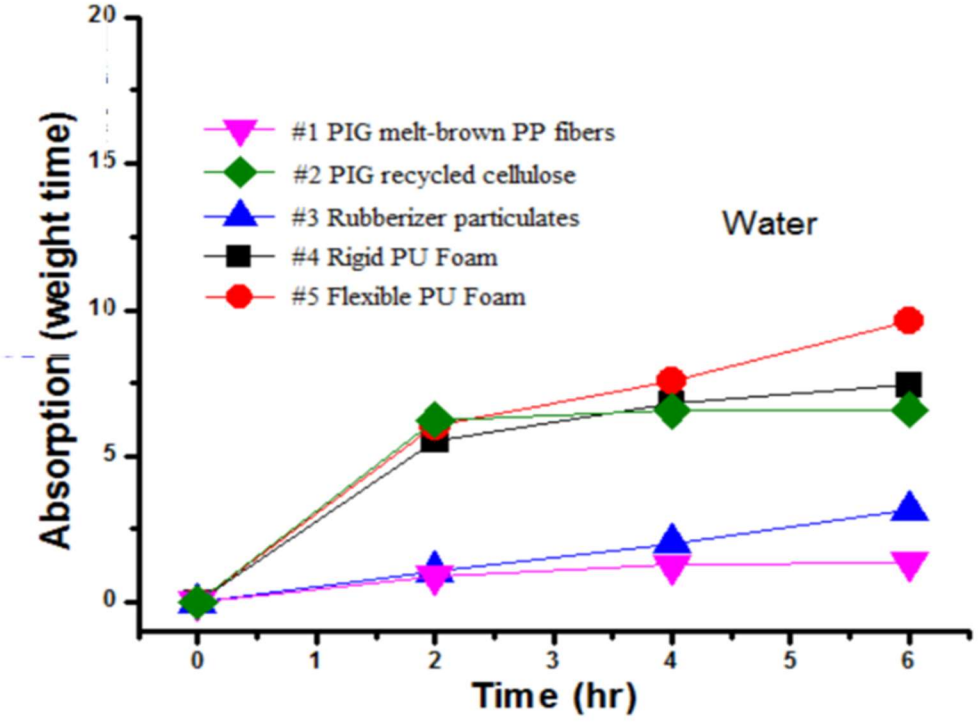

Figure 5.8 Water sorption capacity with different types of commercial sorbents.

5.4 Conclusions

Overall, we have successfully conducted the scale-up i-Petrogel production and field tests and achieved the major milestones and targets required for the practical applications. The operational testing results in Ohmsett were very encouraging. They were consistent with the experimental results observed at the Penn State laboratory. We can draw several conclusions, discussed below:

1. i-Petrogel material: We have identified the most suitable i-Petrogel IPN structure that can effectively and efficiently recover the spilled ANS oil on seawater surfaces. The material scale-up process, including polymer preparation and processing into various forms, has been developed for the mass production of various i-Petrogel products.
2. ANS oil absorption capacity and kinetics: i-Petrogel oil-absorbent is capable of absorbing ANS oil 35-40 times the capacity under 25 and 0 °C. The absorption kinetics are fast in the first 2-3 hours reaching 80-90% saturation. The i-Petrogel with a 1:1 rigid/soft polymer weight ratio absorbs slightly more ANS oil to form the viscous ANS oil/i-Petrogel fluid. On the other hand, the i-Petrogel with a 3:1 rigid/soft polymer weight ratio forms the sheet-like ANS oil/i-Petrogel adduct.
3. Recovery by skimmers and pumping ability: The Elastec TDS 118 oleophilic (HDPE) drum skimmer (with a smooth drum surface) showed effective recovery of the ANS oil/i-Petrogel viscous fluids, involving the i-Petrogel with a 1/1 rigid/soft polymer weight ratio. At a high drum rotational speed (with a high recovery rate), some water drops accompanied the recovered oil/i-Petrogel viscous fluid. The

recovered oil/i-Petrogel fluid can be effectively pumped using the metered pump pallet from the skimmer sump to the storage tank. However, the (sheet-like) gel requires some assistance to be picked up by the rotating drum skimmer. In addition, the recovered viscous adducts also show some difficulties during pumping.

4. Water content in the recovered ANS Oil/i-Petrogel adducts: The water content in the recovered sample is associated with the viscosity of the ANS oil/i-Petrogel fluid, the speed of skimmer drum rotation, and the sample setting time to allow for water phase separation. The trapped water content in the samples, using the i-Petrogel (1/1 wt. ratio) absorbent, are significantly less than the samples, using i-Petrogel with a 3/1 wt. ratio.
5. Reusing the recovered ANS oil/i-Petrogel fluids: Based on the GC-Mass measurements, the recovered ANS oil/i-Petrogel fluids (without water) show identical spectra with that of the original ANS oil. Combining with the TGA results of i-Petrogel polymer that is completely degraded to small organic molecules at < 400 °C, the recovered ANS oil/i-Petrogel fluids can be refined as ANS oil using regular refining processes, preventing secondary pollution that is caused by the disposal of recovered materials.

Chapter 6

Conclusions and Future Works

6.1 Summary of Present Work

Despite the advance in clean energy technology, we are still largely dependent on crude oil for energy and basic chemicals for the foreseeable future. A large-scale oil spill happens rarely and makes news, but many small scale oil spills are daily occurrances in various transport and storage facilities. Whenever, there is an oil spill accident, we should try to recover the spilled oil as soon as possible before the weathering of the oil, which results in more severe environmental pollutions and increases the recovery difficulties. The oil spill in the ocean can cause wide ranging problems for the environment and biological systems. A polymer-based porous sorbent would be an ideal method to mitigate the damages, with many potential benefits such as easy handling, fast response, fast sorption kinetics, high absorption capacity, and easy recovery. However, the current oil sorbent technology has many limitations and is still not suitable for the large-scale crude oil spillage. In this study, I have conducted a systematic study on polyolefin based oil absorbents (Petrogel) by examining both semicrystalline polyolefin thermoplastics and amorphous polyolefin elastomers to understand their advantages and disadvantages and the structure-property relationship. The research results direct us to the discovery of a polyolefin absorbent with an interpenetrated network (i-Petrogel), which contains both elastic (soft) and thermoplastic (rigid) intertwined networks. Some key results are summarized in the following sections.

6.1.1 Amorphous and Semi-Crystalline Polyolefin Polymers

In this research (Chapter 3), we have systemically studied the relationship between the polymer morphology and oil absorption capacity in both amorphous and semi-crystalline polyolefins that contain large free volume for solvent swelling. The crosslinked amorphous copolymer reveals that the combination of low crosslinking density but a complete network is critical in absorption performance. It is difficult to form the desirable porous structure in the low Tg elastomer with low crosslinking density. In the dense polyolefin elastomer, high absorption capacity (>40 times) can be reached with organic solvents and refined oil products with low viscosity, but the absorption capacity is poor for viscous crude oil with slow kinetics. On the other hand, semi-crystalline LLDPE can be fabricated in different types (pellet, film and sponge) and degrees of density. The resulting foam and casting film were suitable for crude oil absorption with fast kinetics, but the absorption is limited by the degree of crystallinity that is not oil swellable.

6.1.2 IPN Polyolefin-Based Polymers

We have successfully developed a new polyolefin structure with an interpenetrated polymer network (i-Petrogel) that contains both semicrystalline (rigid) and amorphous low Tg (soft) polyolefin chains (Chapter 4). The i-Petrogel was directly fabricated by mixing LLDPE and 1-decene/DVB copolymer and the subsequent thermal crosslinking reaction. TEM micrographs and strain-stress curves provide the experimental evidence to show the IPN structure The homogeneous distribution of rigid polymer segments offers the stability of porous morphology with high surface area and short oil diffusion path, as well as high free volume in the elastic polymer matrix. The combination is essential for the absorption of viscous crude oil with >40 times absorption capacity and fast kinetics. Although the DVB monomer units are necessary to create the network structure, too much DVB crosslinkers can restrict the network swelling and reduce the overall oil absorption capacity. In addition, the i-Petrogel composition can be conveniently adjusted to alter the uptake and recovery properties by applying different LLDPE polymers with various degrees of crystallinity and melting temperatures. Changing the mixing ratio between 1-decene/DVB and LLDPE will also affect the oil absorption capacity and recovery properties. It is interesting to note that the absorption capacity is not much affected by the operational temperature, even in the icy water condition.

6.1.3 Scale Up and Practical Applications

A systematic scale-up study (using 20-liter reactor) was conducted with various reaction conditions, including catalyst concentration, to identify the most suitable condition to prepare the 1-decene/DVB copolymer with the desirable molecular structure, i.e. high molecular weight and controllable DVB (crosslinker) content with a narrow copolymer composition distribution. The copolymerization reactions were monitored by reaction temperature and polymer yield. Only a quarter of catalyst used in conventional polymerization is required for large scale D/DVB synthesis, which excreted low heating energy during the polymerization and the reaction temperature was maintained low and stable, similar to that in lab scale (500 ml reactor) polymerization. The combination with low catalyst concentration, the resulting D/DVB copolymer shows molecular weight, low DVB content, and narrow composition distribution. This copolymer structure is most suitable for the fabrication of i-Petrogel absorbent with high ANS oil absorption capacity (>40 times). The results reveal that 25% (original catalyst ratio to the monomer in lab scale) concentration of catalyst is the optimal condition for the large scale production. BSEE also conducted large scale crude oil clean up test at the Ohmsett facility. Both i-Petrogel, with 1/1 and 1/3 (x- D/DVB: LLDPE) weight ratio, shows high oil absorption capacity (40 times), consistent with the lab scale tests, and the resulting absorbed ANS oil/i-Petrogel adducts can be easily recovered by regular drum skimmer and transport by pumping to storage tank. (Chapter 5).

6.2 Suggested Future Works

In the commercialization of i-Petrogel, both performance and economic considerations are very important. The current i-Petrogel production process involves solution casting film and subsequent breaking the resulting (dry) film into flake form by blender, which is slow, expensive, and not suitable for large scale production. It is still an engineering challenge to design an alternative economically feasible method, involving polymer melt and extrusion/foaming to create new i-Petrogel products with similar high surface area and short oil diffusion path morphology.

In addition, it may be possible to extend the application to various operational areas and conditions, involving various crude oils from all over the world. The i-Petrogel may also be designed in different product forms that can be conveniently deployed in many small-scale oil spills to recover and prevent the spilled oil. Like Hydrogels, it may be further developed this i-Petrogel technology for the storage and slow release applications.

References

(1) Lee, K.; Levy, E. M. Bioremediation: Waxy Crude Oils Stranded on Low-Energy Shorelines. *Int. Oil Spill Conf. Proc.* **1991**, *1991* (1), 541–547.

(2) Rogowska, J.; Namieśnik, J. Environmental Implications of Oil Spills from Shipping Accidents. In *Reviews of Environmental Contamination and Toxicology Volume 206*; Whitacre, M. D., Ed.; Springer New York: New York, NY, 2010; pp 95–114.

(3) Moles, A.; Holland, L.; Short, J. Effectiveness in the Laboratory of Corexit 9527 and 9500 in Dispersing Fresh, Weathered, and Emulsion of Alaska North Slope Crude Oil under Subarctic Conditions. *Spill Sci. Technol. Bull.* **2002**, *7* (5–6), 241–247.

(4) Cheng, M.; Gao, Y.; Guo, X.; Shi, Z.; Chen, J. F.; Shi, F. A Functionally Integrated Device for Effective and Facile Oil Spill Cleanup. *Langmuir* **2011**, *27*, 7371–7375.

(5) Wang, C. F.; Tzeng, F. S.; Chen, H. G.; Chang, C. J. Ultraviolet-Durable Superhydrophobic Zinc Oxide-Coated Mesh Films for Surface and Underwater-Oil Capture and Transportation. *Langmuir* **2012**, *28* (26), 10015–10019.

(6) Wong, K. F. V.; Barin, E. Oil Spill Containment by a Flexible Boom System. *Spill Sci. Technol. Bull.* **2003**, *8* (5–6), 509–520.

(7) Xue, Z.; Cao, Y.; Liu, N.; Feng, L.; Jiang, L. Special Wettable Materials for Oil/water Separation. *J. Mater. Chem. A* **2014**, *2*, 2445–2460.

(8) Office of the Auditor General of Canada. *Report of the Commissioner of the Environment and Sustainable Development to the House of Commons: Chapter 1—Oil Spills from Ships*; 2010.

(9) Ochoa, J. E.; Guerra, C. R.; Stern, C. *Experimental and Theoretical Advances in Fluid Dynamics*; 2012.

(10) Ceylan, D.; Dogu, S.; Karacik, B.; Yakan, S. D.; Okay, O. S.; Okay, O. Evaluation of Butyl Rubber as Sorbent Material for the Removal of Oil and Polycyclic Aromatic Hydrocarbons from Seawater. *Environ. Sci. Technol.* **2009**, *43* (10), 3846–3852.

(11) Wu, D.; Fang, L.; Qin, Y.; Wu, W.; Mao, C.; Zhu, H. Oil Sorbents with High Sorption Capacity, Oil/water Selectivity and Reusability for Oil Spill Cleanup. *Mar. Pollut. Bull.* **2014**, *84* (1–2), 263–267.

(12) Radeti??, M. M.; Joci??, D. M.; Jovan??i??, P. M.; Petrovi??, Z. L.; Thomas, H. F. Recycled Wool-Based Nonwoven Material as an Oil Sorbent. *Environ. Sci. Technol.* **2003**, *37* (5), 1008–1012.

(13) Zhu, H.; Qiu, S.; Jiang, W.; Wu, D.; Zhang, C. Evaluation of Electrospun Polyvinyl Chloride/Polystyrene Fibers As Sorbent Materials for Oil Spill Cleanup. *Environ. Sci. Technol.* **2011**, *45* (10), 4527–4531.

(14) Li, H.; Liu, L.; Yang, F. Hydrophobic Modification of Polyurethane Foam for Oil Spill Cleanup. *Mar. Pollut. Bull.* **2012**, *64* (8), 1648–1653.

(15) Kujawinski, E. B.; Kido Soule, M. C.; Valentine, D. L.; Boysen, A. K.;

Longnecker, K.; Redmond, M. C. Fate of Dispersants Associated with the Deepwater Horizon Oil Spill. *Environ. Sci. Technol.* **2011**, *45* (4), 1298–1306.
(16) Shigenaka, G. *Twenty-Five Years After the Exxon Valdez Oil Spill: NOAA's Scientific Support, Monitoring, and Research. Seattle: NOAA Office of Response and Restoration*; 2014.
(17) Mutelet, F.; Ekulu, G.; Solimando, R.; Rogalski, M. Solubility Parameters of Crude Oils and Asphaltenes. *Energy & Fuels* **2004**, *18* (3), 667–673.
(18) WICHTERLE, O.; LIM, D. Hydrophilic Gels for Biological Use. *Nature* **1960**, *185* (4706), 117–118.
(19) Tokatlian, T.; Cam, C.; Segura, T. Porous Hyaluronic Acid Hydrogels for Localized Nonviral DNA Delivery in a Diabetic Wound Healing Model. *Adv. Healthc. Mater.* **2015**, *4* (7), 1084–1091.
(20) Bagheri Marandi, G.; Mahdavinia, G. R.; Ghafary, S. Swelling Behavior of Novel Protein-Based Superabsorbent Nanocomposite. *J. Appl. Polym. Sci.* **2011**, *120* (2), 1170–1179.
(21) Zhang, L.; Cao, Z.; Bai, T.; Carr, L.; Ella-Menye, J.-R.; Irvin, C.; Ratner, B. D.; Jiang, S. Zwitterionic Hydrogels Implanted in Mice Resist the Foreign-Body Reaction. *Nat Biotech* **2013**, *31* (6), 553–556.
(22) Guilherme, M. R.; Reis, A. V; Takahashi, S. H.; Rubira, A. F.; Feitosa, J. P. A.; Muniz, E. C. Synthesis of a Novel Superabsorbent Hydrogel by Copolymerization of Acrylamide and Cashew Gum Modified with Glycidyl Methacrylate. *Carbohydr. Polym.* **2005**, *61* (4), 464–471.
(23) Mudiyanselage, T. K.; Neckers, D. C. Highly Absorbing Superabsorbent Polymer. *J. Polym. Sci. Part A Polym. Chem.* **2008**, *46* (4), 1357–1364.
(24) Cipriano, B. H.; Banik, S. J.; Sharma, R.; Rumore, D.; Hwang, W.; Briber, R. M.; Raghavan, S. R. Superabsorbent Hydrogels That Are Robust and Highly Stretchable. *Macromolecules* **2014**, *47* (13), 4445–4452.
(25) Liu, Z.; Miao, Y.; Wang, Z.; Yin, G. Synthesis and Characterization of a Novel Super-Absorbent Based on Chemically Modified Pulverized Wheat Straw and Acrylic Acid. *Carbohydr. Polym.* **2009**, *77* (1), 131–135.
(26) Holst, J. R.; Cooper, A. I. Ultrahigh Surface Area in Porous Solids. *Adv. Mater.* **2010**, *22* (45), 5212–5216.
(27) Chahine, R.; Bénard, P. Advances in Cryogenic Engineering; Kittel, P., Ed.; Springer US: Boston, MA, 1998; pp 1257–1264.
(28) Yaghi, O. M.; O'Keeffe, M.; Ockwig, N. W.; Chae, H. K.; Eddaoudi, M.; Kim, J. Reticular Synthesis and the Design of New Materials. *Nature* **2003**, *423* (6941), 705–714.
(29) Dillon, A. C.; Jones, K. M.; Bekkedahl, T. A.; Kiang, C. H.; Bethune, D. S.; Heben, M. J. Storage of Hydrogen in Single-Walled Carbon Nanotubes. *Nature* **1997**, *386* (6623), 377–379.
(30) Chung, T. C. M.; Jeong, Y.; Chen, Q.; Kleinhammes, A.; Wu, Y. Synthesis of Microporous Boron-Substituted Carbon (B/C) Materials Using Polymeric Precursors for Hydrogen Physisorption. *J. Am. Chem. Soc.* **2008**, *130* (21), 6668–6669.
(31) Wood, C. D.; Tan, B.; Trewin, A.; Su, F.; Rosseinsky, M. J.; Bradshaw, D.; Sun,

Y.; Zhou, L.; Cooper, A. I. Microporous Organic Polymers for Methane Storage. *Adv. Mater.* **2008**, *20* (10), 1916–1921.

(32) Tokarev, I.; Minko, S. Stimuli-Responsive Porous Hydrogels at Interfaces for Molecular Filtration, Separation, Controlled Release, and Gating in Capsules and Membranes. *Adv. Mater.* **2010**, *22* (31), 3446–3462.

(33) Chen, Q.; Luo, M.; Hammershøj, P.; Zhou, D.; Han, Y.; Laursen, B. W.; Yan, C.-G.; Han, B.-H. Microporous Polycarbazole with High Specific Surface Area for Gas Storage and Separation. *J. Am. Chem. Soc.* **2012**, *134* (14), 6084–6087.

(34) Buchholz, F.; Graham, A. *Modern Superabsorbent Polymer Technology*; Wiley Subscription Services, Inc., A Wiley Company: New York, 1998.

(35) Zohuriaan-Mehr, M. J.; Omidian, H.; Doroudiani, S.; Kabiri, K. Advances in Non-Hygienic Applications of Superabsorbent Hydrogel Materials. *J. Mater. Sci.* **2010**, *45* (21), 5711–5735.

(36) Kim, S. J.; Park, S. J.; Kim, S. I. Swelling Behavior of Interpenetrating Polymer Network Hydrogels Composed of Poly(vinyl Alcohol) and Chitosan. *React. Funct. Polym.* **2003**, *55* (1), 53–59.

(37) Haraguchi, K.; Li, H.-J.; Okumura, N. Hydrogels with Hydrophobic Surfaces: Abnormally High Contact Angles for Water on PNIPA Nanocomposite Hydrogels. *Macromolecules* **2007**, *40* (7), 2299–2302.

(38) Shan, G.-R.; Xu, P.-Y.; Weng, Z.-X.; Huang, Z.-M. Synthesis and Properties of Oil Absorption Resins Filled with Polybutadiene. *J. Appl. Polym. Sci.* **2003**, *89* (12), 3309–3314.

(39) Davis, E. M.; Elabd, Y. a. Prediction of Water Solubility in Glassy Polymers Using Nonequilibrium Thermodynamics. *Ind. Eng. Chem. Res.* **2013**, *52* (36), 12865–12875.

(40) Peppas, N. A.; Moynihan, H. J.; Lucht, L. M. The Structure of Highly Crosslinked poly(2-Hydroxyethyl Methacrylate) Hydrogels. *J. Biomed. Mater. Res.* **1985**, *19* (4), 397–411.

(41) Jang, J.; Kim, B.-S. Studies of Crosslinked Styrene–alkyl Acrylate Copolymers for Oil Absorbency Application. I. Synthesis and Characterization. *J. Appl. Polym. Sci.* **2000**, *77* (4), 903–913.

(42) Xue, W.; Hamley, I. W.; Huglin, M. B. Rapid Swelling and Deswelling of Thermoreversible Hydrophobically Modified poly(N-Isopropylacrylamide) Hydrogels Prepared by Freezing Polymerisation. *Polymer (Guildf).* **2002**, *43* (19), 5181–5186.

(43) Osada, Y.; Ping Gong, J.; Tanaka, Y. Polymer Gels. *J. Macromol. Sci. Part C* **2004**, *44* (1), 87–112.

(44) Yu, Y.; Liu, L.; Kong, Y.; Zhang, E.; Liu, Y. Synthesis and Properties of N-Maleyl Chitosan-Cross-Linked Poly(Acrylic Acid-Co-Acrylamide) Superabsorbents. *J. Polym. Environ.* **2011**, *19* (4), 926–934.

(45) Huggins, R. Statistical Mechanics of Cross-Linked Polymer Networks. *J. Adhes.* **1943**, *11* (11), 521–526.

(46) Sperling, L. H. Introduction to Polymer Science. In *Introduction to Physical Polymer Science*; John Wiley & Sons, Inc., 2005; pp 1–28.

(47) Alberda van Ekenstein, G. O. R.; Meyboom, R.; ten Brinke, G.; Ikkala, O.

Determination of the Flory−Huggins Interaction Parameter of Styrene and 4-Vinylpyridine Using Copolymer Blends of Poly(styrene-Co-4-Vinylpyridine) and Polystyrene. *Macromolecules* **2000**, *33* (10), 3752–3756.

(48) Arroyo, M.; López-Manchado, M. A.; Herrero, B. Organo-Montmorillonite as Substitute of Carbon Black in Natural Rubber Compounds. *Polymer (Guildf).* **2003**, *44* (8), 2447–2453.

(49) Elliott, J. E.; Macdonald, M.; Nie, J.; Bowman, C. N. Structure and Swelling of Poly(acrylic Acid) Hydrogels: Effect of pH, Ionic Strength, and Dilution on the Crosslinked Polymer Structure. *Polymer (Guildf).* **2004**, *45* (5), 1503–1510.

(50) Atta, A. M.; Arndt, K. F. Swelling of High Oil-Absorptive Network Based on 1-Octene and Isodecyl Acrylate Copolymers. *J. Polym. Res.* **2005**, *12* (2), 77–88.

(51) Yuan, X.; Chung, T. C. M. Novel Solution to Oil Spill Recovery: Using Thermodegradable Polyole Fi N Oil Superabsorbent Polymer (Oil − SAP). **2012**.

(52) Venosa, A. D.; Campo, P.; Suidan, M. T. Biodegradability of Lingering Crude Oil 19 Years after the Exxon Valdez Oil Spill. *Environ. Sci. Technol.* **2010**, *44* (19), 7613–7621.

(53) Wikelski, M.; Wong, V.; Chevalier, B.; Rattenborg, N.; Snell, H. L. Marine Iguanas Die from Trace Oil Pollution. *Nature* **2002**, *417* (6889), 607–608.

(54) Coe, H. The Deepwater Horizon Spill. *Science (80-.).* **2011**, *1273* (March), 10–12.

(55) Schrope, M. Oil Spill: Deep Wounds. *Nature* **2011**, *472* (7342), 152–154.

(56) Peng, L.; Yuan, S.; Yan, G.; Yu, P.; Luo, Y. Hydrophobic Sponge for Spilled Oil Absorption. *J. Appl. Polym. Sci.* **2014**, *131* (20), n/a-n/a.

(57) Saleem, J.; Bazargan, A.; Barford, J.; McKay, G. Super-Fast Oil Uptake Using Porous Ultra-High Molecular Weight Polyethylene Sheets. *Polym. Adv. Technol.* **2014**, *25* (10), 1181–1185.

(58) Wang, J.; Zheng, Y.; Wang, A. Superhydrophobic Kapok Fiber Oil-Absorbent: Preparation and High Oil Absorbency. *Chem. Eng. J.* **2012**, *213*, 1–7.

(59) Zhang, A.; Chen, M.; Du, C.; Guo, H.; Bai, H.; Li, L. Poly(dimethylsiloxane) Oil Absorbent with a Three-Dimensionally Interconnected Porous Structure and Swellable Skeleton. *ACS Appl. Mater. Interfaces* **2013**, *5* (20), 10201–10206.

(60) Zia, K. M.; Bhatti, H. N.; Ahmad Bhatti, I. Methods for Polyurethane and Polyurethane Composites, Recycling and Recovery: A Review. *React. Funct. Polym.* **2007**, *67*, 675–692.

(61) Husseien, M.; Amer, a a; El-Maghraby, a.; Taha, a. Availability of Barley Straw Application on Oil Spill Clean up. *Int. J. Environ. Sci. Technol.* **2009**, *6* (1), 123–130.

(62) Singh, V.; Kendall, R. J.; Hake, K.; Ramkumar, S. Crude Oil Sorption by Raw Cotton. *Ind. Eng. Chem. Res.* **2013**, *52*, 6277–6281.

(63) Spill, F. A. No Title.

(64) Goss, K. U. Predicting Equilibrium Sorption of Neutral Organic Chemicals into Various Polymeric Sorbents with COSMO-RS. *Anal. Chem.* **2011**, *83* (13), 5304–5308.

(65) Zhou, X.; Wei, J.; Li, S.; Chen, Y.; Liu, K.; Wang, L. Evaluation of Different PP Grafted Sorbent for Oil Spill Cleanup. *Desalin. Water Treat.* **2013**, *0* (0), 1–10.

(66) Adebajo, M. O.; Frost, R. L.; Kloprogge, J. T.; Carmody, O.; Kokot, S. Porous

Materials for Oil Spill Cleanup : A Review of Synthesis. *J. Porous Mater.* **2003**, 159–170.

(67) Pan, B.; Pan, B.; Zhang, W.; Lv, L.; Zhang, Q.; Zheng, S. Development of Polymeric and Polymer-Based Hybrid Adsorbents for Pollutants Removal from Waters. **2009**, *151*, 19–29.

(68) Saleem, J.; Ning, C.; Barford, J.; McKay, G. Combating Oil Spill Problem Using Plastic Waste. *Waste Manag.* **2015**, *44*, 34–38.

(69) Ruan, C.; Ai, K.; Li, X.; Lu, L. A Superhydrophobic Sponge with Excellent Absorbency and Flame Retardancy. *Angew. Chemie Int. Ed.* **2014**, *53* (22), 5556–5560.

(70) Atta, A. M.; Arndt, K.-F. Swelling and Network Parameters of High Oil-Absorptive Network Based on 1-Octene and Isodecyl Acrylate Copolymers. *J. Appl. Polym. Sci.* **2005**, *97* (1), 80–91.

(71) Atta, A. M.; El-Hamouly, S. H.; AlSabagh, A. M.; Gabr, M. M. Crosslinked Poly(octadecene-Alt-Maleic Anhydride) Copolymers as Crude Oil Sorbers. *J. Appl. Polym. Sci.* **2007**, *105* (4), 2113–2120.

(72) Loan, L. D. Crosslinking Efficiencies of Dicumyl Peroxide in Unsaturated Synthetic Rubbers. *J. Appl. Polym. Sci.* **1963**, *7* (6), 2259–2268.

(73) Zhou, M. H.; Cho, W.-J. Synthesis and Properties of High Oil-Absorbent 4-Tert-Butylstyrene-EPDM-Divinylbenzene Graft Terpolymer. *J. Appl. Polym. Sci.* **2002**, *85* (10), 2119–2129.

(74) Calcagnile, P.; Fragouli, D.; Bayer, I. S.; Anyfantis, G. C.; Martiradonna, L.; Cozzoli, P. D.; Cingolani, R.; Athanassiou, A. Magnetically Driven Floating Foams for the Removal of Oil Contaminants from Water. *ACS Nano* **2012**, *6* (6), 5413–5419.

(75) Qin, X.-H.; Wang, S.-Y. Filtration Properties of Electrospinning Nanofibers. *J. Appl. Polym. Sci.* **2006**, *102* (2), 1285–1290.

(76) Robinson, T.; Chandran, B.; Nigam, P. Effect of Pretreatments of Three Waste Residues, Wheat Straw, Corncobs and Barley Husks on Dye Adsorption. *Bioresour. Technol.* **2002**, *85* (2), 119–124.

(77) Paakko, M.; Vapaavuori, J.; Silvennoinen, R.; Kosonen, H.; Ankerfors, M.; Lindstrom, T.; Berglund, L. A.; Ikkala, O. Long and Entangled Native Cellulose I Nanofibers Allow Flexible Aerogels and Hierarchically Porous Templates for Functionalities. *Soft Matter* **2008**, *4* (12), 2492–2499.

(78) Yuan, J.; Liu, X.; Akbulut, O.; Hu, J.; Suib, S. L.; Kong, J.; Stellacci, F. Superwetting Nanowire Membranes for Selective Absorption. *Nat Nano* **2008**, *3* (6), 332–336.

(79) Li, D.; Zhu, F. Z.; Li, J. Y.; Na, P.; Wang, N. Preparation and Characterization of Cellulose Fibers from Corn Straw as Natural Oil Sorbents. *Ind. Eng. Chem. Res.* **2013**, *52* (1), 516–524.

(80) Sun, X. F.; Sun, R.; Sun, J. X. Acetylation of Rice Straw with or without Catalysts and Its Characterization as a Natural Sorbent in Oil Spill Cleanup. *J. Agric. Food Chem.* **2002**, *50* (22), 6428–6433.

(81) Cloud, R. M.; Sound, W. Natural Sorbents in Oil Spill Cleanup. **1992**, No. 11, 772–776.

(82) Singh, V.; Jinka, S.; Hake, K.; Parameswaran, S.; Kendall, R. J.; Ramkumar, S. Novel Natural Sorbent for Oil Spill Cleanup. **2014**.
(83) Wang, J.; Zheng, Y.; Wang, A. Coated Kapok Fiber for Removal of Spilled Oil. *Mar. Pollut. Bull.* **2013**, *69* (1–2), 91–96.
(84) Johnson, R. F.; Manjreker, T. G.; Halligan, J. E. Removal of Oil from Water Surfaces by Sorption on Unstructured Fibers. *Environ. Sci. Technol.* **1973**, *7* (5), 439–443.
(85) Kang, Y.; Park, B.; Park, S.; Kang, N. G.; Kim, H. Sorption Behaviors of Cotton , Kapok , and Rayon Fibers in Heavy Metal Solutions. **2011**, *48* (6), 386–392.
(86) Wang, J.; Zheng, Y.; Wang, A. Superhydrophobic Kapok Fiber Oil-Absorbent: Preparation and High Oil Absorbency. *Chem. Eng. J.* **2012**, *213*, 1–7.
(87) Bowen, B. H. J. M. 1082 J. Chem. **1970**, No. 1082.
(88) Pinto, J.; Athanassiou, A.; Fragouli, D. Effect of the Porous Structure of Polymer Foams on the Remediation of Oil Spills. *J. Phys. D. Appl. Phys.* **2016**, *49* (14), 145601.
(89) Adebajo, M. O.; Frost, R. L.; Kloprogge, J. T.; Carmody, O.; Kokot, S. Porous Materials for Oil Spill Cleanup: A Review of Synthesis and Absorbing Properties. *J. Porous Mater.* **2003**, *10* (3), 159–170.
(90) Li, X.; Guo, Y.; Zhang, J.; Zhang, L. Preparation of Polysulfone Microspheres with a Hollow Core/porous Shell Structure and Their Application for Oil Spill Cleanup. *J. Appl. Polym. Sci.* **2013**, *128* (5), 2994–2999.
(91) Wu, J.; Wang, N.; Wang, L.; Dong, H.; Zhao, Y.; Jiang, L. Electrospun Porous Structure Fibrous Film with High Oil Adsorption Capacity. *ACS Appl. Mater. Interfaces* **2012**, *4* (6), 3207–3212.
(92) Pier, S. M.; Gould, J. R. Treating Agents. **1971**, 219–233.
(93) Peng, L.; Yuan, S.; Yan, G.; Yu, P.; Luo, Y. Hydrophobic Sponge for Spilled Oil Absorption. *J. Appl. Polym. Sci.* **2014**, *131* (20), n/a-n/a.
(94) de Lima, J. A.; Felisberti, M. I. Porous Polymer Structures Obtained via the TIPS Process from EVOH/PMMA/DMF Solutions. *J. Memb. Sci.* **2009**, *344* (1–2), 237–243.
(95) McCann, J. T.; Marquez, M.; Xia, Y. Highly Porous Fibers by Electrospinning into a Cryogenic Liquid. *J. Am. Chem. Soc.* **2006**, *128* (5), 1436–1437.
(96) Zhao, X.; Li, L.; Li, B.; Zhang, J.; Wang, A. Durable Superhydrophobic/superoleophilic PDMS Sponges and Their Applications in Selective Oil Absorption and in Plugging Oil Leakages. *J. Mater. Chem. A* **2014**, *2* (43), 18281–18287.
(97) Raza, A.; Ding, B.; Zainab, G.; El-Newehy, M.; Al-Deyab, S. S.; Yu, J. In Situ Cross-Linked Superwetting Nanofibrous Membranes for Ultrafast Oil-Water Separation. *J. Mater. Chem. A* **2014**, *2* (26), 10137–10145.
(98) Li, J.-J.; Zhu, L.-T.; Luo, Z.-H. Electrospun Fibrous Membrane with Enhanced Swithchable Oil/water Wettability for Oily Water Separation. *Chem. Eng. J.* **2016**, *287*, 474–481.
(99) Obaid, M.; Barakat, N. A. M.; Fadali, O. A.; Motlak, M.; Almajid, A. A.; Khalil, K. A. Effective and Reusable Oil/water Separation Membranes Based on Modified Polysulfone Electrospun Nanofiber Mats. *Chem. Eng. J.* **2015**, *259*, 449–456.

(100) Sarbatly, R.; Krishnaiah, D.; Kamin, Z. A Review of Polymer Nanofibres by Electrospinning and Their Application in Oil–water Separation for Cleaning up Marine Oil Spills. *Mar. Pollut. Bull.* **2016**, *106* (1–2), 8–16.
(101) Hou, Y.; Wang, Z.; Guo, J.; Shen, H.; Zhang, H.; Zhao, N.; Zhao, Y.; Chen, L.; Liang, S.; Jin, Y.; Xu, J. Facile Fabrication of Robust Superhydrophobic Porous Materials and Their Application in Oil/water Separation. *J. Mater. Chem. A* **2015**, *3* (46), 23252–23260.
(102) Li, A.; Sun, H.-X.; Tan, D.-Z.; Fan, W.-J.; Wen, S.-H.; Qing, X.-J.; Li, G.-X.; Li, S.-Y.; Deng, W.-Q. Superhydrophobic Conjugated Microporous Polymers for Separation and Adsorption. *Energy Environ. Sci.* **2011**, *4* (6), 2062–2065.
(103) Shimizu, T.; Koshiro, S.; Yamada, Y.; Tada, K. Effect of Cell Structure on Oil Absorption of Highly Oil Absorptive Polyurethane Foam for on-Site Use. *J. Appl. Polym. Sci.* **1997**, *65* (1), 179–186.
(104) Jayaramulu, K.; Datta, K. K. R.; Rösler, C.; Petr, M.; Otyepka, M.; Zboril, R.; Fischer, R. A. Biomimetic Superhydrophobic/Superoleophilic Highly Fluorinated Graphene Oxide and ZIF-8 Composites for Oil–Water Separation. *Angew. Chemie Int. Ed.* **2016**, *55* (3), 1178–1182.
(105) Zhang, J.; Seeger, S. Polyester Materials with Superwetting Silicone Nanofilaments for Oil/water Separation and Selective Oil Absorption. *Adv. Funct. Mater.* **2011**, *21* (24), 4699–4704.
(106) Zhu, Q.; Pan, Q.; Liu, F. Facile Removal and Collection of Oils from Water Surfaces through Superhydrophobic and Superoleophilic Sponges. *J. Phys. Chem. C* **2011**, *115* (35), 17464–17470.
(107) Wang, B.; Karthikeyan, R.; Lu, X.-Y.; Xuan, J.; Leung, M. K. H. Hollow Carbon Fibers Derived from Natural Cotton as Effective Sorbents for Oil Spill Cleanup. *Ind. Eng. Chem. Res.* **2013**, *52* (51), 18251–18261.
(108) Li, B.; Liu, X.; Zhang, X.; Zou, J.; Chai, W.; Xu, J. Oil-Absorbent Polyurethane Sponge Coated with KH-570-Modified Graphene. *J. Appl. Polym. Sci.* **2015**, *132* (16), n/a-n/a.
(109) UV and Spontaneously Cured Polyethylene Glycol-Based Hydrogels for Soft and Hard Tissue Scaffolds Kambiz Farbod. **2010**.
(110) Zustiak, S. P.; Boukari, H.; Leach, J. B. Solute Diffusion and Interactions in Cross-Linked Poly(ethylene Glycol) Hydrogels Studied by Fluorescence Correlation Spectroscopy. *Soft Matter* **2010**, *6* (15), 3609–3618.
(111) National, B. Method for Measuring Water Diffusion in a Coating Applied to a Substrate.
(112) George, S. C.; Thomas, S. Transport Phenomena through Polymeric Systems. **2001**, *26*.
(113) Zhao, J.; Xiao, C. F.; Xu, N. K. Diffusion and Swelling Behavior in Treatment of Oil Spill to Semi-Interpenetrating Polymer Network from Oil-Absorptive Fiber. *J. Dispers. Sci. Technol.* **2012**, *33* (8), 1197–1203.
(114) Barlkani, M.; Hepburn, C. Determination of Crosslink Density by Swelling in the Castable Polyurethane Elastomer Based on 1/4-Cyclohexane Diisocyanate and Para-Phenylene. *Iran. J. Polym. Sci. Tech* **1992**, *1* (1), 1–5.
(115) Xing, Q.; Yates, K.; Vogt, C.; Qian, Z.; Frost, M. C.; Zhao, F. Increasing

Mechanical Strength of Gelatin Hydrogels by Divalent Metal Ion Removal. *Sci. Rep.* **2014**, *4*, 4706.
(116) Lazfir, M.; Influence, M. Crosslinking of Polyolefins. **1988**.
(117) Lin, J.; Ding, B.; Yang, J.; Yu, J.; Sun, G. Subtle Regulation of the Micro- and Nanostructures of Electrospun Polystyrene Fibers and Their Application in Oil Absorption. *Nanoscale* **2012**, *4* (1), 176–182.
(118) Wu, B.; Zhou, M.; Lu, D. Studies on Swelling Behaviour, Compressive Properties, and Network Parameters of EPDM/4-. **2006**, *15* (12), 989–995.
(119) Yuan, X.; Chung, T. C. M. Novel Solution to Oil Spill Recovery: Using Thermodegradable Polyolefin Oil Superabsorbent Polymer (Oil–SAP). *Energy & Fuels* **2012**, *26* (8), 4896–4902.
(120) Omidian, H.; Hasherni, S.; Askari, F.; Nafisi, S. Swelling and Crosslink Density Measurements for Hydrogels. **1994**, *3* (2), 115–119.
(121) Lohse, D. J. The Influence of Chemical Structure on Polyolefin Melt Rheology and Miscibility. *J. Macromol. Sci. Part C* **2005**, *45* (4), 289–308.
(122) Lin, W.; Shao, Z.; Dong, J.; Chung, T. C. M. Cross-Linked Polypropylene Prepared by PP Copolymers Containing Flexible Styrene Groups. *Macromolecules* **2009**, *42* (11), 3750–3754.
(123) Chung, T. C. M. Functional Polyolefins for Energy Applications. *Macromolecules* **2013**, *46* (17), 6671–6698.
(124) Mayo, F. R. Chain Transfer in the Polymerization of Styrene. VIII. Chain Transfer with Bromobenzene and Mechanism of Thermal Initiation1. *J. Am. Chem. Soc.* **1953**, *75* (24), 6133–6141.
(125) Mayo, F. R. The Dimerization of Styrene. *J. Am. Chem. Soc.* **1968**, *90* (5), 1289–1295.
(126) Neuburger, N. A.; Eichinger, B. E. Critical Experimental Test of the Flory-Rehner Theory of Swelling. *Macromolecules* **1988**, *21* (10), 3060–3070.
(127) Hansen, C. Absorption and Diffusion in Polymers. In *Hansen Solubility Parameters*; CRC Press, 2007; pp 293–310.
(128) Milner, S. T.; Lacasse, M.-D.; Graessley, W. W. Why χ Is Seldom Zero for Polymer−Solvent Mixtures. *Macromolecules* **2009**, *42* (3), 876–886.
(129) Bi, H.; Yin, Z.; Cao, X.; Xie, X.; Tan, C.; Huang, X.; Chen, B.; Chen, F.; Yang, Q.; Bu, X.; Lu, X.; Sun, L.; Zhang, H. Carbon Fiber Aerogel Made from Raw Cotton: A Novel, Efficient and Recyclable Sorbent for Oils and Organic Solvents. *Adv. Mater.* **2013**, *25* (41), 5916–5921.
(130) Wen, Q.; Di, J.; Jiang, L.; Yu, J.; Xu, R. Zeolite-Coated Mesh Film for Efficient Oil-Water Separation. *Chem. Sci.* **2013**, *4* (2), 591–595.
(131) Bi, H.; Xie, X.; Yin, K.; Zhou, Y.; Wan, S.; He, L.; Xu, F.; Banhart, F.; Sun, L.; Ruoff, R. S. Spongy Graphene as a Highly Efficient and Recyclable Sorbent for Oils and Organic Solvents. *Adv. Funct. Mater.* **2012**, *22* (21), 4421–4425.
(132) Xue, Z.; Wang, S.; Lin, L.; Chen, L.; Liu, M.; Feng, L.; Jiang, L. A Novel Superhydrophilic and Underwater Superoleophobic Hydrogel-Coated Mesh for Oil/water Separation. *Adv. Mater.* **2011**, *23*, 4270–4273.
(133) Dana, S. F.; Nguyen, D.-V.; Kochhar, J. S.; Liu, X.-Y.; Kang, L. UV-Curable Pressure Sensitive Adhesive Films: Effects of Biocompatible Plasticizers on

Mechanical and Adhesion Properties. *Soft Matter* **2013**, *9* (27), 6270–6281.
(134) Hoffman, A. S. Hydrogels for Biomedical Applications. *Adv. Drug Deliv. Rev.* **2012**, *64*, 18–23.
(135) Tokarev, I.; Minko, S. Stimuli-Responsive Hydrogel Thin Films. *Soft Matter* **2009**, *5* (3), 511.
(136) Avnir, D.; Coradin, T.; Lev, O.; Livage, J. Recent Bio-Applications of Sol–gel Materials. *J. Mater. Chem.* **2006**, *16* (11), 1013.
(137) Rana, D.; Matsuura, T. Surface Modifications for Antifouling Membranes. *Chem. Rev.* **2010**, *110* (4), 2448–2471.
(138) Buenger, D.; Topuz, F.; Groll, J. Hydrogels in Sensing Applications. *Prog. Polym. Sci.* **2012**, *37* (12), 1678–1719.
(139) Zhu, J. Bioactive Modification of Poly(ethylene Glycol) Hydrogels for Tissue Engineering. *Biomaterials* **2010**, *31* (17), 4639–4656.
(140) Hou, Y.; Schoener, C. A.; Regan, K. R.; Munoz-Pinto, D.; Hahn, M. S.; Grunlan, M. A. Photo-Cross-Linked PDMSstar-PEG Hydrogels: Synthesis, Characterization, and Potential Application for Tissue Engineering Scaffolds. *Biomacromolecules* **2010**, *11* (3), 648–656.
(141) Cipriano, B. H.; Banik, S. J.; Sharma, R.; Rumore, D.; Hwang, W.; Briber, R. M.; Raghavan, S. R. Superabsorbent Hydrogels That Are Robust and Highly Stretchable. *Macromolecules* **2014**, *47* (13), 4445–4452.
(142) Kumar, A.; Sharma, G.; Naushad, M.; Thakur, S. SPION/β-Cyclodextrin Core–shell Nanostructures for Oil Spill Remediation and Organic Pollutant Removal from Waste Water. *Chem. Eng. J.* **2015**, *280*, 175–187.
(143) Zhao, J.; Xiao, C.; Xu, N.; Feng, Y. Preparation and Properties of Oil-Absorptive Fiber Based on Polybutyl Methacrylate-Inter-Polyhydroxyethyl Methacrylate via Wet Spinning. *Polym. Plast. Technol. Eng.* **2011**, *50* (8), 818–824.
(144) Hu, H.; Zhao, Z.; Gogotsi, Y.; Qiu, J. Compressible Carbon Nanotube–Graphene Hybrid Aerogels with Superhydrophobicity and Superoleophilicity for Oil Sorption. *Environ. Sci. Technol. Lett.* **2014**, *1* (3), 214–220.
(145) Chen, P.-C.; Xu, Z.-K. Mineral-Coated Polymer Membranes with Superhydrophilicity and Underwater Superoleophobicity for Effective Oil/Water Separation. *Sci. Rep.* **2013**, *3*, 2776.
(146) Yang, Y.; Tong, Z.; Ngai, T.; Wang, C. Nitrogen-Rich and Fire-Resistant Carbon Aerogels for the Removal of Oil Contaminants from Water. *ACS Appl. Mater. Interfaces* **2014**, *6* (9), 6351–6360.
(147) Li, X.; Wang, M.; Wang, C.; Cheng, C.; Wang, X. Facile Immobilization of Ag Nanocluster on Nanofibrous Membrane for Oil/Water Separation. *ACS Appl. Mater. Interfaces* **2014**, *6* (17), 15272–15282.
(148) He, K.; Duan, H.; Chen, G. Y.; Liu, X.; Yang, W.; Wang, D. Cleaning of Oil Fouling with Water Enabled by Zwitterionic Polyelectrolyte Coatings: Overcoming the Imperative Challenge of Oil–Water Separation Membranes. *ACS Nano* **2015**, *9* (9), 9188–9198.
(149) Zhang, J.; Seeger, S. Polyester Materials with Superwetting Silicone Nanofilaments for Oil/Water Separation and Selective Oil Absorption. *Adv. Funct. Mater.* **2011**, *21* (24), 4699–4704.

(150) Li, A.; Sun, H.-X.; Tan, D.-Z.; Fan, W.-J.; Wen, S.-H.; Qing, X.-J.; Li, G.-X.; Li, S.-Y.; Deng, W.-Q. Superhydrophobic Conjugated Microporous Polymers for Separation and Adsorption. *Energy Environ. Sci.* **2011**, *4* (6), 2062.
(151) Lei, W.; Portehault, D.; Liu, D.; Qin, S.; Chen, Y. Porous Boron Nitride Nanosheets for Effective Water Cleaning. *Nat Commun* **2013**, *4*, 1777.
(152) Kota, A. K.; Kwon, G.; Choi, W.; Mabry, J. M.; Tuteja, A. Hygro-Responsive Membranes for Effective Oil-Water Separation. *Nat. Commun.* **2012**, *3*, 1025.
(153) Solomon, B. R.; Hyder, M. N.; Varanasi, K. K. Separating Oil-Water Nanoemulsions Using Flux-Enhanced Hierarchical Membranes. *Sci. Rep.* **2014**, *4*, 5504.
(154) Bergamelli, F.; Iannelli, M.; Marafie, J. A.; Moseley, J. D. A Commercial Continuous Flow Microwave Reactor Evaluated for Scale-Up. *Org. Process Res. Dev.* **2010**, *14* (4), 926–930.
(155) Mulligan, C. J.; Wilson, M.; Bryant, G.; Vaughan, B.; Zhou, X.; Belcher, W. J.; Dastoor, P. C. A Projection of Commercial-Scale Organic Photovoltaic Module Costs. *Sol. Energy Mater. Sol. Cells* **2014**, *120*, *Part*, 9–17.
(156) Tang, C.; Zhang, C.; Liu, J.; Qu, X.; Li, J.; Yang, Z. Large Scale Synthesis of Janus Submicrometer Sized Colloids by Seeded Emulsion Polymerization. *Macromolecules* **2010**, *43* (11), 5114–5120.
(157) Matyjaszewski, K.; Xia, J. Atom Transfer Radical Polymerization. *Chem. Rev.* **2001**, *101* (9), 2921–2990.
(158) Parvez, M. A.; Rahaman, M.; Suleiman, M. A.; Soares, J. B. P.; Hussein, I. A. Correlation of Polymerization Conditions with Thermal and Mechanical Properties of Polyethylenes Made with Ziegler-Natta Catalysts. *Int. J. Polym. Sci.* **2014**, *2014*.

VITA

Changwoo Nam

Changwoo Nam was born in Changwon, South Korea. He received his Bachelor (August, 2005) degree in Chemical engineering from Pukyong National University and Master (August, 2007) degree in Chemical and biological engineering from Seoul National University under a Brain Korea 21 (BK21) graduate fellowship. Following graduation 2007, he joined the Daewoo Shipbuilding and Marine Engineering (DSME) in Korea. After 5.2 years of work for material division in DSME, he came to U.S for his graduate study in 2012. He joined the research group of Dr. Michael Hickner in the Materials Science and Engineering Department at the Pennsylvania State University. He started his Ph.D. research focusing on the molecules absorption behavior on hydrogel. After 2 years, he moved to Dr. T.C. Mike Chung's group, he broadened his research area to oil molecules absorption on polyolefin based absorbents and his research was developing polyolefin interpenetrated network absorbent for oil spill recovery supported by Department of the Interior.